AD-A074 273 OREGON STATE UNIV CORVALLIS SCHOOL OF OCEANOGRAPHY F/G 8/3
TOWED OBSERVATIONS OF INTERNAL WAVES IN THE UPPER OCEAN.(U)
JUL 79 T J SPOERING N00014-76-C-0067
UNCLASSIFIED REF-79-10 NL

1 OF 2
AD A074273

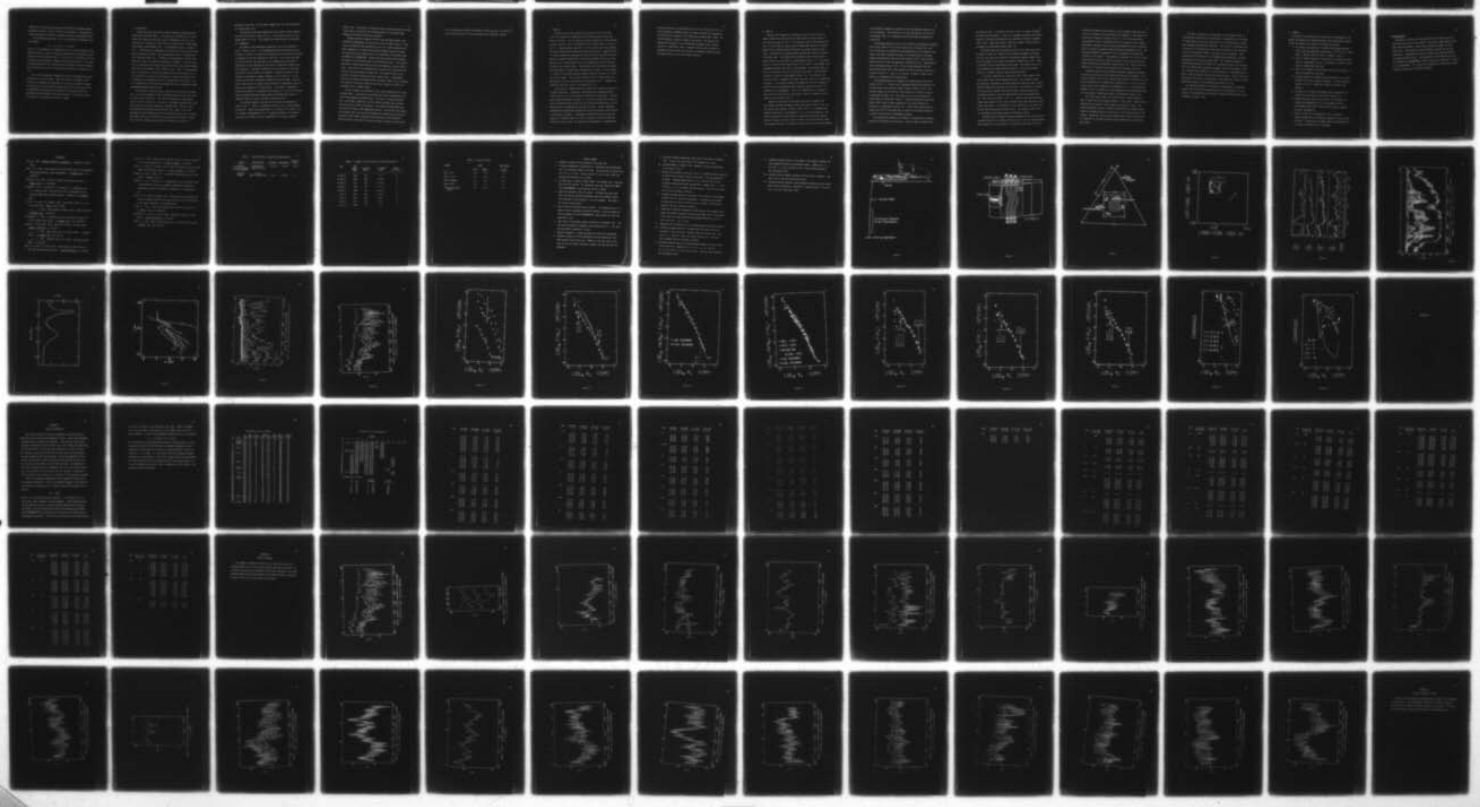

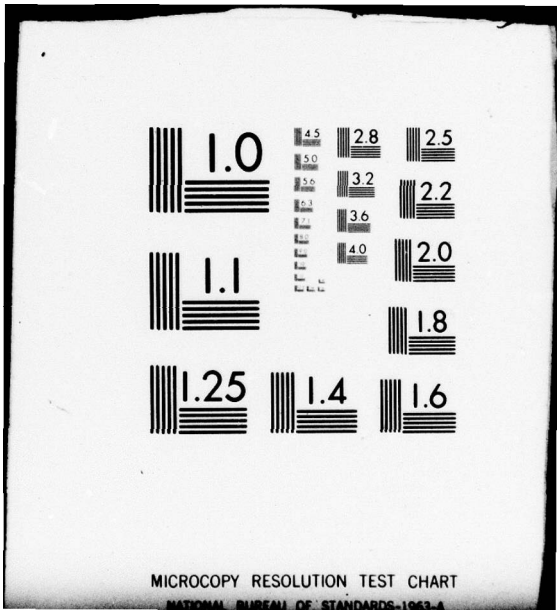
1.0
1.1
1.25
1.4
1.6
1.8
2.0
2.2
2.5
2.8
3.2
3.6
4.0
4.5
5.0
MICROCOPY RESOLUTION TEST CHART
NATIONAL BUREAU OF STANDARDS-1963-A

OCEANOGRAPHY

Vessel Observations of Internal Waves in the Upper Ocean

by
Thomas J. Spoering

Office of Naval Research
N00014-75-C-0207

unclassified

SECURITY CLASSIFICATION OF THIS PAGE (When Data Entered)

REPORT DOCUMENTATION PAGE		READ INSTRUCTIONS BEFORE COMPLETING FORM
1. REPORT NUMBER 79-10	2. GOVT ACCESSION NO.	3. RECIPIENT'S CATALOG NUMBER
4. TITLE (and Subtitle) (6) TOWED OBSERVATIONS OF INTERNAL WAVES IN THE UPPER OCEAN.		5. TYPE OF REPORT & PERIOD COVERED M.S. Thesis, May 1979 6. PERFORMING ORG. REPORT NUMBER
7. AUTHOR(s) (10) Thomas [redacted] Spoering James		8. CONTRACT OR GRANT NUMBER(s) (15) N00014-76-C-0067 N00014-79-C-0004
9. PERFORMING ORGANIZATION NAME AND ADDRESS School of Oceanography Oregon State University Corvallis, Oregon 97331		10. PROGRAM ELEMENT, PROJECT, TASK AREA & WORK UNIT NUMBERS NR 083-102
11. CONTROLLING OFFICE NAME AND ADDRESS Office of Naval Research Ocean Science & Technology Division Arlington, VA 22217		(11) 12. REPORT DATE July [redacted]79 13. NUMBER OF PAGES 121
14. MONITORING AGENCY NAME & ADDRESS (if different from Controlling Office) (12) 129p.		15. SECURITY CLASS. (of this report) unclassified 15a. DECLASSIFICATION/DOWNGRADING SCHEDULE

16. DISTRIBUTION STATEMENT (of this Report)

Approved for public release, distribution unlimited

(9) Master's Thesis.

17. DISTRIBUTION STATEMENT (of the abstract entered in Block 20, if different from Report)

(14) REF-79-10

18. SUPPLEMENTARY NOTES

19. KEY WORDS (Continue on reverse side if necessary and identify by block number)

Internal Waves
Towed Thermistor Chain
Mixed Layer Experiment (MILE)

20. ABSTRACT (Continue on reverse side if necessary and identify by block number)

Observations between 20 and 40 m depth were made with a towed thermister chain in the North Pacific. Despite the rapid vertical variation of buoyancy frequency, spectra of isotherm displacements are in fair agreement with other observations and with the Garrett-Munk model. The spectra show evidence of a shoulder and break in slope at a wavelength of 1 km. There is no evidence of significant variation of spectral levels as a function of buoyancy frequency, tow direction or wind (over)

DD FORM 1 JAN 73 1473 EDITION OF 1 NOV 65 IS OBSOLETE
S/N 0102-014-6601

unclassified
SECURITY CLASSIFICATION OF THIS PAGE (When Data Entered)

272 268

speed. A peak at a wavelength of 1 km in coherence spectra between pairs of isotherms separated in the vertical suggests that internal wave energy at this wavelength is dominated by the low modes.

Towed Observations of Internal Waves in the Upper Ocean

by

Thomas James Spoering

A THESIS

submitted to

Oregon State University

in partial fulfillment of the requirements for the degree of

Master of Science

Completed May 3, 1979

Commencement June 1979

AN ABSTRACT OF THE THESIS OF

Thomas James Spoering for the degree of Master of Science

in the School of Oceanography presented on May 3, 1979

Title: Towed Observations of Internal Waves in the Upper Ocean

Abstract approved: _____

Clayton A. Paulson

Observations between 20 and 40 m depth were made with a towed thermostor chain in the North Pacific. Despite the rapid vertical variation of buoyancy frequency, spectra of isotherm displacements are in fair agreement with other observations and with the Garrett-Munk model. The spectra show evidence of a shoulder and break in slope at a wavelength of 1 km. There is no evidence of significant variation of spectral levels as a function of buoyancy frequency, tow direction, or wind speed. A peak at a wavelength of 1 km in coherence spectra between pairs of isotherms separated in the vertical suggests that internal wave energy at this wavelength is dominated by the low modes.

APPROVED:

Associate Professor of Oceanography
in charge of major

Dean of the School of Oceanography

Dean of Graduate School

Date thesis is presented May 3, 1979

Typed by Gail Henwood for Thomas J. Spoering

TABLE OF CONTENTS

Preface

This paper has been written in manuscript format rather than the traditional thesis format. The School of Oceanography encourages this approach to reduce the work involved in preparing papers stemming from graduate research projects for publication in scientific journals. For this reason, some deviations from the ordering of a traditional thesis are present: 1) no list of Tables or Figures appears; 2) Tables appear in order at the end of the main text; 3) a list of Figure legends, followed by the Figures, are placed after the Tables; 4) acknowledgments are placed after the text, rather than before. This paper will be submitted to the Journal of Physical Oceanography with Thomas J. Spoering as first author and Clayton A. Paulson as second.

1. Introduction

The investigation of internal gravity waves in the open ocean has produced an extensive theoretical and observational literature. Recent advances in the observations and interpretation have been excellently reviewed by Garrett and Munk (1979). For the most part, the theory and observations have applied to regions of the ocean in which the buoyancy frequency, N, defined by $N^2 = g\,\rho^{-1}\,\partial\rho/\partial z$, is nearly constant or changes slowly with depth. In the upper ocean, N usually varies rapidly with depth, reaching a maximum below the base of the surface mixed layer and then decreasing with depth in the seasonal thermocline.

Garrett and Munk (1972, 1975) successfully modeled the distribution of the internal wave energy in wavenumber and frequency space. This model spectrum was based on observations from many sources together with simplifying assumptions. The applicability of the Garrett-Munk model near the base of the surface mixed layer is doubtful.

Pinkel (1975) reported observations from FLIP between 60 and 400 m depth from which spectra of isotherm displacement and slope were computed. Pinkel found that the first mode is strongly dominant above 2 cph while below 2 cph the bandwidth of energetic wavenumbers is broader, corresponding to multiple energetic modes.

Käse and Clarke (1978) analyzed moored and profiling CTD measurements in the upper thermocline during the GARP Atlantic and Tropical Experiment (GATE). They found a peak in the internal wave spectrum in the frequency band from 2 to 5 cph. Waves in this band are coherent and in phase within the upper 30 m of the thermocline. Käse and Clarke suggest a model showing how surface wind stress forcing may produce a spectral peak in

the upper thermocline at frequencies higher than the buoyancy frequency of the thickest underlying layer of constant N.

Nelson and Milder (1979) analyzed towed thermistor chain observations in the upper 150 m of the Eastern Tropical Pacific. Spectra of isotherm depths agreed with the Garrett-Munk model although there was evidence of horizontal anisotropy at wavenumbers below 1 c/km. They found that towed vertical coherence was substantially higher throughout the horizontal wavenumber band when compared to previous deeper observations and the Garrett-Munk model.

Dillon and Caldwell (1979) reported observations in the upper 200 m of the vertical velocity of internal waves obtained from a nearly free-falling vehicle. The spectrum of vertical velocity has a maximum at a band in the spectrum centered at 3 cph. They found that most of the internal wave energy in this band was in the first and second modes.

The objective of this paper is to describe observations of internal waves in the upper North Pacific. The measurements were made by use of a towed thermistor chain at depths between 20 and 40 m. Horizontal wavenumber spectra of the vertical displacement of isotherms are presented and compared to previous observations and to the Garrett-Munk model. Variability of the spectra with the local value of N, tow direction, and wind speed are investigated. Coherence spectra between isotherms separated in the vertical are also presented.

2. Instrumentation

The design of the towed thermistor chain was based on the design of a similar system constructed by the Applied Physics Laboratory of Johns Hopkins University (Mobley et al., 1976). The main difference in our design is the incorporation of the bridge/amplifiers into the chain near each of the thermistors rather than having the bridge/amplifiers located in the ship's laboratory. A more complete description of the design and construction of our system is given by Mesecar and Evans (1977).

A schematic diagram of the thermistor chain in operation is shown in Fig. 1. The chain was constructed using plastic fairing manufactured by Fathom Oceanology Ltd. (Model 770T). The fairing effectively reduces drag and vibration and also supports the sensors, bridge/amplifiers and electrical conductors. A steel strain member runs through the nose pieces of the fairing and is attached to a streamlined, lead-filled, cyclindrical depressor which has a mass of 450 kg. The fairing is free to turn around the strain member and align itself parallel to the flow. The angle between the chain and the vertical was less than 10° for tow speeds up to 3 m/s with the depressor at a depth of 40 m.

There were 25 thermistors installed on the chain, each separated by a distance of one meter. Four pressure sensors and associated electronics were installed at intervals of eight meters. The specifications for the temperature and pressure measurements are given in Table 1.

Sensors and associated electronics can be placed anywhere along the length of the chain in modified sections of fairing. The installation of a thermistor and its associated bridge/amplifier is illustrated in Fig. 2. Part of the nosepiece of a fairing section was cut out and replaced by a

nosepiece containing a thermistor. The thermistor was molded into the nosepiece and exposed to the environment through an indentation in the front. The leads from the thermistor run to another molding containing pad resistors used to normalize the calibration. Leads run from the pad resistors to a molding in the tail section containing the bridge/amplifier. The bridge/amplifier is powered from shipboard by electrical conductors running through the tail sections of the fairing. Signals are conducted to the ship by similar means. The signal and power conductors are twisted pairs of teflon-coated, stranded wire. The pressure sensors and associated electronics were installed entirely within tail sections of fairing analogous to the installation of the bridge/amplifiers in Fig. 2.

A specially constructed winch and sheave are part of the system. Because of the stiffness of the chain and the wires running through the tail sections of the fairing, a large turning radius is required. The winch has a drum 1.5 m in diameter which holds a single wrap of faired cable. The drum has a continuous plastic groove attached to its surface which is shaped to accept the fairing nosepieces. The grooved surface eliminates the need for a level-wind. The chain runs out over a sheave 1.2 m in diameter which is suspended from the ship's boom or A-frame.

The signals from the thermistors and pressure sensors are processed and recorded in the ship's lab. The signals are amplified, offset, digitized and recorded on magnetic tape by use of a minicomputer system. Means and standard deviations are computed simultaneous to recording.

The thermistors, together with the bridge/amplifiers, were calibrated in a stirred calibration bath which was stable to better than 0.001°C.

Comparison of calibrations before and following the experiment showed agreement to within ± 0.01°C for most of the sensors. Disagreement was caused by rupture of the glass insulation covering the thermistor bead.

The calibration data were fit to a curve proposed by Steinhart and Hart (1968):

$$T^{-1} = A + B \ln R + C (\ln R)^3$$

where T is the temperature in degrees Kelvin, R is the resistance of the thermistor and A, B and C are constants determined by the method of least squares from the calibration data. In our case, we substituted for R the resistance of the thermistor together with the pad resistors. The errors introduced because of this substitution are expected to be small because the calibration and the use of the chain was limited to a range of 5 to 15°C.

The pressure transducers together with their bridge/amplifiers were calibrated in a pressure bomb. There was evidence of changes in the calibration throughout the experiment of as much as one meter in depth. The chain was very nearly vertical while under tow so that we were able to independently determine the mean depth of the sensors during the experiment from the length of the chain deployed. The pressure sensors were relied on to determine variations in depth.

3. Observations

Observations were made with the towed thermistor chain during the Mixed Layer Experiment (MILE). The objective of the MILE was to investigate the response of the upper ocean to atmospheric forcing. The experiment was conducted in the vicinity of Ocean Station P (50N, 145W) during August and September, 1977. The experimental array is shown in Fig. 3. Observations of temperature and velocity in the upper 100 m were made at moorings M1 and M2. Wave observations by use of a moored wave-rider buoy were made at M3. In addition to measurements with the towed thermistor chain, the shipborne observations included: 1) vertical profiles of temperature and conductivity microstructure (Dillon and Caldwell, 1978; Dillon and Caldwell, 1979; Caldwell et al., 1979; 2) towed measurements of temperature, velocity and conductivity microstructure; 3) vertical profiles of velocity microstructure; 4) towed saw-tooth profiles of temperature and conductivity; and 5) conventional CTD profiles. Vertical temperature profiles were also measured by use of expendable bathythermographs dropped from aircraft.

The thermistor chain was usually towed once around the 20-km square (Fig. 3) with the midpoint of the instrumented section of the chain near the base of the mixed layer. The times and locations of the tows are given in Table 2 and Fig. 4. The tow on 5 September proceeded four times around the five-km square centered on the mooring M1. The tow tracks and speeds were determined from satellite fixes, radar fixes on the moorings and dead reckoning by use of the output from the ship's log and gyrocompass which were recorded on our data acquisition system. During tows, the ship's heading and speed were maintained as constant as

possible on each leg. The tow speed ranged from 1 to 3 m/s and usually was greater than 2 m/s.

The periods of the tows together with wave height, surface temperature and wind speed are shown in Fig. 5. Wind speeds during the tows ranged from 2 to 12 m/s. The highest wind speed during a tow occurred on 1 September.

An example of the temperature measured by use of the thermistor chain is shown in Fig. 6. The temperature oscillations having periods of about 10 seconds are caused by the thermistor chain moving up and down in response to the pitch and heave of the ship. For a given amplitude of vertical motion, the amplitude of the temperature oscillations is proportional to the magnitude of the vertical temperature gradient near each thermistor. The upper thermistors are occasionally in the mixed layer where no oscillations are apparent. Occasional patches of high-frequency fluctuations, perhaps turbulence, can be seen, e.g. in the record from the lowest thermistor between 2313 and 2314 GMT. Also evident in the records are larger-scale variations in temperature which are taken to be signatures of internal waves. The change in temperature along the horizontal is occasionally very abrupt as is seen in the record from the lowest thermistor between 2304 and 2305 GMT where there is a change of nearly 2°C over a horizontal distance of 30 m.

The average buoyancy frequency profile during the experiment is shown in Fig. 7. There is a maximum of 18 cph in N at a depth between 25 and 50 m. Below this maximum there is a minimum in N of about 3 cph at a depth of approximately 75 m. A secondary maximum in N of about 7 cph occurs at a depth of 125 m. Below 200 m, N is nearly constant,

about 2 cph. The maximum in N below the base of the mixed layer was much larger than 18 cph during and following periods of high winds when deepening of the well-mixed layer occurred.

Average buoyancy frequency profiles over the depth range of the temperature measurements for each of the tows are shown in Fig. 8. Density was determined from temperature by use of a linear regression between temperature and density observations between 20 and 50 m depth. The observations were taken by use of a conventional CTD operated from the NOAA ship OCEANOGRAPHER. Observations were chosen which preceded, followed or occurred during tows of the thermistor chain. The standard deviation of the observed density about the regression line was 0.06 σ_t units. The errors in N introduced by not having direct observations of salinity are not expected to exceed 10%. The largest values of N occurred on 24 August following the most intense storm. Instantaneous profiles of N would show larger values than those shown in Fig. 8 because of horizontal variability along the tow track, primarily vertical displacements due to internal waves.

In most respects, the thermistor chain system performed well during the experiment. Launching and retrieving were easily accomplished, and the fairing reduced drag effectively. The winch and sheave performed well, and bridges, amplifiers, and the digital recorder were reliable, had low noise and stable calibrations. The biggest disappointment was the failure of many of the temperature sensors. The failures were caused by saltwater leaks into the potting between the thermistors and the pad resistors and by leaks through the glass coatings of the thermistors. These failures, which have since been corrected, resulted in having only

4 to 10 thermistors working simultaneously during any tow. The vertical depth range and density of the measurements were therefore reduced.

4. Analysis

The first step in the analysis was to low-pass filter the time series to eliminate the temperature oscillations caused by pitch and heave of the ship. This was done by computing sequential, nonoverlapping averages, each 30 s long. An example of the filtered series is shown in Fig. 9. Isotherm depths, usually at 0.5°C intervals, were then computed by linear interpolation between the temperature records. Separate series of isotherm depths were generated for each tow leg of constant direction. Records of isotherm depth often could not be computed for an entire leg because of the limited depth range of the thermistors and the large amplitude of the internal waves. Records which were more than 80% complete were completed by extrapolation from adjacent isotherms. This procedure is justified by the high coherence between adjacent isotherms for scales of 1 km and larger. The resulting records varied in length from 50 to 500 points, each point representing an average over 30 s. Isotherms computed from the data in Fig. 9 are shown in Fig. 10.

The records of isotherm depth were spectrally analyzed by the use of standard techniques. The Fourier coefficients were computed directly rather than by use of a Fast Fourier Transform (FFT) algorithm. This was done because the number of points in a record was seldom near a power of two as required for use of the FFT and to avoid discarding data or introducing errors by extending the records with zeros. Various windowing, detrending and prewhitening methods were tried to determine their effects on the spectal estimates. Frankignoul (1974) found that the end point jump was an important source of error in spectra of internal waves computed from short records. On the basis of Frankignoul's recommendation

and our own tests, we prewhitenend each series by taking the first forward difference, computed spectra, and then recolored the spectrum by dividing by the transform of the differencing scheme (Bath, 1974). We did not detrend or apply a window to the series. The spectra were smoothed by averaging in non-overlapping wavenumber bands, equally spaced on a logarithmic scale. Frequency spectra were converted to wavenumber spectra by the use of Taylor's hypothesis taking the mean tow speed during a leg as the relevant velocity.

5. Results

Spectra from 20 August of the depth of the 10.0 and 11.5°C isotherms together with the spectrum of depth from a pressure sensor on the chain are shown in Fig. 11. The spectral level of the depth of the chain is well below the other spectra showing that spectra of isotherm depth are not signficiantly contaminated by vertical motion of the chain. The spectra of isotherm depth show features typical of spectra from other tows. The energy density decreases with increasing wavenumber except for a shoulder at a wavelength of about 1 km. The energy density is approximately proportional to k^{-3}, where k is wavenumber, for wavenumbers greater than those at the shoulder. The shoulder does not occur in the spectra from all of the tows, but there is nearly always a change in slope at a wavelength of about 1 km. The slopes of the spectra in Fig. 11 together with those from other sources are summarized in Table 3. The spectral energy of the depth of the 10.0°C isotherm is nearly an order of magnitude greater than the spectrum of the 11.5°C isotherm at all wavenumbers. The 11.5°C isotherm was in a region of weak vertical stratification lying above a layer of stronger stratification as can be seen in Fig. 10.

Spectra of the depth of the lowest and highest isotherm from individiaul tows were averaged to obtain the spectra shown in Fig. 12. The spectra show features similar to those in Fig. 11, althrough the shoulder occurring at a wavelength of 1 km is not as pronounced. This might be epxected since the effects of doppler-shifting and sampling packets of waves at various angles to their crests would tend to smear the averaged spectrum. The spectral energy of the vertical displacements

of the highest isotherms is lower than the corresponding energy of the lowest isotherms. The difference is in the same sense as for the tow on 20 August (Fig. 11), although not nearly as large and perhaps not significant.

The averaged spectra in Fig. 13 are scaled by the buoyancy frequency ratio, N/N_0, where N is the local value and N_0 is taken to be 3 cph. This scaling does not collapse the averaged spectra of the depth of the lowest and highest isotherms because, as discussed above, the lowest isotherm displacements tend to be more energetic and in layers having higher values of N than the uppermost isotherms (Fig. 8). Nevertheless, the two averaged spectra in Fig. 13 are in good agreement with the Garrett-Munk model (1972, 1975) despite the rapid vertical variation of the local value of N. There is, of course, no break in slope in the model as is suggested by the observations.

The averaged spectra are compared with towed spectra from other sources in Fig. 14. There is fair agreement between the different sets of observations, with spectral levels within a factor of five. The spectral shapes are also similar with evidence of a break in slope at a wavelength of about 1 km. The slopes of the various spectra and slope-breaks are tabulated in Table 3. Spectra reported by Nelson and Milder (1979) from the upper thermocline also show evidence of a shoulder at a wavelength of about 1 km. Pinkel (1975) reported observations from FLIP in the upper 200 m in which he too found evidence of a should in the horizontal wavenumber spectrum.

The spectra were examined for evidence of anisotropy by averaging spectra from different tow directions. Only the lowest isotherm from

each leg was used. The results, plotted in Fig. 15, show no evidence of significant anisotropy. This is in agreement with most other observations in the open ocean and with the assumption of Garrett and Munk (1972, 1975). Nelson and Milder (1979) did, however, find evidence of anisotropy at wavelengths greater than 1 km.

The spectra were also averaged according to the local value of N, as shown in Figure 16. Owing to the correlation between N and depth (Fig. 8), the results are similar to difference between averaged spectra of the depth of the lowest and highest isotherms (Fig. 12). There is evidence that for wavelengths greater than 1 km, higher values of N are associated with higher spectral energies. The usual N-scaling results in a greater spread of the spectral estimates.

It has been suggested (e.g. Käse and Clarke, 1978; Wunsch, 1975) that internal waves may be generated by wind. As a possible though not necessary consequence, one might expect that spectral energy levels would be higher during periods of high winds. The spectra of the depth of the uppermost isotherm from each tow were therefore grouped and averaged according to the wind speed range during and preceding each tow. The results are shown in Fig. 17. Spectra from tows during the lowest wind speeds (3-5 m/s) are on average lower than from tows during higher wind speeds. The difference is not significant at the 95% level and may have been caused by other factors. The spectral levels from the two highest wind speed ranges are remarkably similar.

Coherence spectra between isotherms separated in the vertical were computed from pairs of isotherms from each leg. Pairs of isotherms which were computed from the same pair of thermistors more than 23% of the

time were excluded from the analysis so as to greatly reduce the possibility of introducing an artificially high coherence. The results from the tow on 20 August are shown in Fig. 18. All of the spectra are qualitatively similar, having high values of coherence at the longest wavelengths, decreasing with increasing wavenumber and then increasing again to a peak in coherence centered around a wavelength of 1 km. The coherence between the uppermost (11.5°C) isotherm and the remaining isotherms is the lowest. The uppermost isotherm was in a layer of weak stratification overlying a layer of stronger, nearly uniform stratification containing the remaining isotherms (Fig. 10). Phase spectra between pairs of isotherms are insignificantly different from zero.

Coherence spectra from individual tows were grouped and averaged according to the mean vertical separation between the isotherms. The results plotted in Fig. 19 are qualitatively similar in shape to Fig. 18. With the exception of isotherm pairs separated by 1 to 3 m, all of the spectra show a peak centered at a wavelength of 1 km. For separations between 1 and 3 m, coherence is high throughout the low wavenumber band of the spectrum, dropping only beyond a wavelength of about 0.5 km.

Katz and Briscoe (1979) also found evidence at 350 m depth of a peak in towed vertical coherence between 0.7 and 2 cpkm. Towed vertical coherence from a depth of 750 m showed no evidence of a peak. The Garrett-Munk model predicts coherence decreasing with increasing wavenumber in agreement with Katz and Briscoe's (1979) observations at 750 m depth. Nelson and Milder (1979) found higher values of towed vertical coherence in the upper thermocline than predicted by the Garrett-Munk model.

The peak in coherence at a wavelength of 1 km suggests that the internal wave spectrum at this wavelength is dominated by the low modes. If higher modes are present, they would result in destructive interference, thereby decreasing the coherence. This result is consistent with the analysis of fluctuations of the vertical velocity of internal waves by Dillon and Caldwell (1979) in the upper 200 m during MILE. They found that the fluctuations in a frequency-band centered at 3 cph were dominated by the first and second modes. The frequency spectrum of isotherm displacement during MILE has a shoulder at about 3 cph and then falls off rapidly with increasing frequency (Dillon and Caldwell, 1979). The frequency band centered at 3 cph corresponds to a wavenumber band at about 1 cpkm as deduced from the dispersion relation. Pinkel (1975) also concluded on the basis of observations in the upper 400 m that the lowest modes were dominant in the frequency band from 3 to 6 cph.

We therefore tentatively interpret our observations of a spectral shoulder and towed vertical coherence peak at a wavelength of 1 km as evidence of the penetration from below of low-mode internal waves having a frequency of about 3 cph.

6. Summary

On the basis of the analysis of the vertical displacement of isotherms interpolated from towed thermistor chain measurements between 20 and 40 m depth we can draw the following conclusions:

1) On average, the spectrum of isotherm displacement decreases with increasing wavenumber proportional to $k^{-3/2}$ out to 1 cpkm. Above 1 cpkm the spectral slope is between -2 and -3.
2) There is often a shoulder in the spectra of isotherm displacement at a wavelength of 1 km. This feature is smeared in the spectra averaged from many tows.
3) There is no evidence of significant horizontal anisotropy in spectra averaged over many tows.
4) Averaged spectra of isotherm displacement appear to be independent of the local buoyancy frequency. Scaling individual spectra by N, as is often done, therefore increases the scatter.
5) The spectra of isotherm displacement does not depend significantly on wind speed for wind speeds below 10 m/s.
6) Despite the rapid vertical variation of N, the spectra of isotherm displacements are in fair agreement with the Garrett-Munk model (1972, 1975) and with spectra reported by other investigators.
7) There is a peak at a wavelength of 1 km in coherence spectra between pairs of isotherms separated in the vertical. The peak is interpreted as evidence that the wavenumber band at 1 cpkm is dominated by the low modes.

Acknowledgments

The design, construction and maintenance of the thermistor chain system was carried out by Rod Mesecar, Frank Evans, James Wagner, Orrie Page and Milton Rowland. Donald Denbo developed software for data acquisition. Stanley Hayes and David Halpern provided CTD and wave height data. Temperature data from 5 m depth was provided by Roland de Szoeke and Peter Niiler. The cooperation of the officers and crew of the NOAA Ship OCEANOGRAPHER, Captain George Poor commanding, is gratefully acknowledged. This research was supported by the Office of Naval Research through contract N00014-76-C-0067.

REFERENCES

Bath, M., 1974: Spectral analysis in geophysics. Amsterdam, Elsevier, 563 p.

Bell, T. H., 1976: The structure of internal wave spectra as determined from towed thermistor chain measurements. J. Geophys. Res., 81, 3709-3714.

Briscoe, M. G., 1972: A note on internal gravity wave spectra. J. Geophys. Res., 77, 3278-3280.

Caldwell, D. R., T. M. Dillon, J. M. Brubaker, P. A. Newburger, and C. A. Paulson, 1979: Scaling of the cut-off wavenumber of the vertical temperature gradient spectrum. Submitted to J. Geophys. Res.

Dillon, T. M. and D. R. Caldwell, 1978: Catastrophic events in a surface mixed layer. Nature, 276, 601-602.

_____, 1979: High frequency internal waves at Ocean Station P. J. Geophys. Res., (in press).

Frankignoul, C., 1974: A cautionary note on the spectral analysis of short internal wave records. J. Geophys. Res., 79, 3459-3462.

Garrett, C. and W. Munk, 1972: Space-time scales of internal waves. Geophys. Fluid Dyn., 2, 225-264.

_____, 1975: Space-time scales of internal waves: a progress report. J. Geophys. Res., 80, 291-297.

_____, 1979: Internal waves in the ocean. Ann. Rev. Fluid Mech., 11, 339-369.

Käse, R. H. and R. A. Clarke, 1978: High frequency internal waves in the upper thermocline during GATE. Deep-Sea Research, 25, 815-825.

Katz, E. J., 1973: Profile of an isopycnal surface in the main thermocline of the Sargasso Sea. J. Phys. Oceanogr., 3, 448-457.

Katz, E. J. and M. G. Briscoe, 1979: Vertical coherence of the internal wave field from towed sensors. J. Phys. Oceanogr., (in press).

Mesecar, R. and F. Evans, 1977: Distributed instrumentation profiling system. Exposure, 5(3), 1-7.

Mobley, F. F., A. C. Sadilek, C. J. Gundersdorff and D. Speranza, 1976: A new thermistor chain for underwater temperature measurement. Proceedings, Oceans 76 Conference, September 13-15, Washington, D.C.

Nelson, K. W. and D. M. Milder, 1979: Internal wave displacement and vertical coherence spectra from towed thermistor chain measurements in the upper thermocline (to be published).

Pinkel, R., 1975: Upper ocean internal wave observations from Flip. J. Geophys. Res., 80, 3892-3910.

Steinhart, J. S. and S. R. Hart, 1968: Calibration curves for thermistors. Deep-Sea Research, 15, 497-503.

Wunsch, C., 1975: Deep ocean internal waves: what do we really know?. J. Geophys. Res., 80, 339-343.

TABLE 1. Specifications of Towed Chain Measurements

Sensor	Manufacturer	Accuracy	Resolution	Response Time
Thermistor, glass-coated bead, 0.2 mm diameter	Thermometrics Model P 85 B10	± 0.01°C	± 0.001°C	0.12s
Pressure (Depth)	Kulite Model PTQH-360-250	± 0.5 m	± 0.05 m	1s

TABLE 2. Summary of Towed Thermistor Chain Observations

Date	Time Begin (GMT)	Duration (Min)	Tow Speed (m/s)	Track (see Fig. 4)
20 Aug 77	1846	195	1.6	A
24 Aug 77	1654	465	1.6-2.0	B
26 Aug 77	1521	534	2.3-3.0	C
28 Aug 77	1515	718	1.1-3.3	C
30 Aug 77	1736	575	2.5-3.2	C
1 Sep 77	1723	440	2.2-2.3	D
3 Sep 77	1811	520	2.3-3.1	C
5 Sep 77	1817	487	2.6	E
8 Sep 77	1814	173	2.8	F

TABLE 3. Spectral Slopes

SOURCE	SLOPE		SLOPE BREAK
	Low k	High k	(c/km)
Run 1, 10°	-1.3	-3.0	1.0
Run 1, 11.5°	-1.5	-3.6	1.0
MILE, Ensemble	-1.6	-2.2	0.8
Katz (1973)	-1.5	-2.3	1.8
Nelson and Milder (1979)	-1.5	-2.5	1.3

FIGURE LEGENDS

1. Schematic diagram of the thermistor chain under tow.
2. A diagram showing the installation of a thermistor and bridge/amplifier in a modified section of fairing. The dimensions of the fairing are 15.5 x 2 x 10 cm. The nose-pieces fit over a steel cable and overlap with adjacent tail sections.
3. The MILE array. Station P (50N, 145W) is at northern apex. Moorings are at M1, M2, and M3. The thermistor chain was towed by the NOAA ship OCEANOGRAPHER, usually around the 20 km square.
4. Idealized thermistor chain tow tracks. Clockwise tows were made about the squares, generally beginning near the southwest corner. Tow A was made to the northwest, F to the southwest. See Table 2 for time and towing speed.
5. Near-surface observations during the MILE. The temperatures at 5 m depth are hourly averages from the M1 mooring. The wind speeds are hourly averages from the OCEANOGRAPHER. Wave heights are from the wave-rider at M3.
6. Time series of thermistor outputs recorded on 3 September 1977. The data were recorded at 8 samples/s and plotted over 0.5 s. The ship was proceeding southward at 3.0 m/s.
7. Buoyancy frequency vs. depth averaged over the entire experiment.
8. Buoyancy frequency profiles determined from the thermistor chain data averaged over entire tows. Numbers on the plot refer to the date of tow, two digits referring to August 1977 and one digit to September.

9. Low pass filtered temperature time series of the tow on 20 August 1977. The ship was traveling to the northeast at 1.6 m/s.
10. Isotherm depths, 20 August 1977, computed by linear interpolation to the data in Fig. 9.
11. Spectra of the depth of the 10.0° and 11.5° isotherms and the spectrum of depth from a pressure sensor on the chain. The tow occurred on 20 August. Average depths were 37.2, 27.3, and 33.8 m, for the isotherms and pressure sensor respectively. Symbols are: +, 10.0°C isotherm; X, 11.5°C isotherm; and □, pressure. Vertical bars represent the 95% confidence intervals.
12. Ensemble-averaged spectra of the depth of the lowest (+) and highest isotherms (X) for the entire experiment. Averaging was performed without regard to actual isotherm values or depths. Vertical bars represent the 95% confidence intervals.
13. Comparison of ensemble-averaged N-scaled spectra of the depth of the lowest and highest isotherms and the Garrett-Munk (1972, 1975) models. Local values of N were derived from averaged thermistor data for each time series. N_0 is 3 cph.
14. Comparison of N-scaled spectra of isotherm depth from several sources.
15. Ensemble-averaged spectra of isotherm depth from tows in various directions. Only the lowest isotherm from each tow was used. Symbols are: X, north; +, east; □, south; and ◇, west. Vertical bars represent the 95% confidence intervals.
16. Ensemble-averaged spectra of isotherm depth grouped according to the local value of N. Symbols are: X, $N < 5$; +, $5 < N < 10$; □, $10 < N < 15$; ◇, $N > 15$ (all units in cph). Vertical bars represent 95% confidence limits.

17. Ensemble-averaged spectra of the depth of the highest isotherms for tows grouped according to average wind speed. Symbols are: X, 8-10 m/s; +, 5-7 m/s; and □, 3-5 m/s Vertical bars represent 95% confidence limits.

18. Coherence spectra between isotherms from the tow on 20 August. The solid line is the 95% significance level.

19. Ensemble-averaged coherence spectra between isotherms having various mean vertical separations, regardless of absolute depth. The solid line is the 95% signficance level.

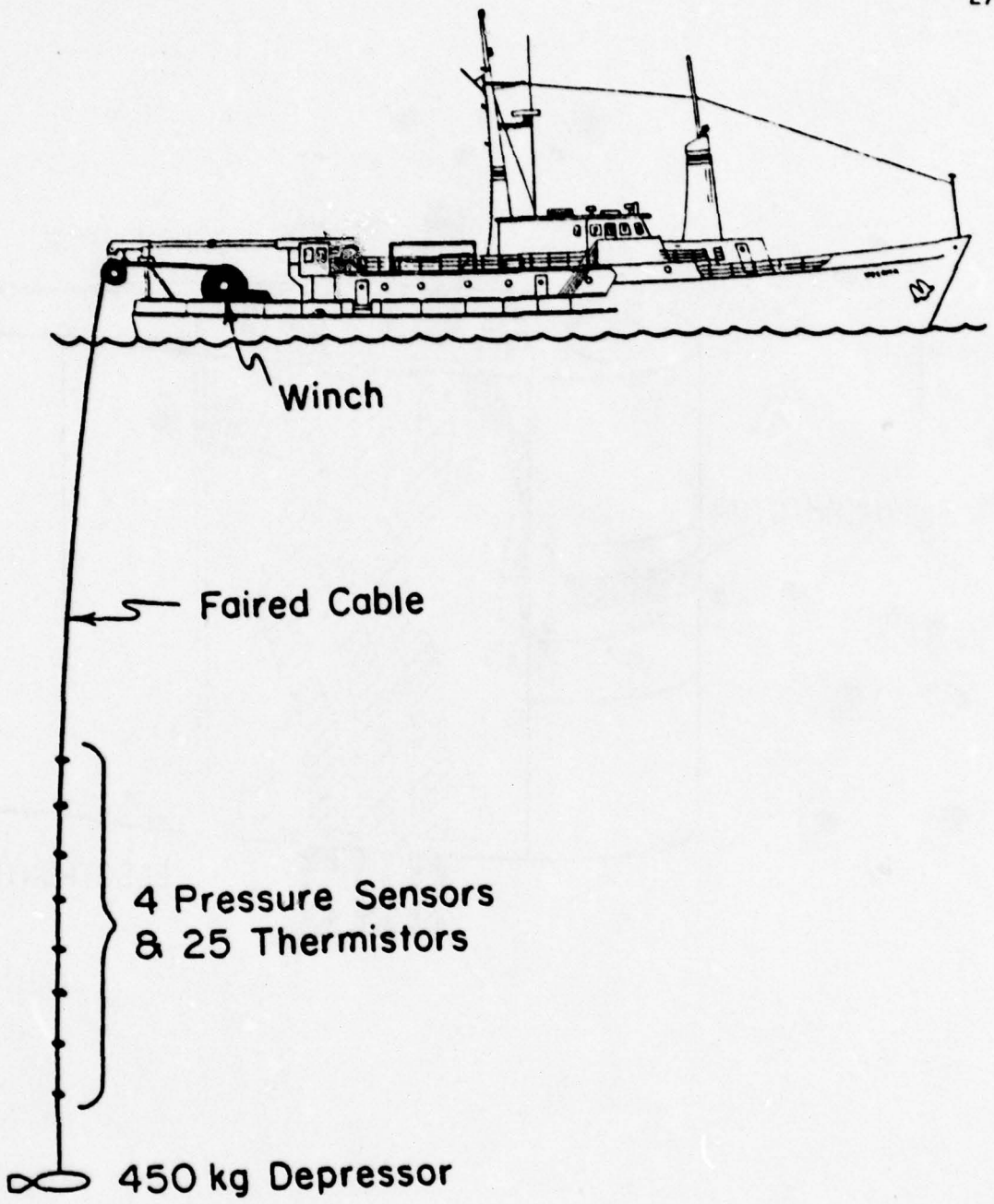
Winch
Faired Cable
4 Pressure Sensors
& 25 Thermistors
450 kg Depressor

Figure 1.

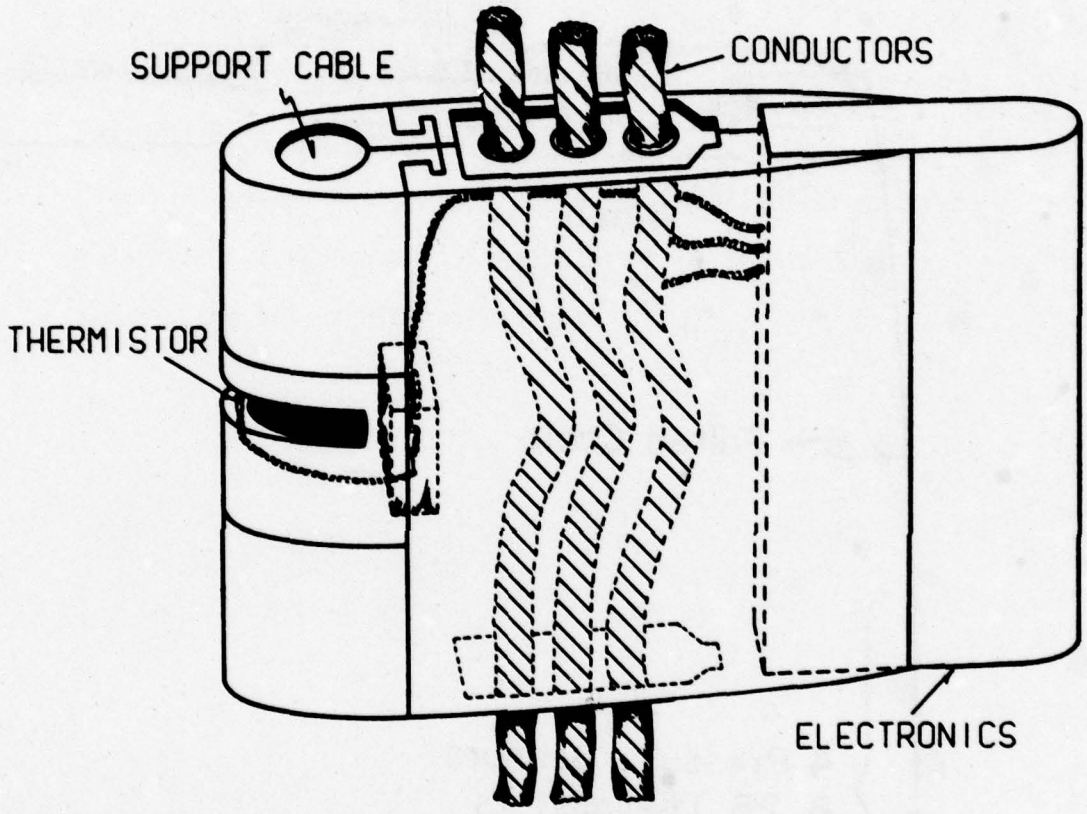

Figure 2.

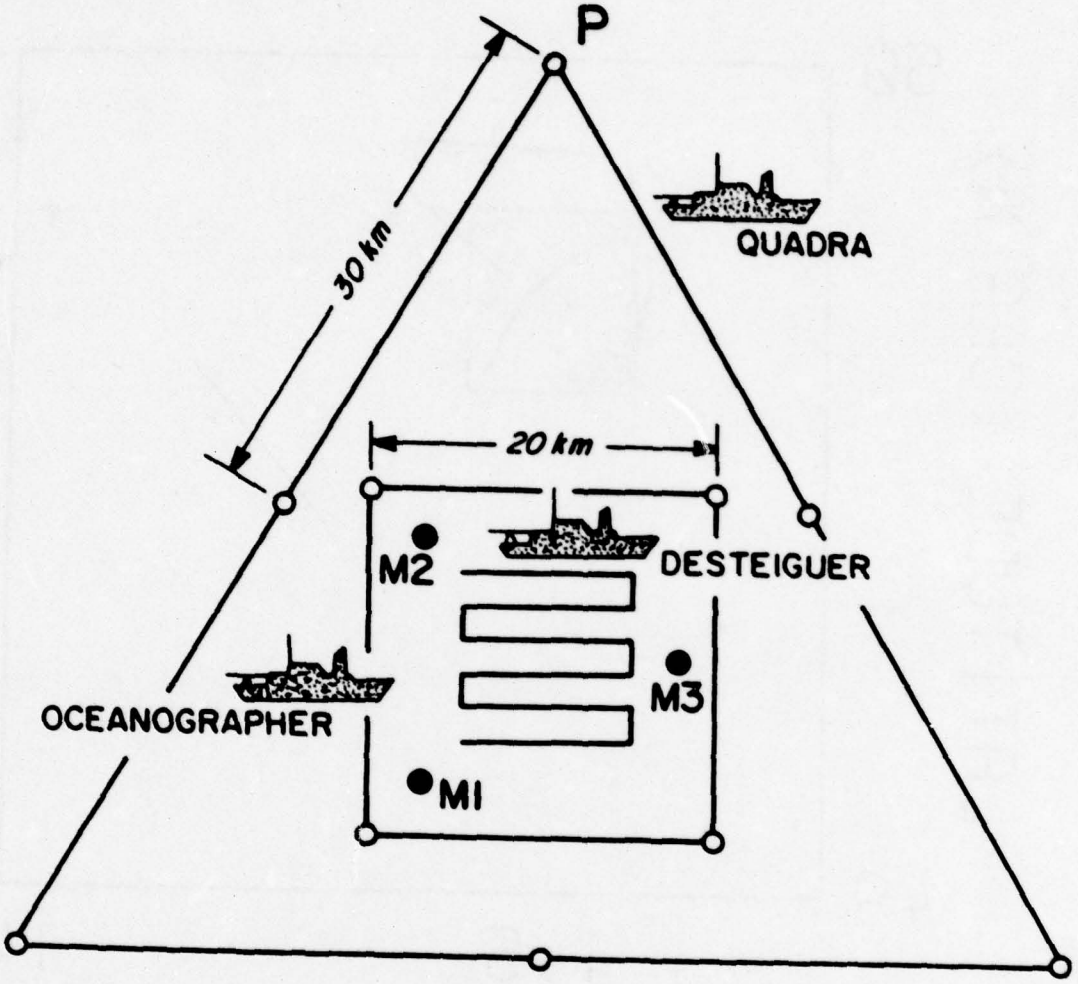

Figure 3.

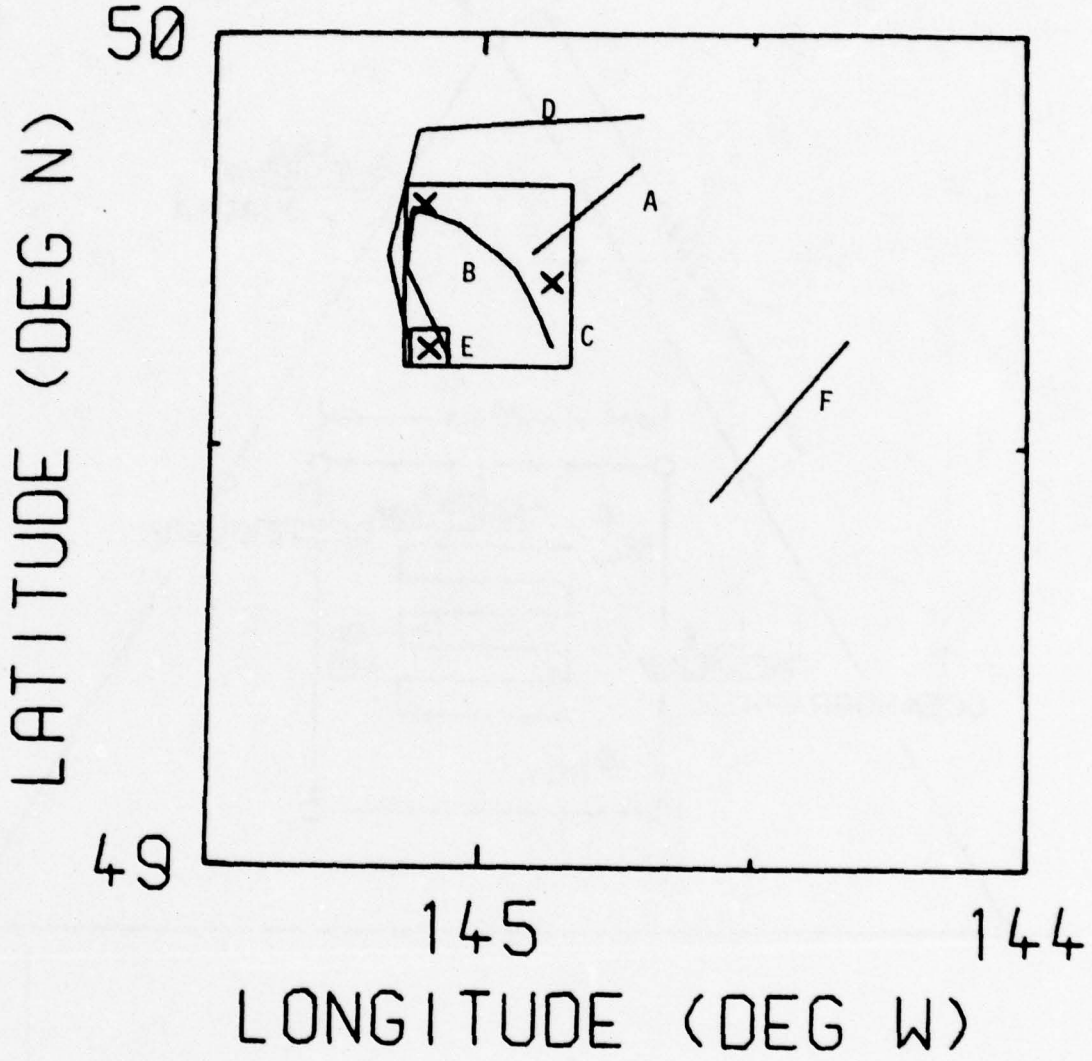

Figure 4.

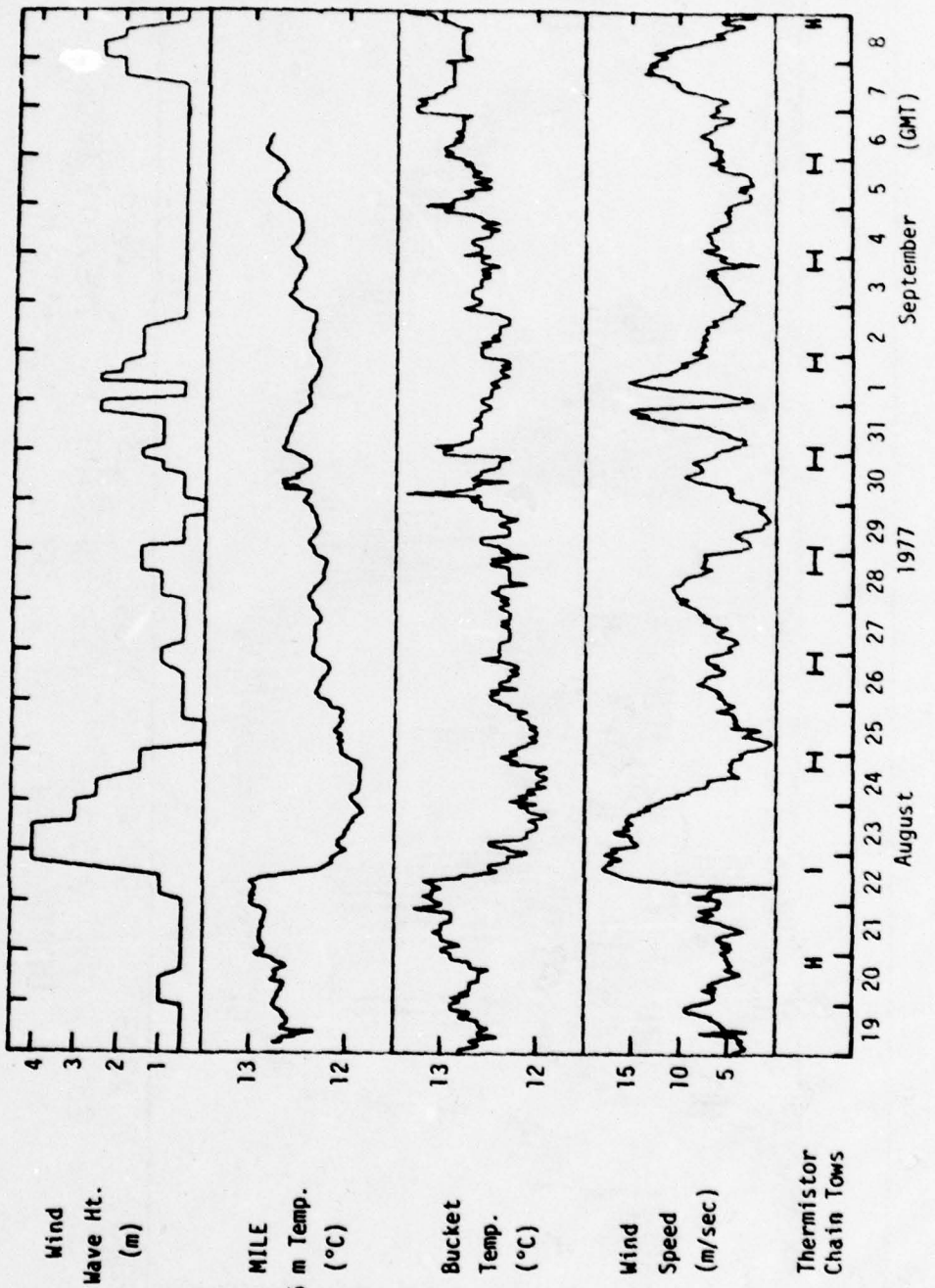
Wind
Wave Ht.
(m)
4
3
2
1
MILE
5 m Temp.
(°C)
13
12
Bucket
Temp.
(°C)
13
12
Wind
Speed
(m/sec)
15
10
5
Thermistor
Chain Tows
19 20 21 22 23 24 25 26 27 28 29 30 31 1 2 3 4 5 6 7 8
August
1977
September
(GMT)

Figure 5.

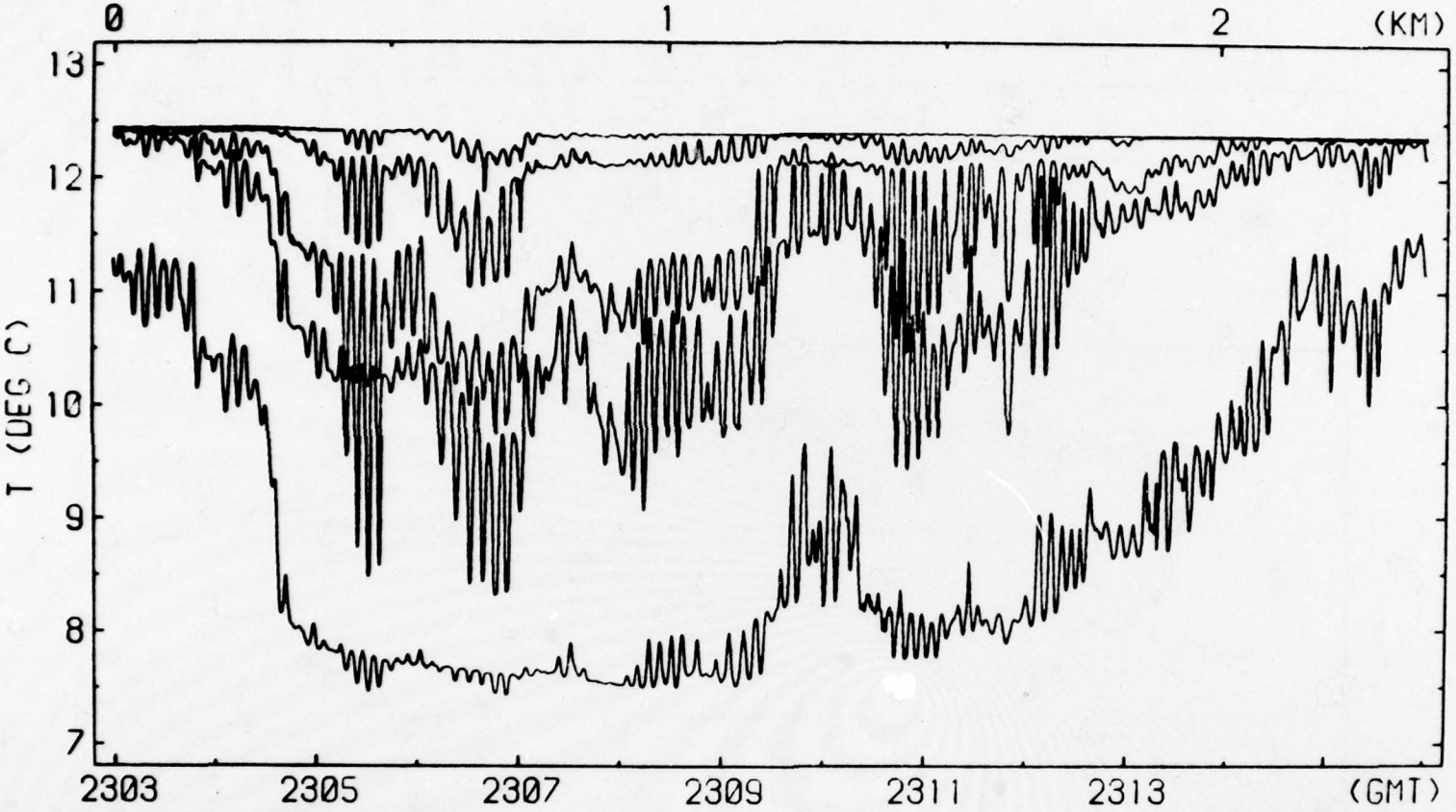
0
1
2
(KM)
13
12
11
10
9
8
7
T (DEG C)
2303
2305
2307
2309
2311
2313
(GMT)
03 SEP 77 0 5 SEC TEMPERATURE AVE VS TIME/DISTANCE
DEPTH = 29 1, 31 2, 33 3, 34 4, 37 5 M

Figure 6.

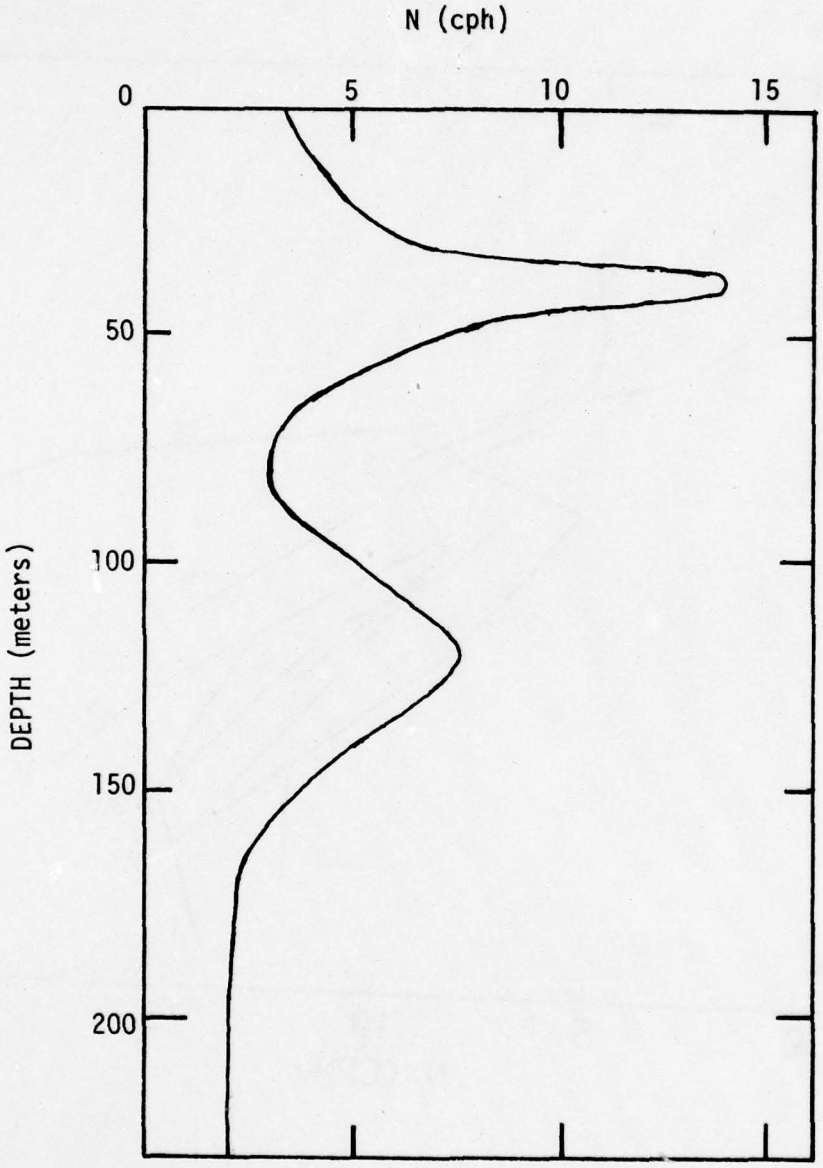

Figure 7.

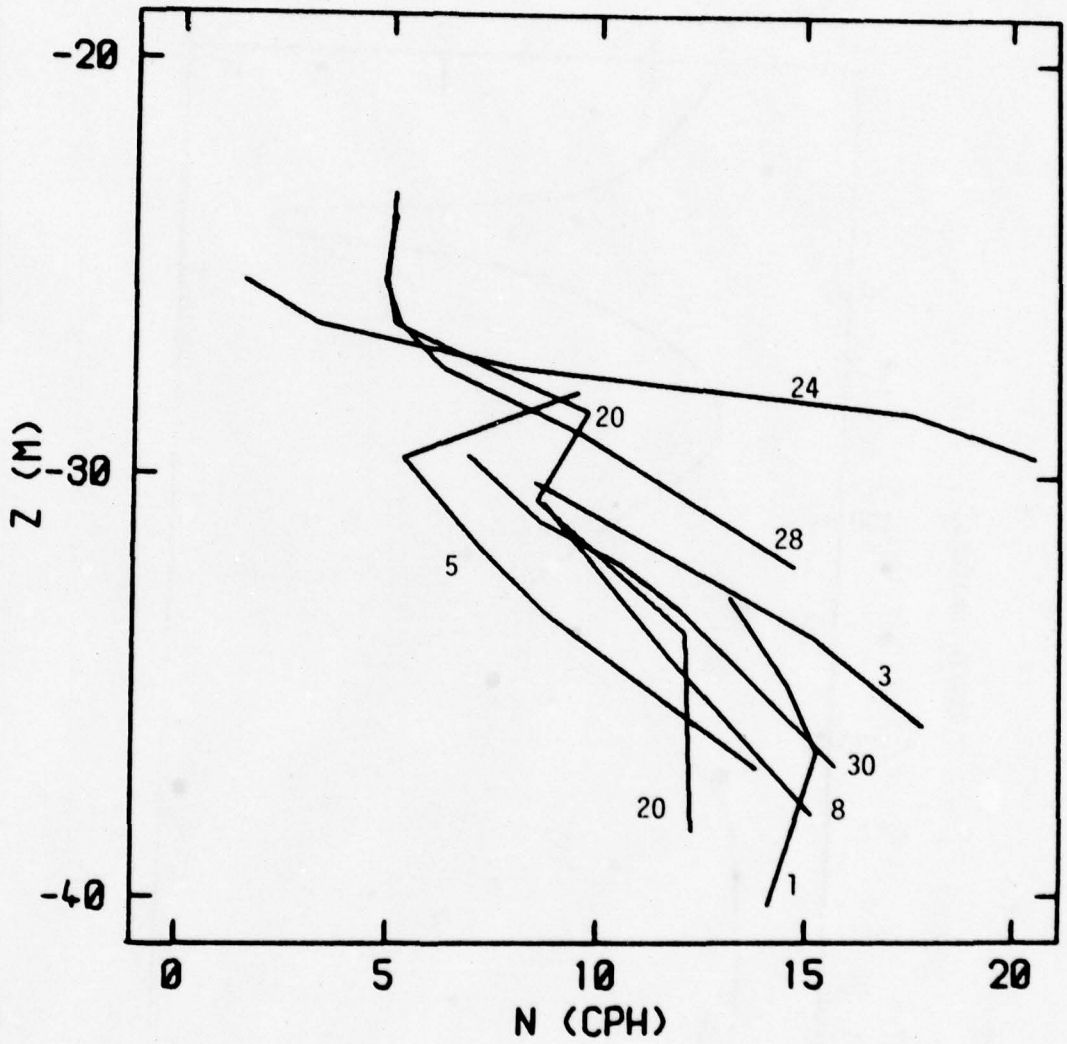

Figure 8.

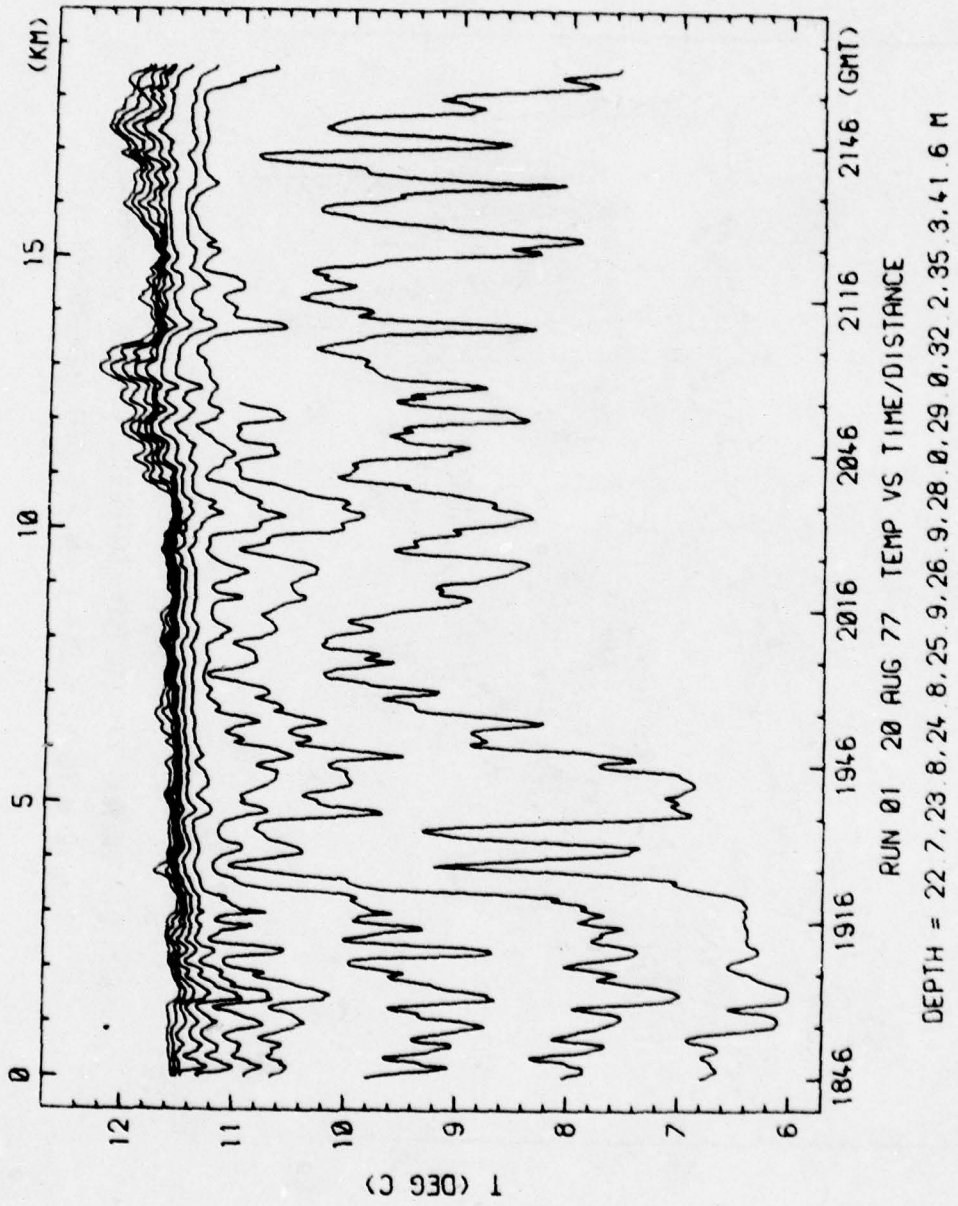
T (DEG C)
12
11
10
9
8
7
6
0
5
10
15
(KM)
1846
1916
1946
2016
2046
2116
2146 (GMT)
RUN 01 20 AUG 77 TEMP VS TIME/DISTANCE
DEPTH = 22.7,23.8,24.8,25.9,26.9,28.0,29.0,32 2.35 3.41.6 M

Figure 9.

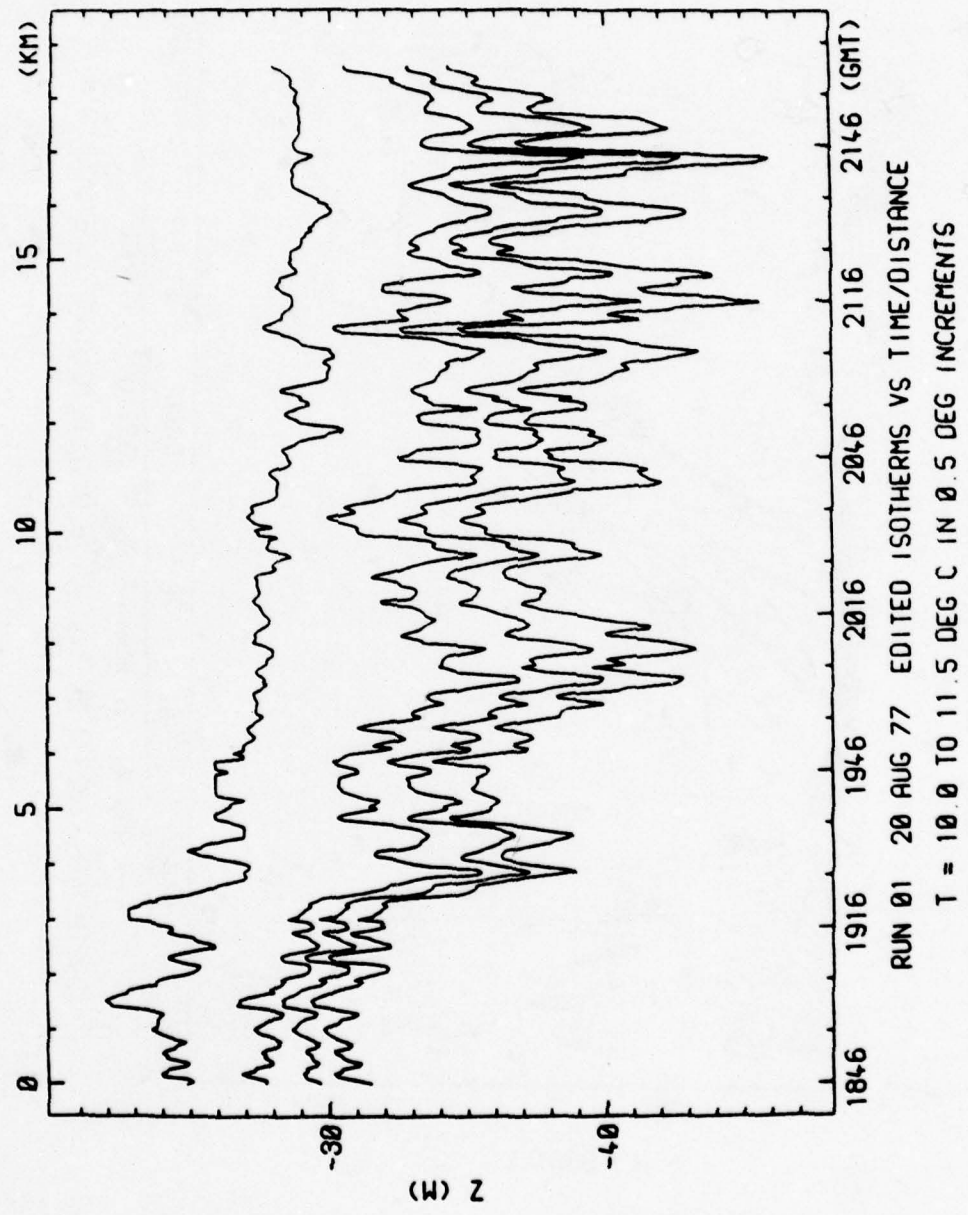
(KM)
0
5
10
15
1846
1916
1946
2016
2046
2116
2146 (GMT)
-30
-40
Z (M)
RUN 01 20 AUG 77 EDITED ISOTHERMS VS TIME/DISTANCE
T = 10 0 TO 11.5 DEG C IN 0.5 DEG INCREMENTS

Figure 10.

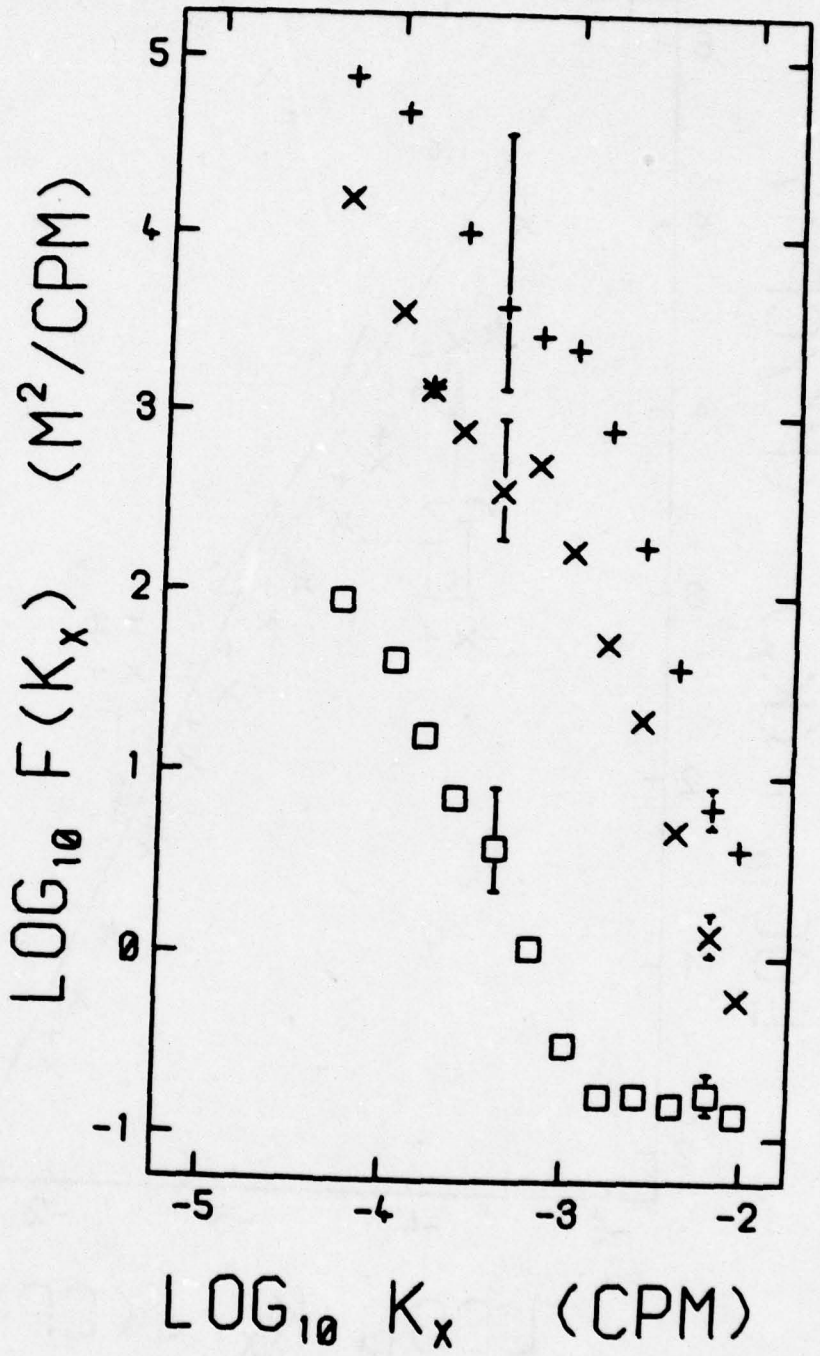

Figure 11.

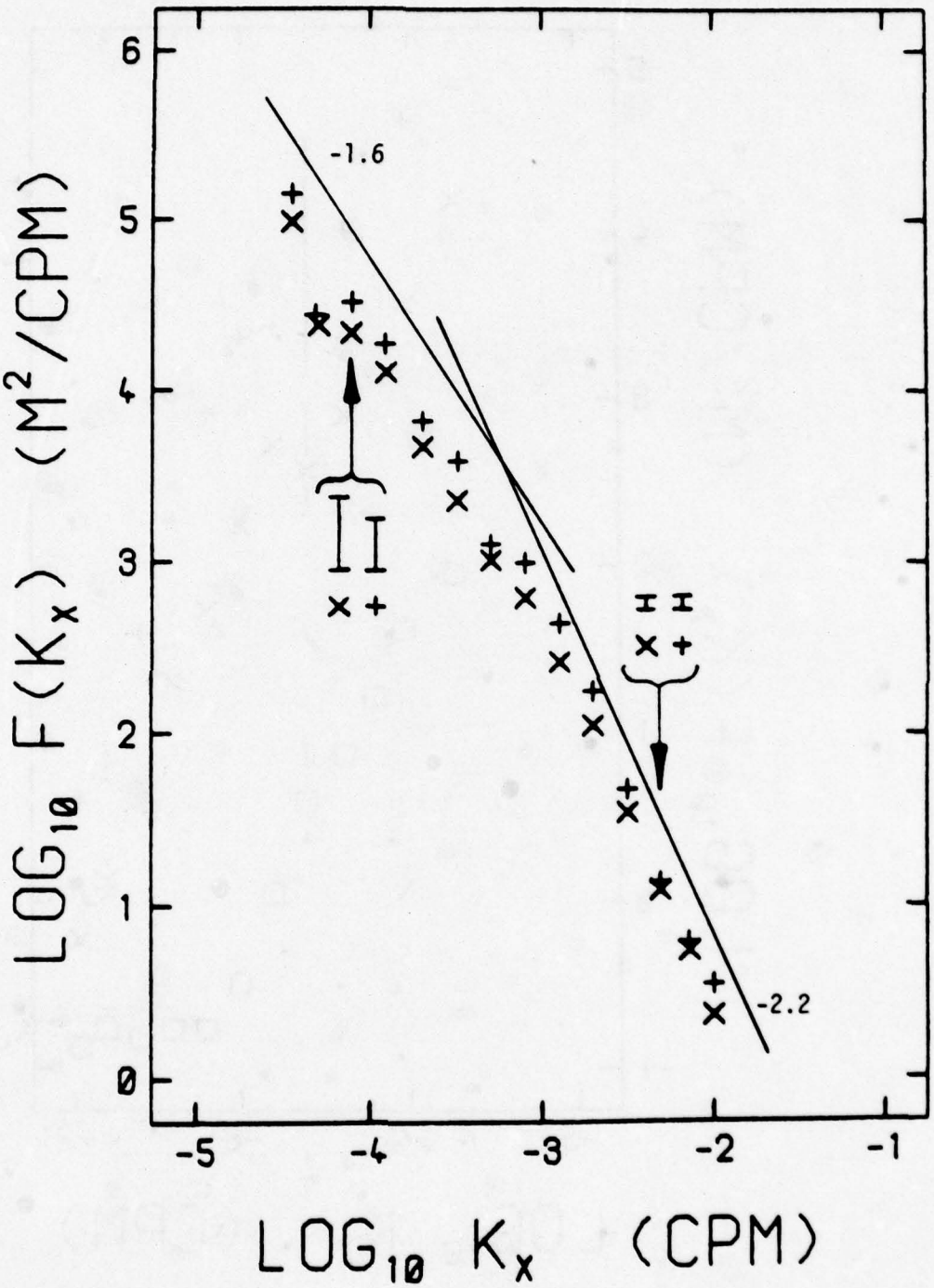

Figure 12.

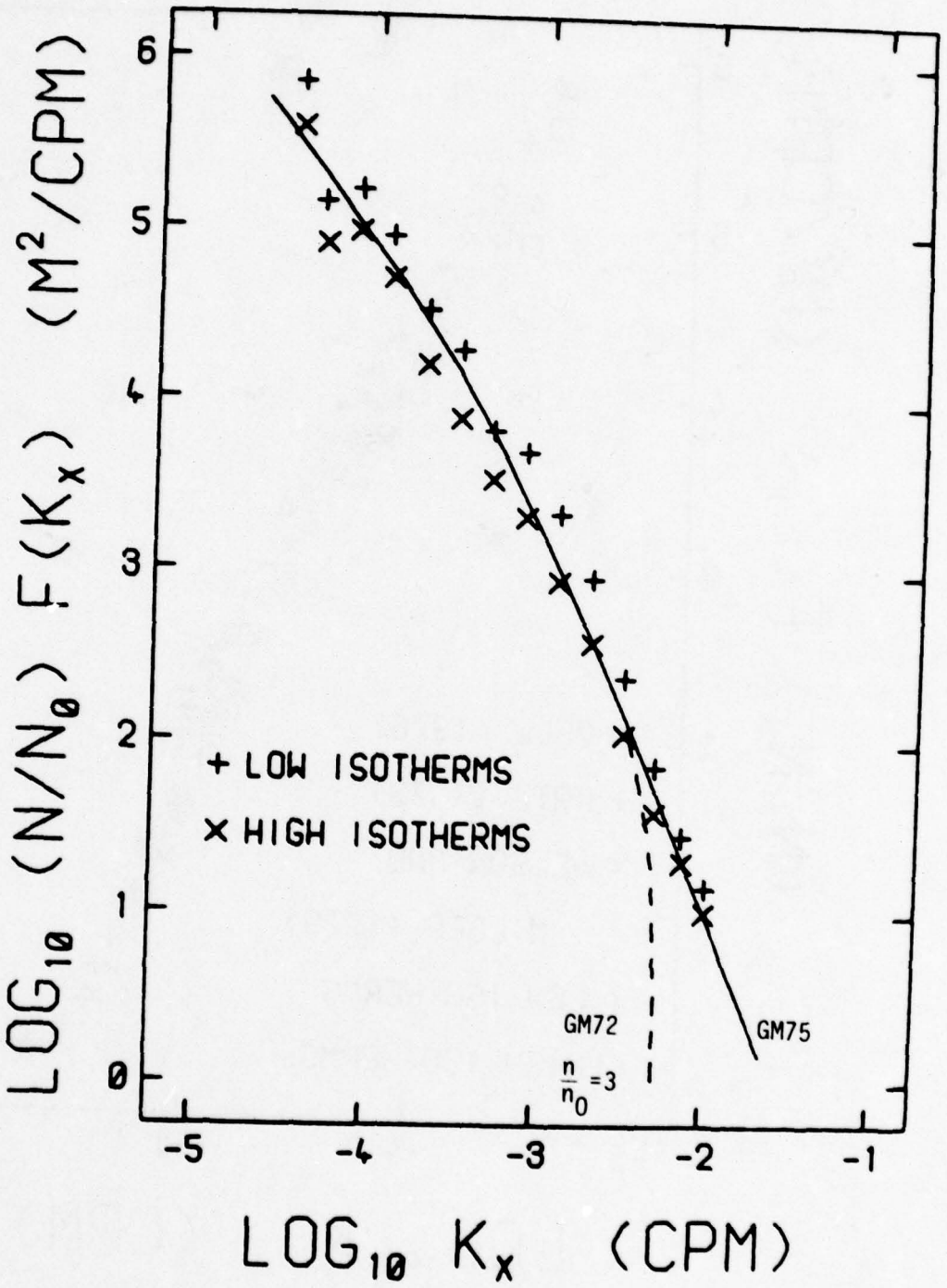
LOG10 (N/N0) F(Kx) (M2/CPM)
LOG10 Kx (CPM)
+ LOW ISOTHERMS
× HIGH ISOTHERMS
GM72
n/n0 =3
GM75
6
5
4
3
2
1
0
-5
-4
-3
-2
-1

Figure 13.

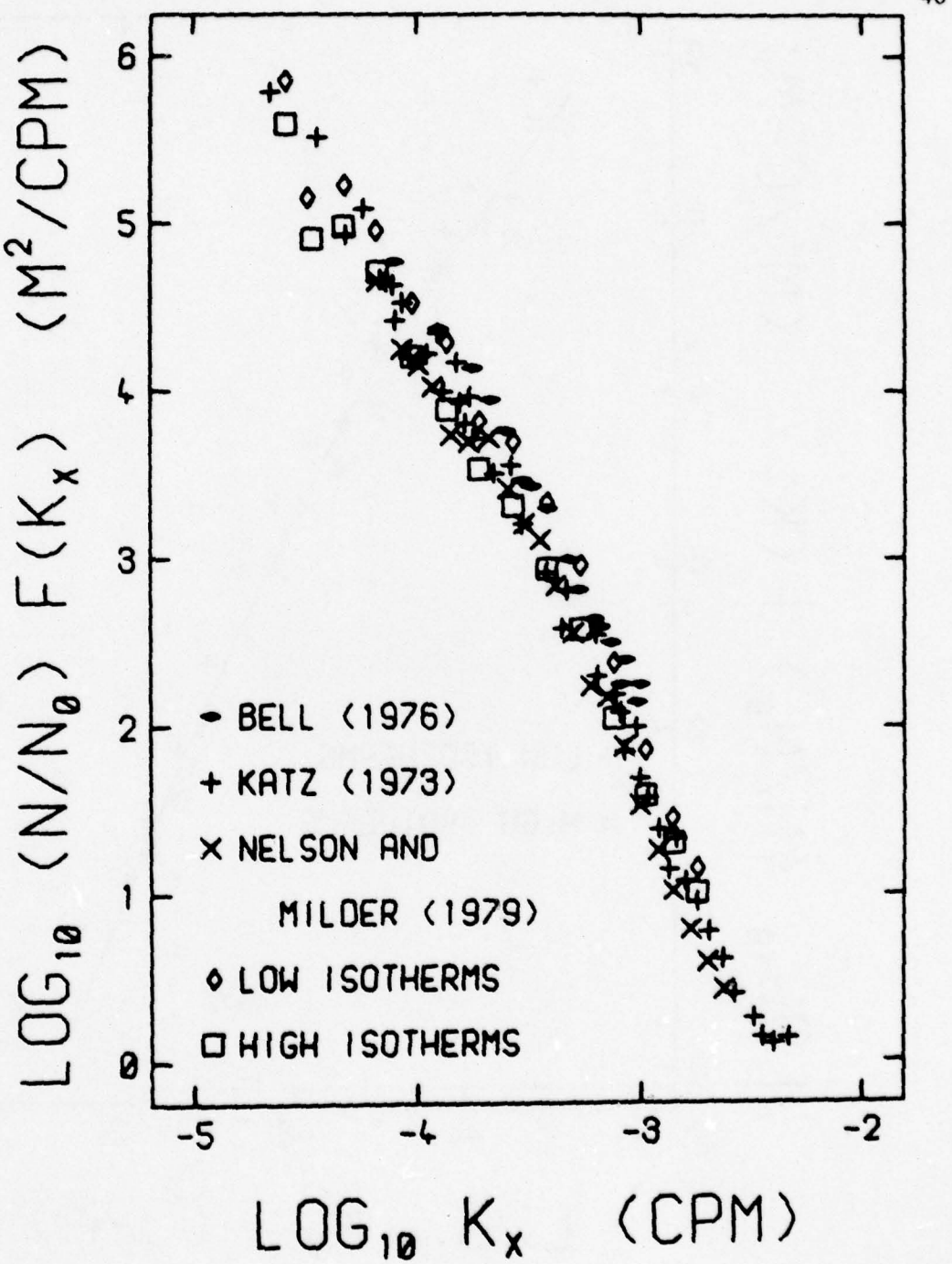
LOG10 (N/N0) F(Kx) (M2/CPM)
LOG10 Kx (CPM)
6
5
4
3
2
1
0
-5
-4
-3
-2
BELL (1976)
KATZ (1973)
NELSON AND MILDER (1979)
LOW ISOTHERMS
HIGH ISOTHERMS

Figure 14.

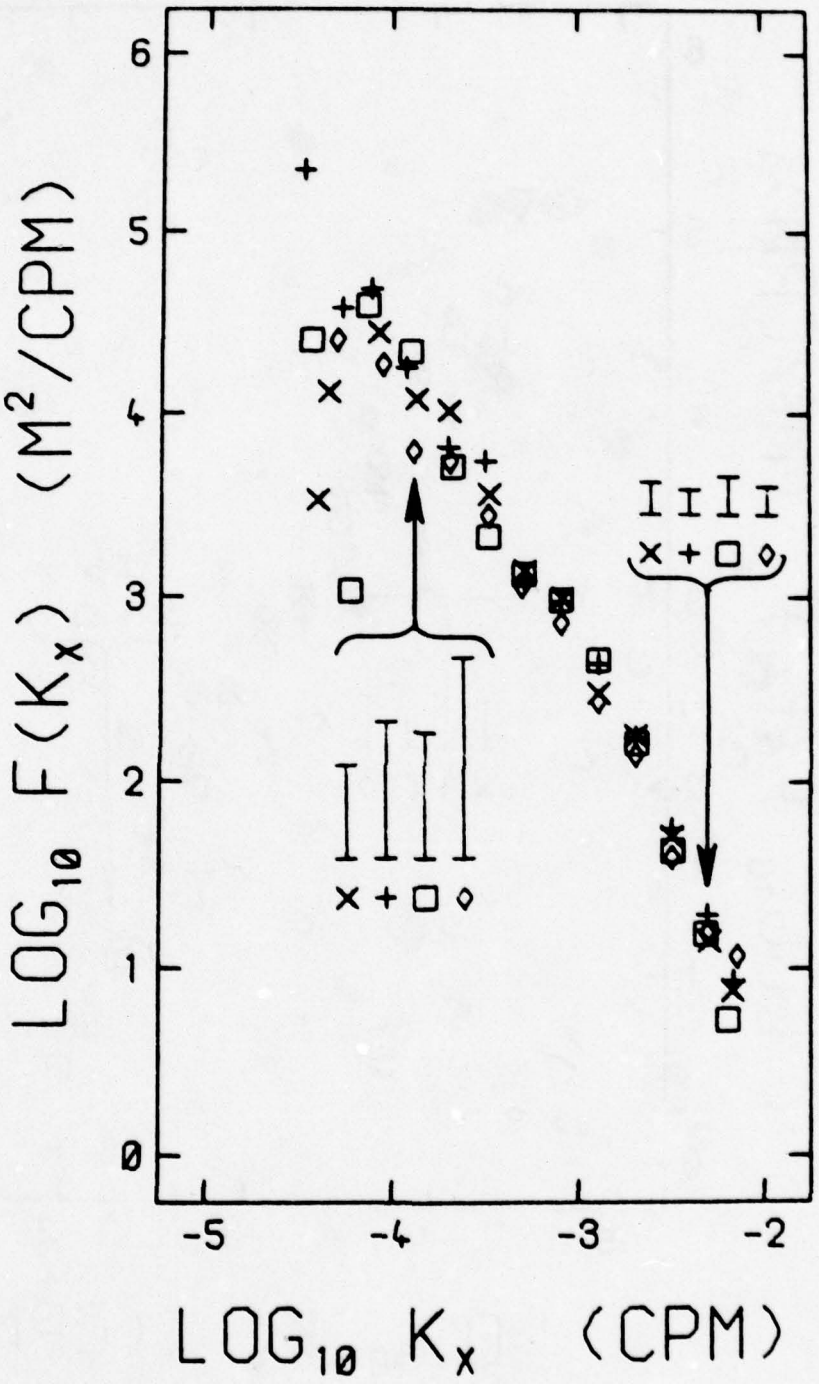

Figure 15.

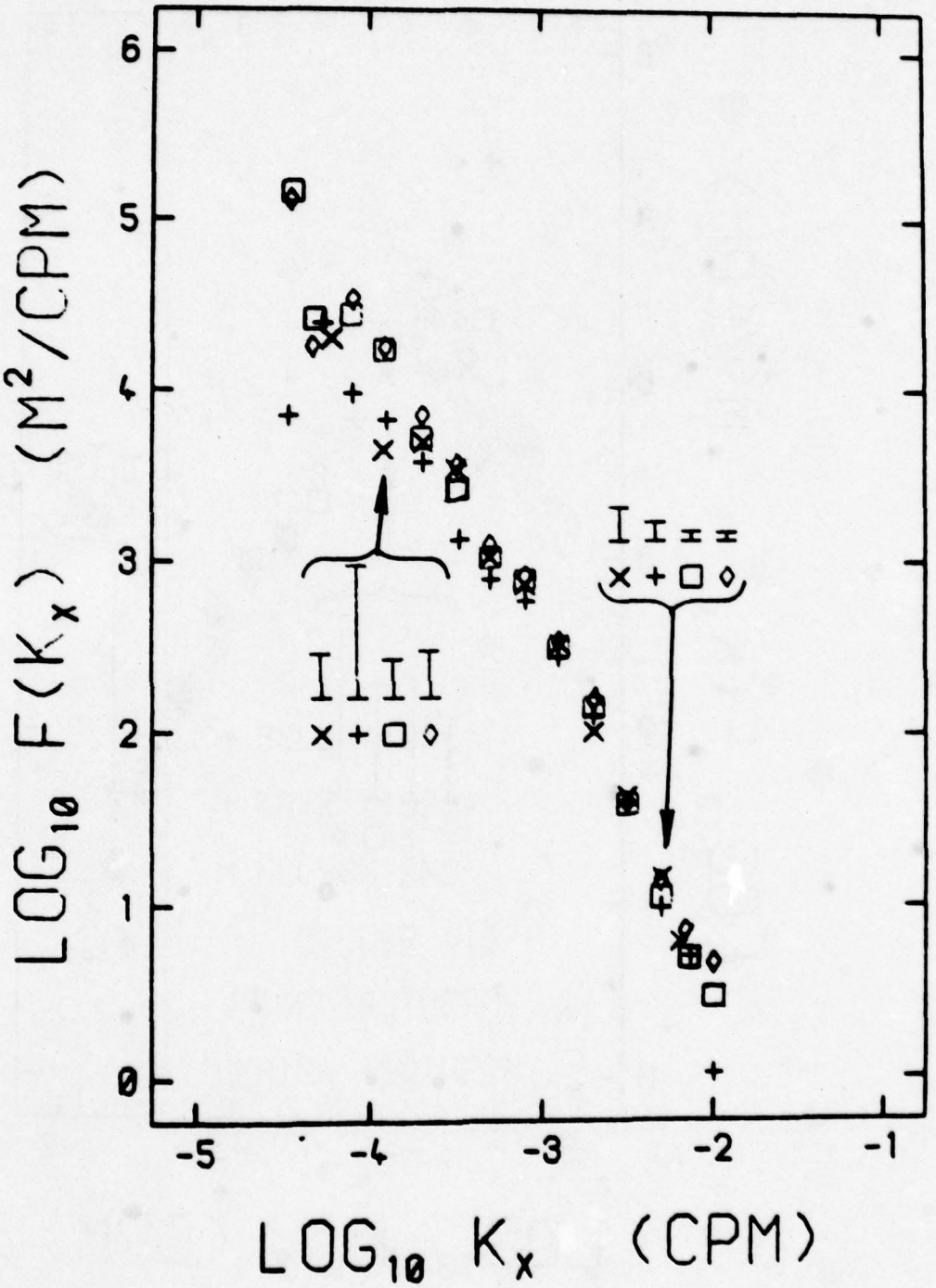

Figure 16.

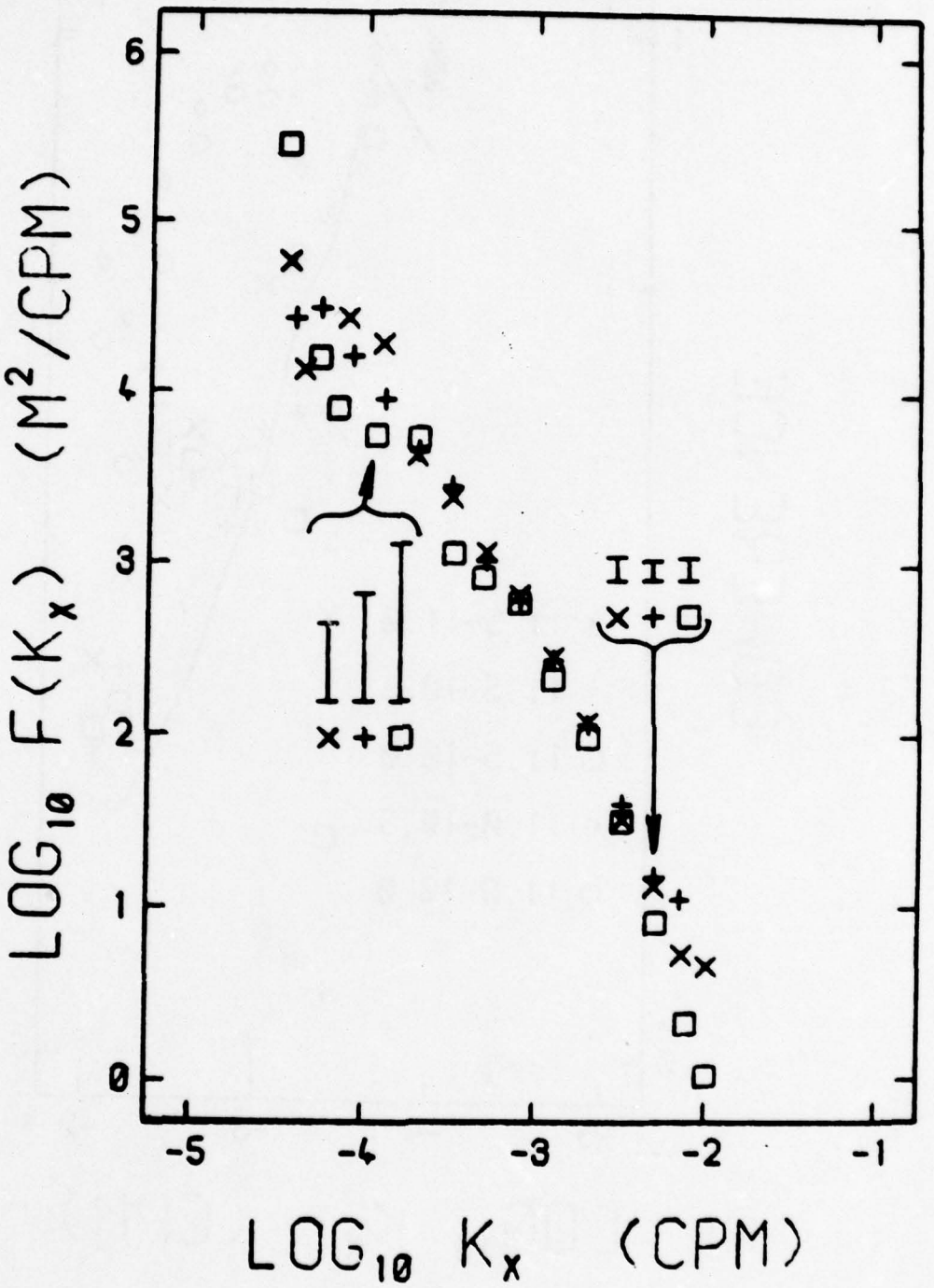

Figure 17.

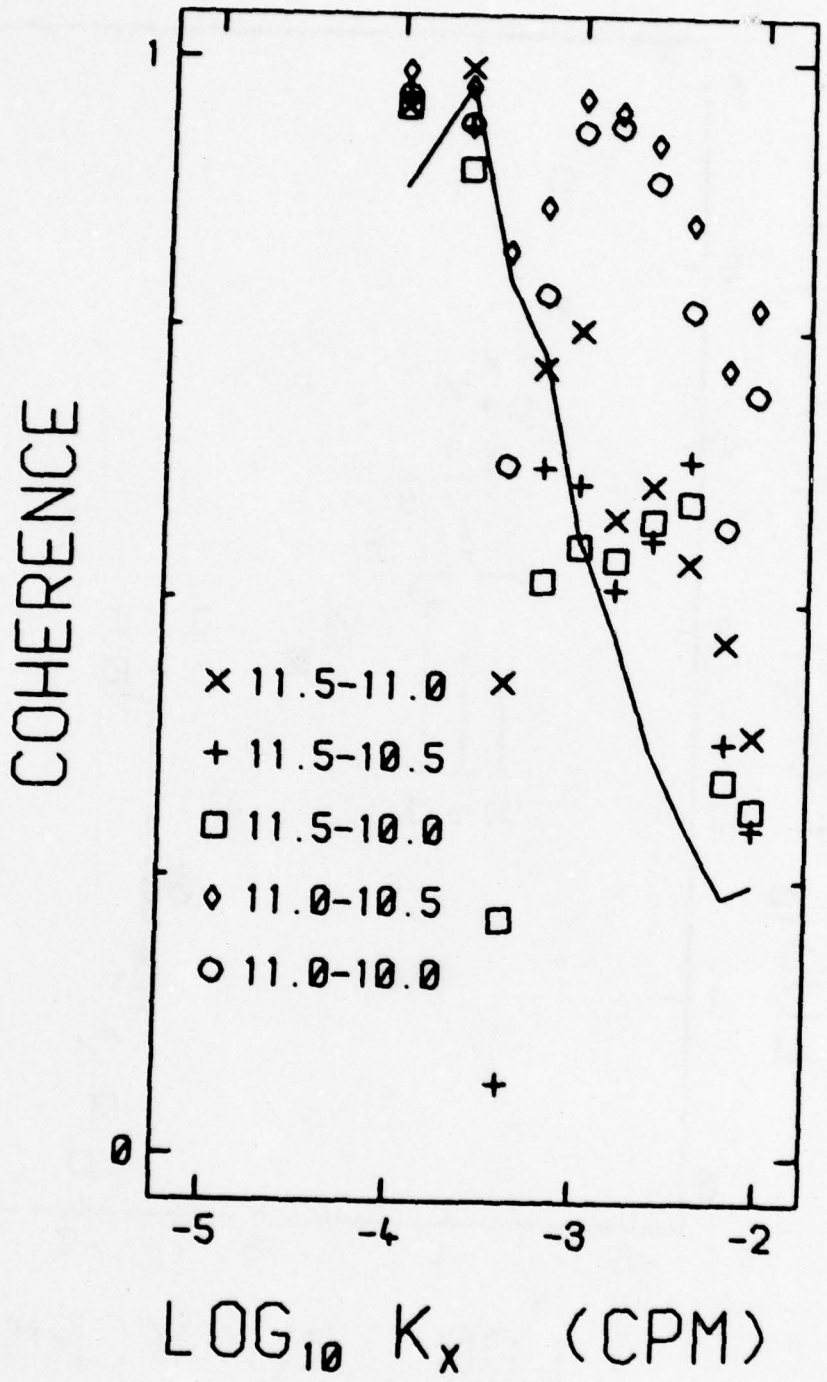
COHERENCE
1
0
-5
-4
-3
-2
LOG10 Kx (CPM)
× 11.5-11.0
+ 11.5-10.5
□ 11.5-10.0
◇ 11.0-10.5
○ 11.0-10.0

Figure 18.

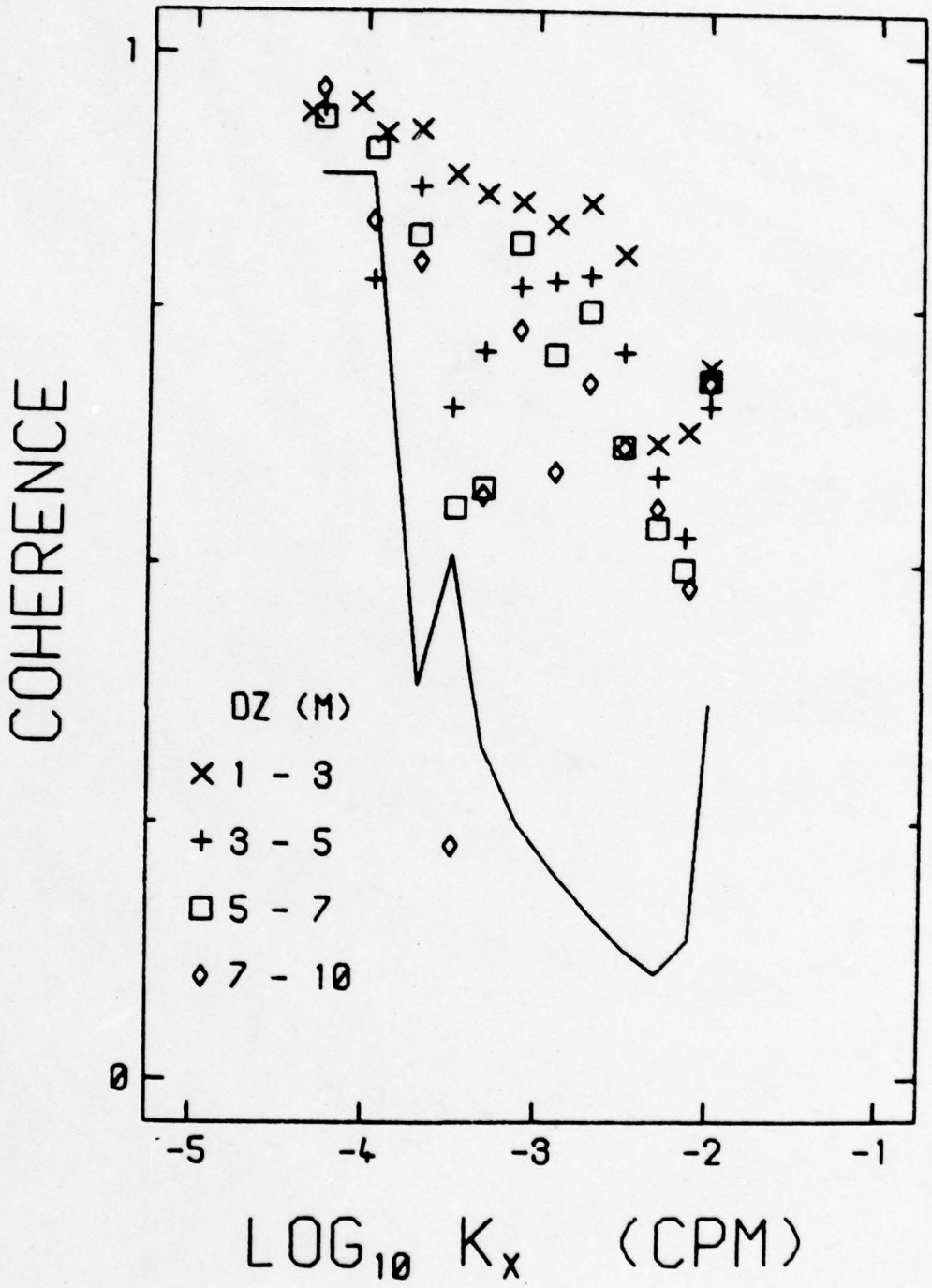

Figure 19.

APPENDICES

APPENDIX A

MILE Tow Parameters

This section contains listings of parameters associated with the thermistor chain tows and some elementary results. During the experiment, tows were made on a total of 10 occasions. Data from the sensors were recorded in continuous sections called runs, with a single tow comprising of one or more runs. The 10 tows were recorded in a total of 24 runs. For analysis, each tow was broken up into legs, which are tow segments of nearly constant direction and speed. Run and leg boundaries had no specific relationship so that a single leg could span one or more runs, or a single run could comprise one or more tow legs. The numbering of the legs is derived from the run numbers, and is best described by example. Run 4 and part of run 5 make up leg 4-5, leg 15A is contained in the first half of run 15 and so on. A total of 37 tow legs were recorded.

One of the parameters obtainable from the thermistor chain data is the buoyancy frequency, N. This is the natural frequency of the vertical oscillation of a water parcel in a stably stratified environment and is given by

$$N^2 = - \frac{g}{\rho} \frac{\partial \rho}{\partial z}$$

where g is the acceleration due to gravity, ρ is the density and z is the vertical space coordinate, positive upwards. Since conductivity was not measured on the chain, a relation between temperature and density was needed. This was obtained from CTD profiles measured on the NOAA ship OCEANOGRAPHER by the group led by Stan Hayes of the Pacific Marine Environmental Laboratory. Profiles were selected which were taken during

or within a few hours of the thermistor chain tows. Values of temperature, salinity, and σ_t from every 10 m in the depth range -20 to -50 were assembled. A linear relation between temperature and σ_t was derived:

$$\sigma_t = -0.19179\ T\ (°C) + 27.038$$

The rms deviation of the observations from this line was 0.0647 σ_t units. Using this relation and the horizontally averaged temperature of each thermistor for each tow leg, profiles of σ_t were calculated. Using the relation $\rho = 1.0 + 1000. \times \sigma_t$, the values of N at the midpoints between thermistors were obtainable. Just as the isotherm depths were determined by linear interpolation of the thermistor data, the average values of N for each isotherm were found by linear interpolation of the values at the midpoints between thermistors.

MILE Thermistor Chain Tow Parameters

Run	Date	Time (GMT)	Tow Speed (M/S)	Tow Direction (Deg)	Duration Time (Min)	Duration Distance (KM)	Wind Speed (M/S)	Wind Direction (Deg)	Wind Wave Height (M)
1	20-AUG-77	1846	1.6	NE	195	18.5	5	120	0.5
2	22-AUG-77	1648	1.1	W	6	0.4	18	240	3.0
3	24-AUG-77	1654	1.6	NNW	114	10.9	5	310	1.5
4-5	"	1852	1.6	NW	171	16.4	4	310	1.5
5-6	"	2142	2.0	S	180	21.6	5	300	1.5
7	26-AUG-77	1521	2.3	N	162	22.7	6	250	0.5
8	"	1810	2.7	E	103	16.5	6	240	0.8
9A	"	1959	3.0	S	149	26.4	8	260	1.0
9B	"	2229	3.0	W	120	21.2	7	260	1.0
10-11	28-AUG-77	1515	1.1	W	26	1.7	8	250	1.0
11A	"	1541	2.7	N	123	20.2	7	250	1.5
11B	"	1744	3.3	E	81	15.9	7	280	1.5
11-12	"	1905	1.9	S	240	27.7	8	250	1.5
12A	"	2111	2.5	S	112	16.7	8	240	1.5
12B	"	2303	2.0	W	136	16.3	7	240	1.5
13	30-AUG-77	1736	3.0	S	27	4.9	8	060	1.0
13-14	"	1803	2.5	N	158	23.6	8	050	1.0
14	"	2041	3.2	E	120	22.7	8	040	1.0
15A	"	2258	3.2	S	150	28.8	7	040	1.0
15B	31-AUG-77	0128	3.0	W	120	21.6	5	040	1.5
16	1-SEP-77	1723	2.3	N	25	3.4	12	360	2.5
17	"	1757	2.2	N	190	25.2	10	350	2.5
17-18	"	2107	2.2	E	225	29.7	8	340	2.0
19	3-SEP-77	1811	2.3	N	130	17.9	7	360	0.5
20	"	2025	2.6	E	118	18.6	4	340	0.5
21A	"	2227	3.1	S	140	25.6	5	330	0.5
21B	4-SEP-77	0047	2.9	W	132	22.6	6	320	0.5
22A	5-SEP-77	1817	2.6	W	16	2.5	3	280	0.5
22B	"	1833	2.6	N	33	5.2	3	270	0.5
22C	"	1906	2.6	E	21	3.3	3	270	0.5
22D	"	1927	2.6	S	27	4.2	3	280	0.5
22E	"	1954	2.6	W	33	5.2	3	290	0.5
22F	"	2027	2.6	N	37	5.8	3	300	0.5
22G	"	2104	2.6	E	22	3.4	3	300	0.5
22H	"	2126	2.6	S	29	4.5	3	300	0.5
22I	"	2155	2.6	W	30	4.7	3	300	0.5
22J	"	2225	2.6	N	32	5.0	3	300	0.5
22K	"	2257	2.6	E	28	4.4	2	300	0.5
22L	"	2325	2.6	S	29	4.5	3	290	0.5
22M	"	2354	2.6	W	32	5.0	3	290	0.5
23A	6-SEP-77	0031	2.6	N	28	4.4	3	300	0.5
23B	"	0059	2.6	E	29	4.5	3	300	0.5
23C	"	0128	2.6	S	31	4.8	3	310	0.5
23D	"	0159	2.6	W	30	4.7	2	310	0.5
24	8-SEP-77	1814	2.8	SW	173	28.6	5	250	1.5

MILE Depths (m) of Working Thermistors

	CHANNEL											
Run	15	16	18	19	20	21	22	23	24	27	30	36
1			22.74	23.79	24.84	25.89	26.93	27.98	29.03	32.17	35.32*	41.61
2	21.69*	22.74	24.84	25.89	26.93	27.98	29.03	30.08				
3			24.84	25.89	26.93	27.98		30.08				
4			24.84	25.89	26.93	27.98	29.03	30.08				
5			24.84	25.89	26.93	27.98	29.03*	30.08				
6			24.84	25.89	26.93	27.98		30.08				
7	21.69	22.74	24.84	25.89	26.93	27.98		30.08				
8	21.69*	22.74	24.84	25.89	26.93	27.98		30.08				
9		22.74	24.84	25.89	26.93	27.98		30.08				
10			24.84	25.89	26.93	27.98		30.08				
11		22.74	24.84	25.89	26.93	27.98		30.08				
12		22.74	24.84	25.89	26.93	27.98		30.08*		34.27		
13		28.51	30.60	31.65	32.70	33.75				40.03		
14		28.51	30.60	31.65	32.70	33.75				40.03		
15		28.51	30.60	31.65	32.70	33.75				40.03		
16		18.55	20.65		22.74	23.79				30.08		
17		31.86	33.96		36.05	37.10				43.39		
18		31.86	33.96		36.05	37.10				43.39		
19		29.13	31.23		33.33	34.37						
20		29.13	31.23		33.33	34.37			37.52			
21		29.13	31.23		33.33	34.37			37.52*			
22		28.56	30.65		32.75	33.80				40.09		
23	27.51*	28.56	30.65		32.75	33.80				40.09		
24		29.66	31.75		33.85	34.90				41.19		

* Working for part of run only

Run	Chan	Working 30 Sec Points		Total 30 Sec Points
1	30	1	259	391
2	15	1	7	13
5	22	1	111	310
8	15	1	98	206
12	23	1	440	497
21	24	1	457	545
23	15	55	237	237

RUN	AVERAGE Z (M)	AVERAGE N (CPH)	STD DEV N (CPH)	# 30 SEC POINTS
1				
	-23.27	5.08	1.61	391
	-24.31	5.02	1.61	391
	-25.36	4.89	1.97	391
	-26.41	5.08	2.16	391
	-27.46	7.32	2.03	391
	-28.51	9.72	2.63	391
	-30.60	8.49	3.95	391
	-33.75	12.05	4.12	259
	-38.46	12.22	2.32	259
2				
	-22.22	16.06	1.96	7
	-23.79	10.04	1.51	13
	-25.36	11.36	1.03	13
	-26.41	10.42	1.37	13
	-27.46	8.87	1.70	13
	-28.51	8.39	1.64	13
	-29.55	7.36	1.64	13
4-5				
	-25.36	1.49	2.43	270
	-26.41	3.22	5.01	270
	-27.46	8.01	7.59	270
	-28.51	17.47	7.75	180
	-29.55	20.49	4.95	180
11A				
	-23.79	6.39	2.25	246
	-25.36	7.42	3.97	246
	-26.41	9.58	6.31	246
	-27.46	12.15	6.93	246
	-29.03	14.88	5.72	246
11B				
	-23.79	2.44	1.04	163
	-25.36	2.70	1.70	163
	-26.41	3.47	1.72	163
	-27.46	4.95	2.44	163
	-29.03	7.99	4.69	163
12A				
	-23.79	5.70	1.51	224
	-25.36	4.59	2.25	224
	-26.41	3.56	2.11	224
	-27.46	3.42	1.66	224
	-29.03	6.45	3.95	224
	-32.17	18.34	4.09	224

RUN	AVERAGE Z (M)	AVERAGE N (CPH)	STD DEV N (CPH)	# 30 SEC POINTS
12B				
	-23.79	5.04	1.90	273
	-25.36	4.07	2.07	273
	-26.41	3.68	2.19	273
	-27.46	3.88	2.77	273
	-29.03	7.98	3.30	216
	-32.17	10.82	4.34	216
13				
	-29.55	6.58	2.89	54
	-31.13	10.82	8.70	54
	-32.17	14.22	7.06	54
	-33.22	16.54	5.30	54
	-36.89	17.02	2.21	54
13-14				
	-29.55	8.41	4.54	310
	-31.13	10.28	6.76	310
	-32.17	12.28	6.21	310
	-33.22	13.37	5.87	310
	-36.89	15.92	3.22	310
14				
	-29.55	8.39	4.04	241
	-31.13	11.38	5.81	241
	-32.17	14.24	6.24	241
	-33.22	15.73	6.13	241
	-36.89	15.71	2.13	241
15A				
	-29.55	4.14	2.36	300
	-31.13	3.93	3.47	300
	-32.17	4.59	4.04	300
	-33.22	5.50	4.87	300
	-36.89	14.93	4.24	300
15B				
	-29.55	6.78	4.34	241
	-31.13	8.91	6.66	241
	-32.17	11.36	7.38	241
	-33.22	13.36	7.08	241
	-36.89	15.98	2.74	241
16				
	-19.60	1.33	0.14	50
	-21.69	0.57	0.30	50
	-23.27	1.33	0.28	50
	-26.93	3.88	1.12	50

RUN	AVERAGE Z (M)	AVERAGE N (CPH)	STD DEV N (CPH)	# 30 SEC POINTS
17				
	-32.91	16.95	4.71	380
	-35.00	16.09	4.47	380
	-36.58	14.95	4.31	380
	-40.24	12.26	2.70	380
17-18				
	-32.91	9.83	6.57	440
	-35.00	13.22	6.50	440
	-36.58	15.47	6.13	440
	-40.24	15.62	3.34	440
19				
	-30.18	7.26	7.20	261
	-32.28	8.41	6.94	261
	-33.85	9.84	5.97	261
20				
	-30.18	8.33	6.07	237
	-32.28	12.81	6.08	237
	-33.85	16.10	6.05	237
	-35.95	18.74	3.14	237
21A				
	-30.18	6.64	6.51	280
	-32.28	10.34	5.98	280
	-33.85	14.11	5.50	280
	-35.95	16.72	3.48	280
21B				
	-30.18	11.62	6.45	265
	-32.28	17.63	4.94	265
	-33.85	20.71	4.73	265
	-35.95	18.17	2.57	177
22A				
	-29.61	1.58	0.73	32
	-31.70	1.98	0.85	32
	-33.27	3.14	1.54	32
	-36.94	9.99	2.16	32
22B				
	-29.61	2.41	0.64	66
	-31.70	3.18	1.76	66
	-33.27	5.24	2.35	66
	-36.94	12.06	2.31	66

220				
	27,41	2.44	0.19	60
	41,70	1.55	0.41	60
	44,27	2.12	0.87	60
	46,94	6.79	4.88	60
221				
	27,41	3.91	1.84	64
	41,70	5.55	5.16	64
	44,27	7.53	5.94	64
	46,94	12.93	3.51	64

RUN	AVERAGE Z (M)	AVERAGE N (CPH)	STD DEV N (CPH)	# 30 SEC POINTS
22K				
	-29.61	5.02	2.13	56
	-31.70	10.20	4.33	56
	-33.27	13.01	3.31	56
	-36.94	15.61	1.63	56
22L				
	-29.61	3.49	1.06	58
	-31.70	3.69	2.99	58
	-33.27	5.26	3.49	58
	-36.94	14.46	3.23	58
22M				
	-29.61	3.15	0.75	65
	-31.70	3.97	2.75	65
	-33.27	6.54	3.77	65
	-36.94	15.66	2.13	65
23A				
	-29.61	9.27	6.14	56
	-31.70	12.29	3.48	56
	-33.27	12.88	2.36	56
	-36.94	16.58	0.95	56
23B				
	-28.03	9.38	5.68	58
	-29.61	13.76	3.98	58
	-31.70	15.86	2.94	58
	-33.27	14.95	3.63	58
	-36.94	15.39	1.94	58
23C				
	-28.03	5.87	1.26	62
	-29.61	10.02	5.22	62
	-31.70	17.22	5.80	62
	-33.27	17.66	3.94	62
	-36.94	15.19	1.79	62
23D				
	-28.03	13.19	5.28	61
	-29.61	14.75	5.29	61
	-31.70	18.07	3.99	61
	-33.27	19.79	2.98	61
	-36.94	14.10	3.58	61

RUN	AVERAGE Z (M)	AVERAGE N (CPH)	STD DEV N (CPH)	# 30 SEC POINTS
24				
	-30.71	8.69	4.31	347
	-32.80	10.42	5.29	347
	-34.37	11.72	5.41	347
	-38.04	15.09	1.95	347

RUN	# 30 SEC AVERAGES	ISOTHERM (DEG C)	AVERAGE Z (M)	STD DEV Z (M)	N (CPH)
1	390				
		11.50	-27.28	1.89	6.93
		11.00	-32.34	2.45	10.46
		10.50	-34.94	3.14	12.09
		10.00	-37.17	3.84	12.17
2	12				
		12.00	-22.98	0.67	13.14
		11.50	-25.50	1.01	11.23
		11.00	-28.29	1.15	8.49
4-5	274				
		12.00	-27.67	1.25	9.97
		11.90	-28.32	1.37	15.78
11A	246				
		11.90	-25.94	1.62	8.61
		11.50	-28.08	1.84	13.23
11B	162				
		12.25	-26.92	1.82	4.19
12A	224				
		12.00	-26.35	1.62	3.61
		11.80	-29.97	0.99	10.01
		11.50	-30.80	1.13	13.13
		11.00	-31.73	1.35	16.67
		10.50	-32.57	1.47	19.82
		10.00	-33.35	1.53	22.77
12B	272				
		11.80	-29.90	1.85	8.76
13	54				
		11.50	-32.29	1.44	14.48
		11.00	-33.30	1.53	16.55
		10.50	-34.11	1.79	16.66
		10.00	-34.90	2.10	16.76
		9.50	-35.72	2.34	16.87
		9.00	-36.60	2.50	16.98
13-14	316				
		11.50	-31.93	2.77	11.81
		11.00	-32.99	2.74	13.13
		10.50	-33.89	2.84	13.84
		10.00	-34.84	2.86	14.49
		9.50	-35.82	2.88	15.18
		9.00	-36.90	2.80	15.92

RUN	# 30 SEC AVERAGES	ISOTHERM (DEG C)	AVERAGE Z (M)	STD DEV Z (M)	N (CPH)
14	240				
		11.50	-32.13	2.10	14.12
		11.00	-33.27	2.13	15.73
		10.50	-34.28	2.30	15.72
		10.00	-35.22	2.48	15.72
		9.50	-36.24	2.58	15.71
		9.00	-37.31	2.59	15.71
15A	300				
		11.50	-34.95	1.80	9.95
		11.00	-36.47	2.51	13.84
15B	240				
		11.50	-32.40	2.18	11.79
		11.00	-33.60	2.06	13.63
		10.50	-34.60	2.13	14.35
		10.00	-35.57	2.28	15.04
		9.50	-36.53	2.44	15.72
		9.00	-37.51	2.53	16.43
16	50				
		12.25	-25.68	1.24	3.00
17	380				
		9.00	-34.78	2.93	16.18
		8.50	-35.96	3.00	15.39
		8.00	-37.38	3.07	14.36
		7.50	-39.18	2.85	13.04
		7.00	-41.18	2.53	11.57
17-18	450				
		11.50	-35.33	3.08	13.69
		11.00	-36.28	3.11	15.04
		10.50	-37.08	3.27	15.49
		10.00	-37.91	3.40	15.52
		9.50	-38.78	3.51	15.56
		9.00	-39.70	3.52	15.59
19	190				
		12.35	-31.46	1.94	7.96
20	236				
		12.00	-32.08	2.09	12.39
		11.50	-33.32	2.11	14.99
		11.00	-34.33	2.16	16.71
		10.50	-35.22	2.21	17.82

RUN	# 30 SEC AVERAGES	ISOTHERM (DEG C)	AVERAGE Z (M)	STD DEV Z (M)	N (CPH)
21A	280				
		12.00	-32.55	2.36	10.99
		11.50	-33.67	2.51	13.69
		11.00	-34.59	2.64	15.04
21B	264				
		11.50	-31.56	1.68	15.56
		11.00	-32.40	1.65	17.87
		10.50	-33.08	1.66	19.19
		10.00	-33.68	1.67	20.38
		9.50	-34.31	1.72	20.16
22A	32				
		12.35	-32.92	1.66	2.88
		12.30	-34.09	0.67	4.67
		12.20	-34.94	0.91	6.26
		12.00	-36.30	1.51	8.80
22B	66				
		12.30	-32.57	1.29	4.32
		12.20	-33.88	0.78	6.36
		12.00	-35.04	0.99	8.52
		11.50	-37.22	1.71	12.58
22C	42				
		12.35	-30.11	1.42	3.25
		12.30	-32.29	1.52	5.01
		12.20	-33.38	1.20	6.51
		12.00	-34.40	0.99	8.45
		11.50	-36.28	1.15	12.00
		11.00	-37.99	1.44	15.23
22D	54				
		12.35	-31.88	1.16	2.33
		12.30	-33.58	0.51	5.11
		12.20	-34.04	0.20	6.62
		12.00	-34.53	0.24	8.24
		11.50	-35.71	0.49	12.16
		11.00	-36.90	0.75	16.08
		10.50	-38.08	1.00	19.99

RUN	# 30 SEC AVERAGES	ISOTHERM (DEG C)	AVERAGE Z (M)	STD DEV Z (M)	N (CPH)
22E	66				
		12.35	-31.23	1.59	4.65
		12.30	-32.35	1.36	6.97
		12.20	-33.08	1.15	9.10
		12.00	-33.81	0.97	10.62
		11.50	-35.13	0.93	13.03
		11.00	-36.30	1.16	15.16
		10.50	-37.45	1.36	17.26
		10.00	-38.56	1.50	19.27
22F	74				
		12.30	-30.66	1.22	5.78
		12.20	-32.10	1.28	7.89
		12.00	-33.27	1.18	9.08
		11.50	-34.91	1.01	12.22
		11.00	-36.17	1.27	14.62
		10.50	-37.37	1.55	16.92
		10.00	-38.49	1.71	19.07
22G	44				
		12.35	-31.87	1.15	2.34
		12.30	-33.78	0.81	3.86
		12.20	-34.97	0.83	5.77
		12.00	-36.74	1.61	8.60
22H	58				
		12.35	-32.90	1.22	2.61
		12.30	-34.16	0.92	4.87
		12.20	-35.04	1.64	6.85
		12.00	-36.09	2.02	9.18
22I	60				
		12.35	-34.86	1.96	4.14
22J	64				
		12.35	-30.10	1.74	4.29
		12.30	-32.20	2.04	6.18
		12.20	-33.22	1.96	7.46
		12.00	-34.41	2.33	9.21
		11.50	-36.54	3.01	12.34

RUN	# 30 SEC AVERAGES	ISOTHERM (DEG C)	AVERAGE Z (M)	STD DEV Z (M)	N (CPH)
22K	56				
		12.30	-30.19	1.00	6.47
		12.20	-31.44	1.18	9.56
		12.00	-32.39	1.22	11.42
		11.50	-33.96	1.24	13.50
		11.00	-35.19	1.47	14.37
		10.50	-36.38	1.61	15.21
		10.00	-37.62	1.69	16.09
		9.50	-38.83	1.75	16.96
22L	58				
		12.35	-31.38	2.15	3.66
		12.30	-32.73	1.98	4.71
		12.20	-33.62	1.62	6.13
		12.00	-34.44	1.55	8.19
		11.50	-36.05	1.65	12.21
		11.00	-37.43	1.88	15.68
		10.50	-38.71	1.99	18.88
22M	64				
		12.35	-31.45	1.54	3.88
		12.30	-32.70	1.33	5.60
		12.20	-33.44	0.98	6.94
		12.00	-34.21	0.72	8.85
		11.50	-35.58	0.82	12.27
		11.00	-36.88	1.13	15.52
		10.50	-38.11	1.32	18.56
23A	56				
		12.00	-30.84	1.85	11.05
		11.50	-32.27	2.05	12.50
		11.00	-33.52	2.08	13.13
		10.50	-34.72	2.07	14.34
		10.00	-35.86	2.03	15.49
		9.50	-37.03	1.92	16.66
		9.00	-38.09	1.91	17.74
23B	58				
		11.50	-29.98	1.58	14.13
		11.00	-31.25	1.70	15.41
		10.50	-32.47	1.90	15.41
		10.00	-33.63	2.11	14.99
		9.50	-34.70	2.29	15.12
		9.00	-35.85	2.36	15.26
		8.50	-37.00	2.30	15.40
		8.00	-38.21	2.12	15.55
		7.50	-39.47	1.90	15.70

RUN	# 30 SEC AVERAGES	ISOTHERM (DEG C)	AVERAGE Z (M)	STD DEV Z (M)	N (CPH)
23C	62				
		12.00	-30.63	1.26	13.54
		11.50	-31.91	1.51	17.28
		11.00	-32.78	1.77	17.52
		10.50	-33.61	2.04	17.43
		10.00	-34.51	2.31	16.83
		9.50	-35.49	2.48	16.17
		9.00	-36.59	2.54	15.42
		8.50	-37.83	2.42	14.59
23D	60				
		11.50	-30.03	1.81	15.42
		11.00	-30.90	1.90	16.80
		10.50	-31.70	1.91	18.06
		10.00	-32.48	1.88	18.92
		9.50	-33.29	1.90	19.77
		9.00	-34.14	1.99	18.45
		8.50	-35.03	2.11	17.07
		8.00	-36.13	2.13	15.36
		7.50	-37.60	1.83	13.08
24	346				
		12.00	-33.78	2.39	11.23
		11.50	-35.18	2.56	12.46
		11.00	-36.41	2.78	13.59
		10.50	-37.61	2.94	14.69

APPENDIX B

Edited Isotherms

This appendix contains the entire set of edited time series of isotherm depths used in the spectral analysis and other processing. As mentioned in the section on analysis, only series that were at least 80% complete before editing were chosen to be edited for further processing. Because of this, not all tow legs are represented.

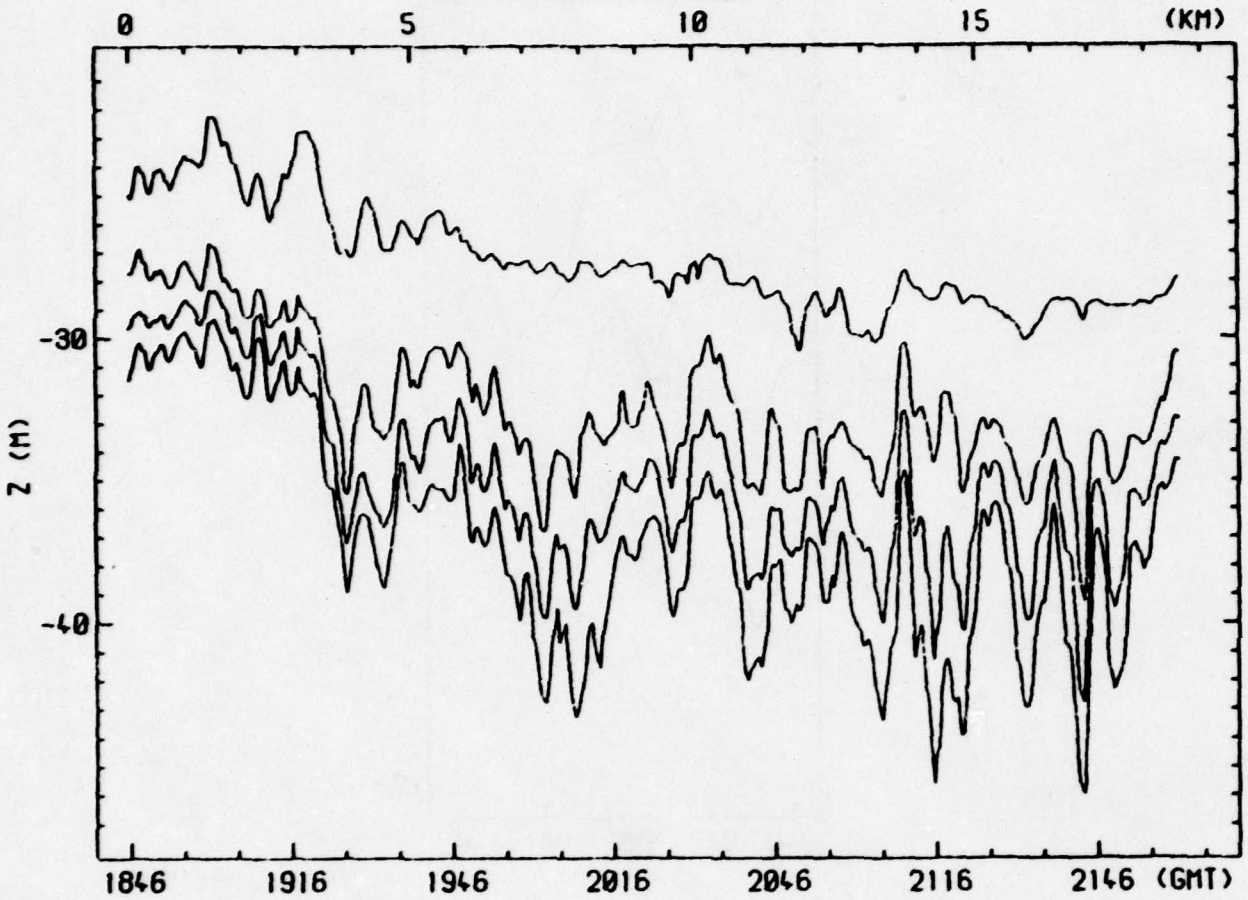

RUN 01 20 AUG 77 EDITED ISOTHERMS VS TIME/DISTANCE

T = 10.0 TO 11.5 DEG C IN 0.5 DEG INCREMENTS

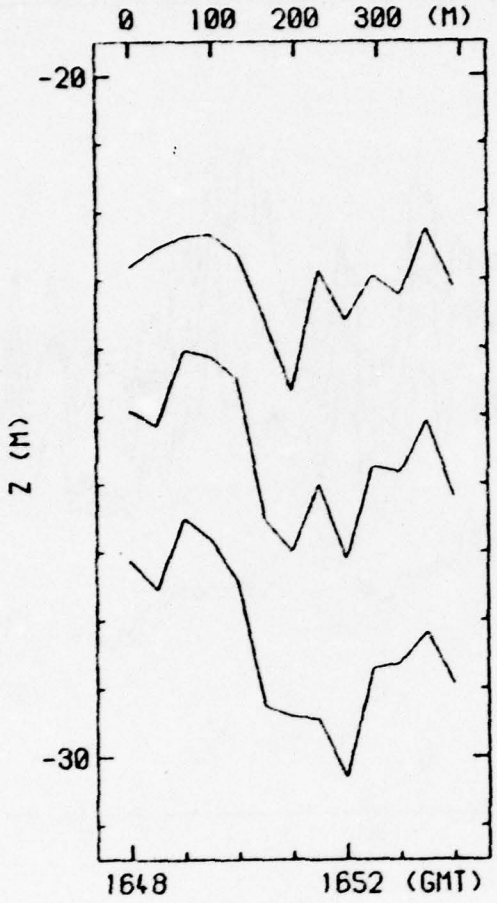

RUN 02 22 AUG 77 EDITED ISOTHERMS VS TIME/DISTANCE

T = 11.0 TO 12.0 DEG C IN 0.5 DEG INCREMENTS

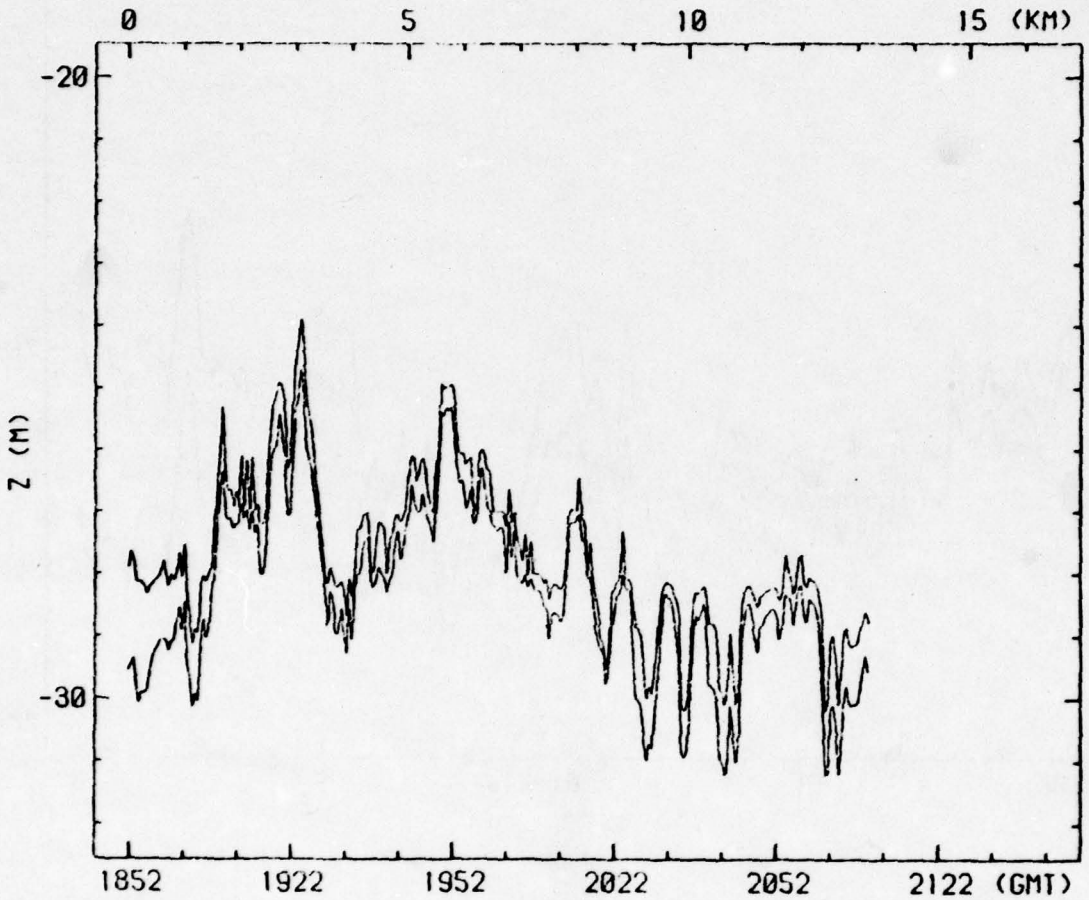

RUNS 04-05 24 AUG 77 EDITED ISOTHERMS VS TIME/DISTANCE

T = 11.9 AND 12.0 DEG C

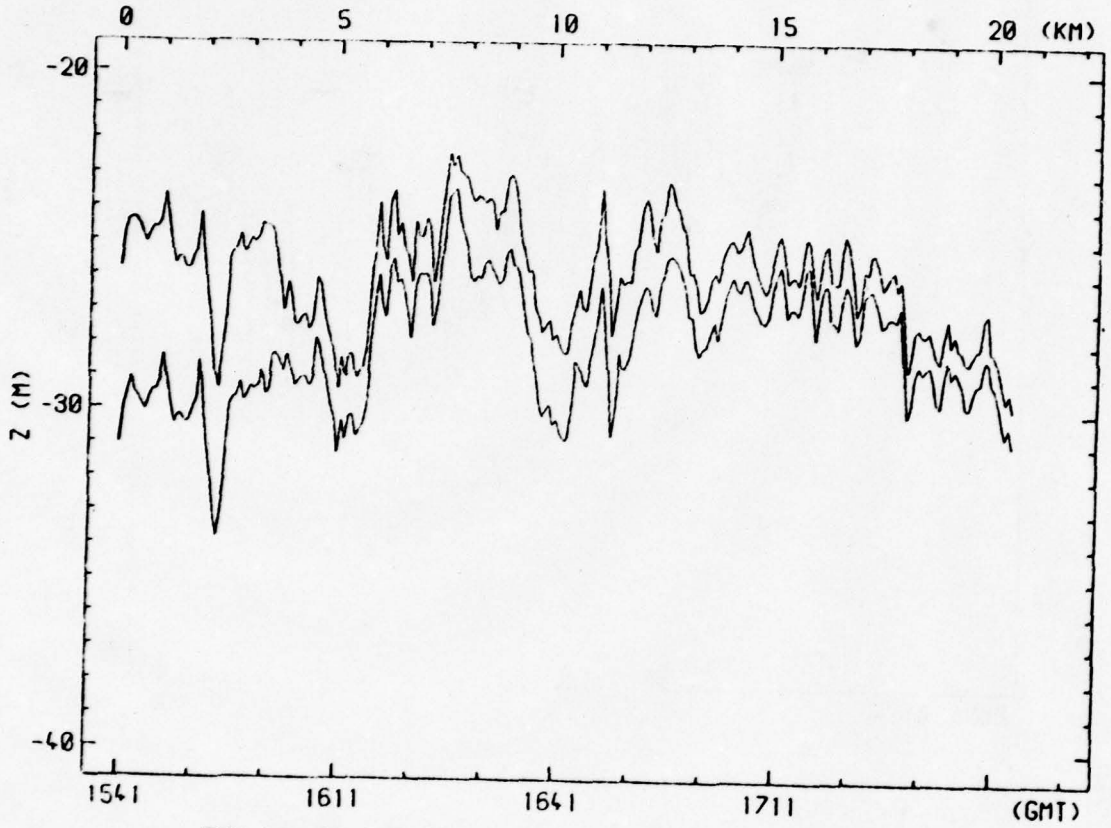

RUN 11 28 AUG 77 EDITED ISOTHERMS VS TIME/DISTANCE

T = 11.5 AND 11.9 DEG C

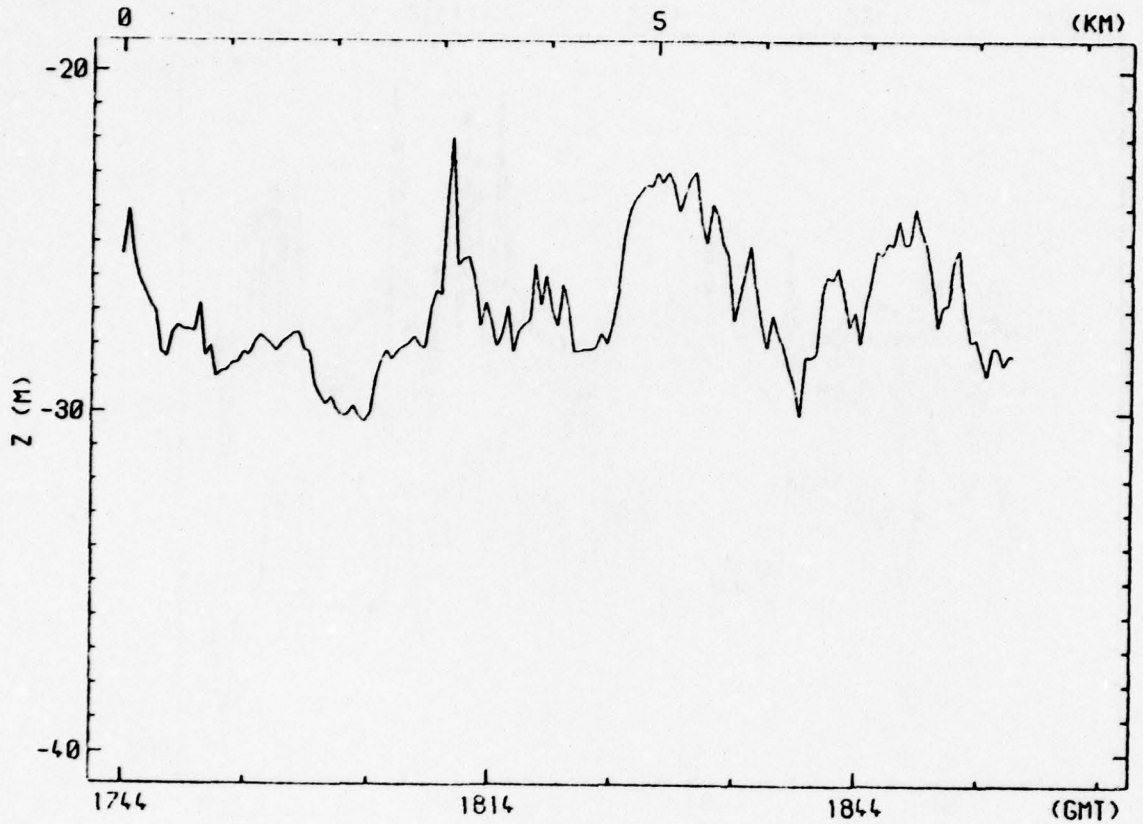

RUN 11 28 AUG 77 EDITED ISOTHERM VS TIME/DISTANCE

T = 12.25 DEG C

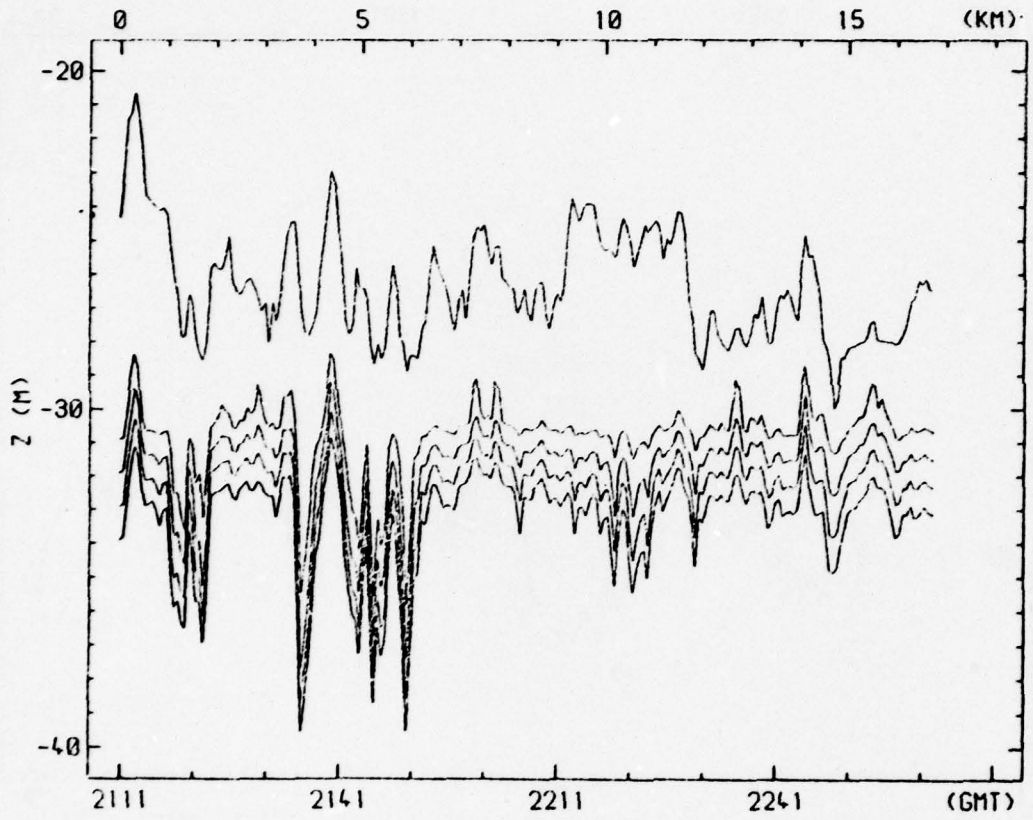

RUN 12 28 AUG 77 EDITED ISOTHERMS VS TIME/DISTANCE

T = 10 0 TO 12 0 DEG C IN 0 5 DEG INCREMENTS

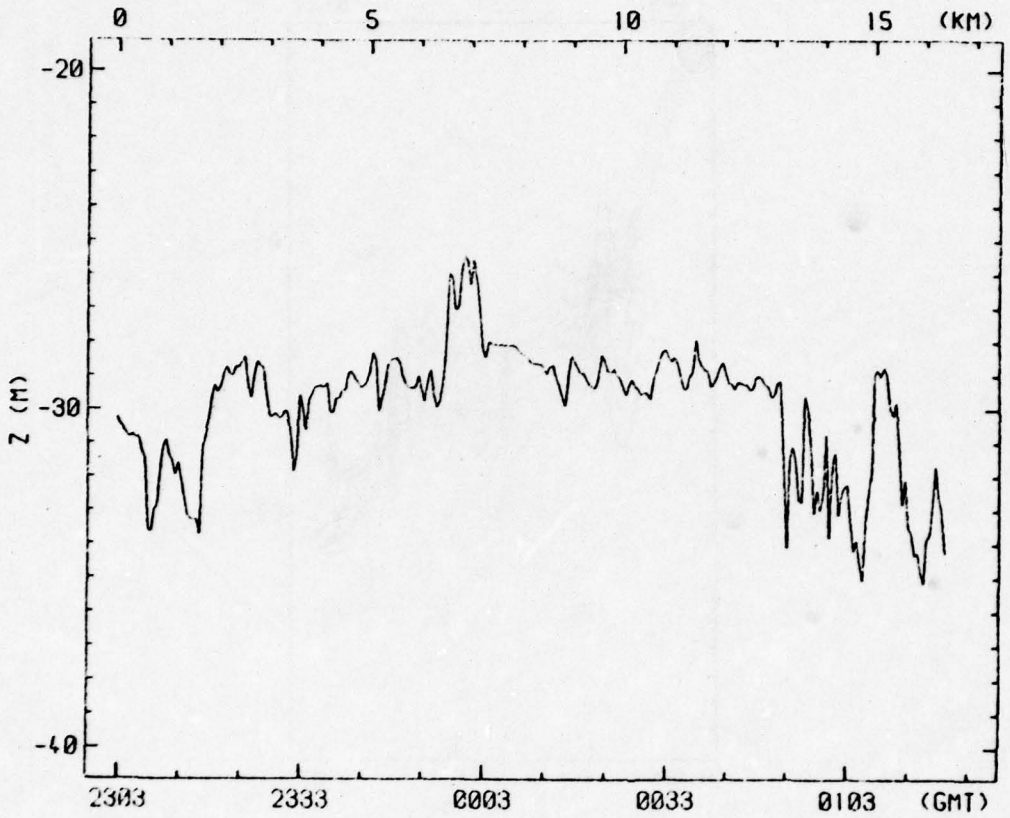

RUN 12 28 AUG 77 EDITED ISOTHERM VS TIME/DISTANCE

T = 11.8 DEG C

10.00	-34.84	2.86	14.49
9.50	-35.82	2.88	15.18
9.00	-36.90	2.80	15.92

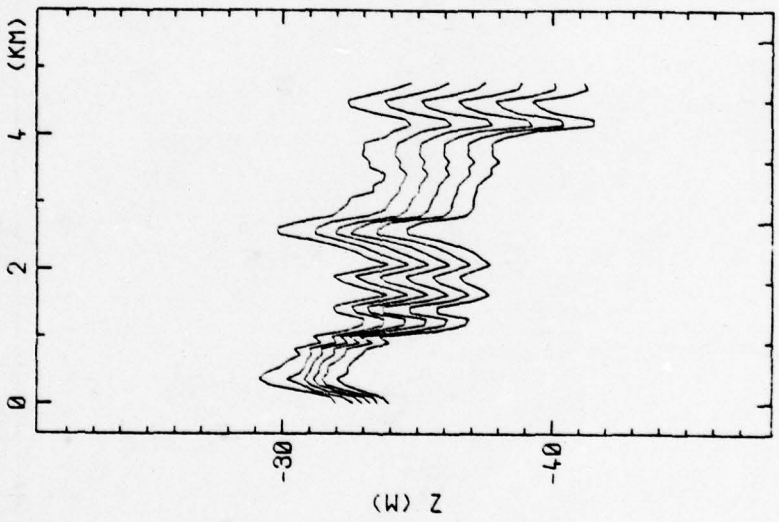

RUN 13 30 AUG 77 EDITED ISOTHERMS VS TIME/DISTANCE
T = 9 0 TO 11 5 DEG C IN 0 5 DEG INCREMENTS

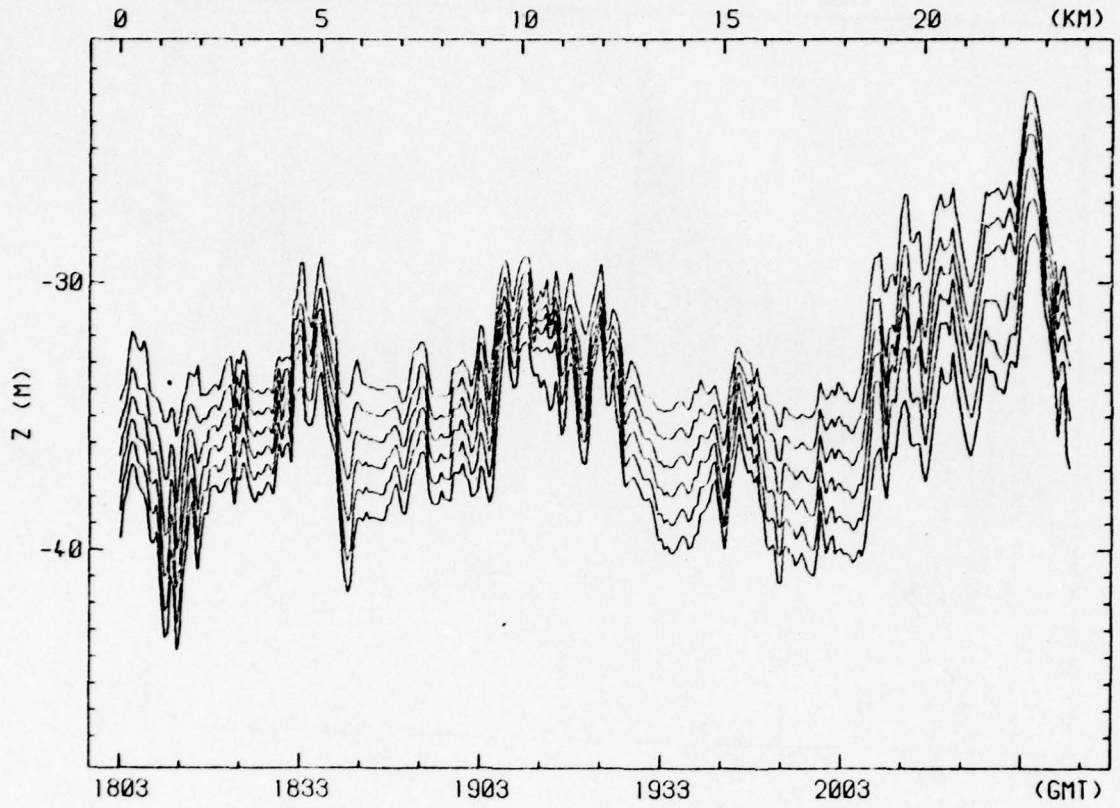

RUNS 13-14 30 AUG 77 EDITED ISOTHERMS VS TIME/DISTANCE

T = 9.0 TO 11.5 DEG C IN 0.5 DEG INCREMENTS

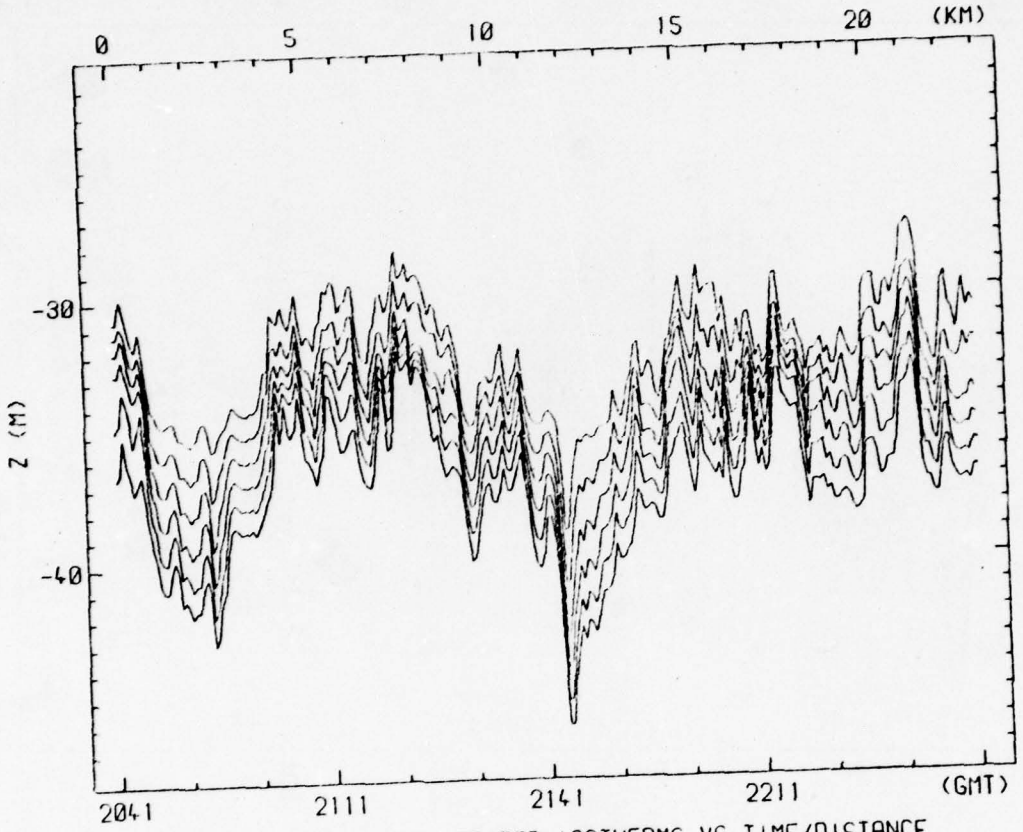

RUN 14 30 AUG 77 EDITED ISOTHERMS VS TIME/DISTANCE

T = 9.0 TO 11.5 DEG C IN 0.5 DEG INCREMENTS

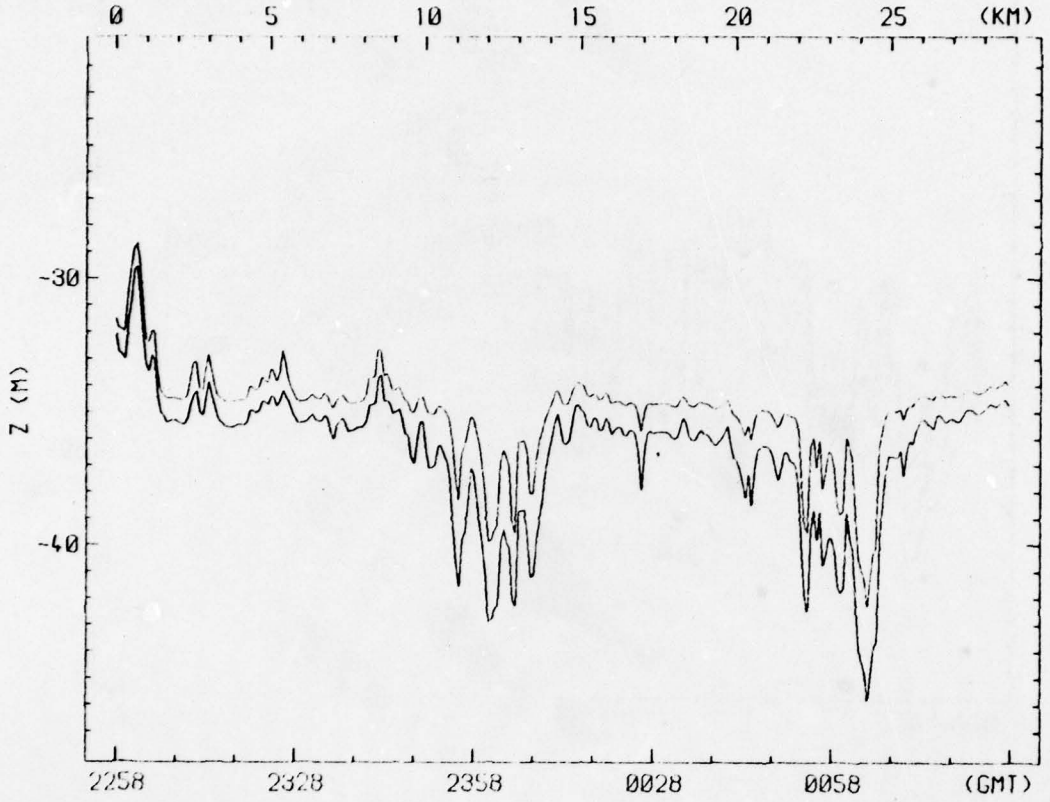

RUN 15 30 AUG 77 EDITED ISOTHERMS VS TIME/DISTANCE

T = 11.0 TO 11.5 DEG C IN 0.5 DEG INCREMENTS

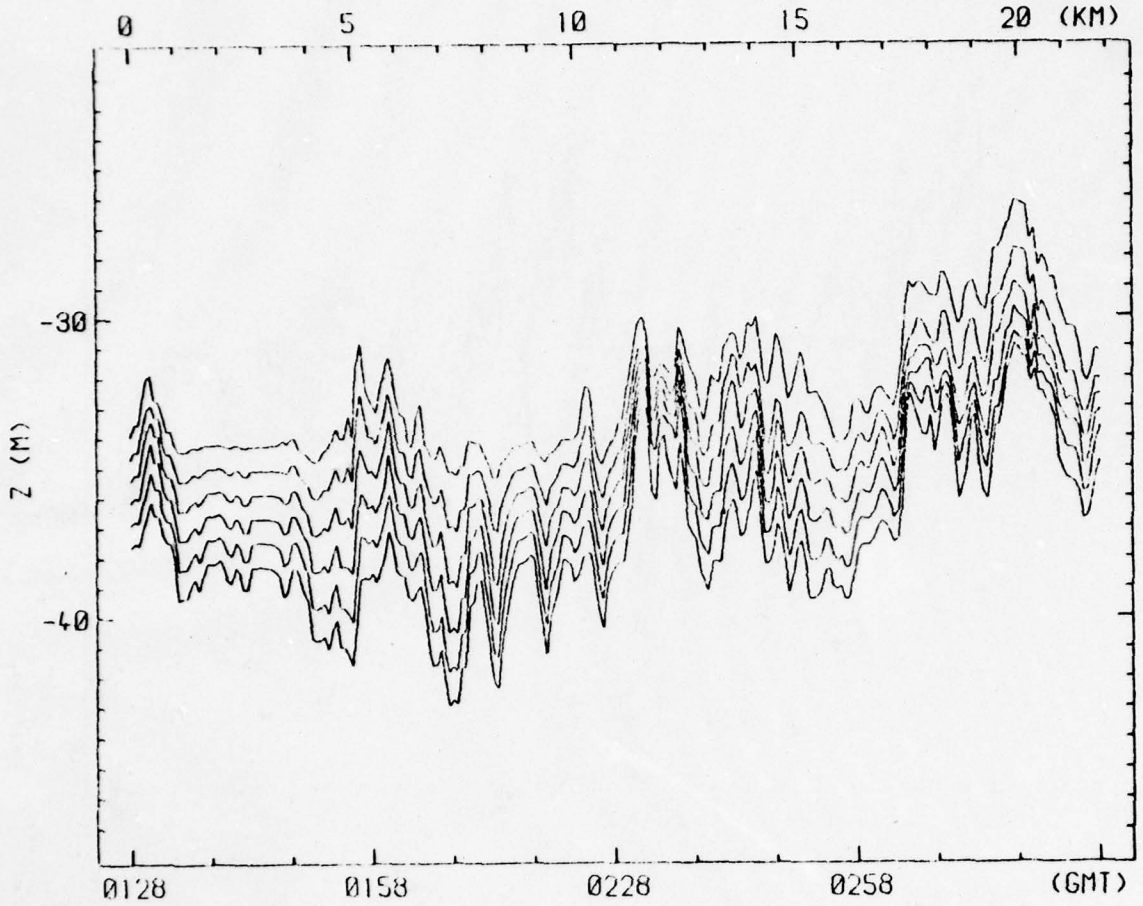

RUN 15 31 AUG 77 EDITED ISOTHERMS VS TIME/DISTANCE

T = 9.0 TO 11.5 DEG C IN 0.5 DEG INCREMENTS

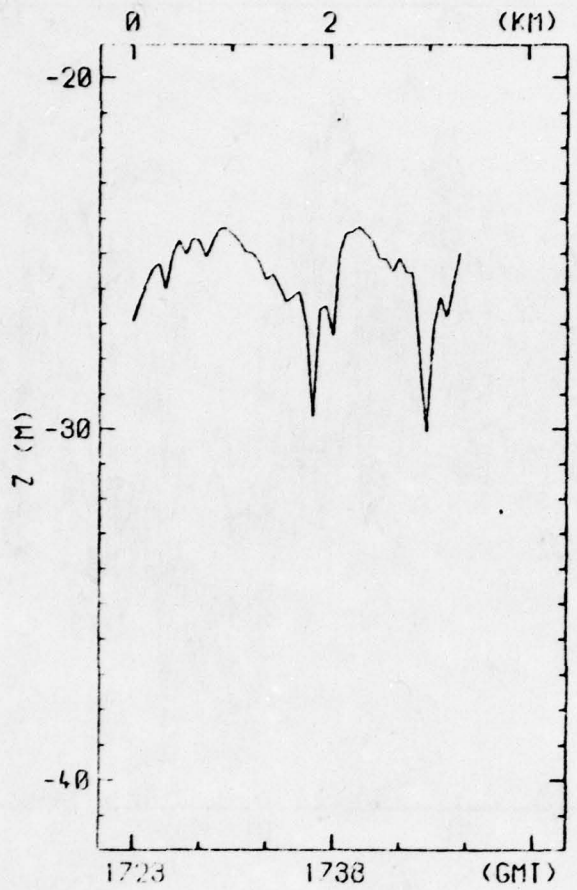

RUN 16 1 SEP 77 EDITED ISOTHERM VS TIME/DISTANCE

T = 12.25 DEG C

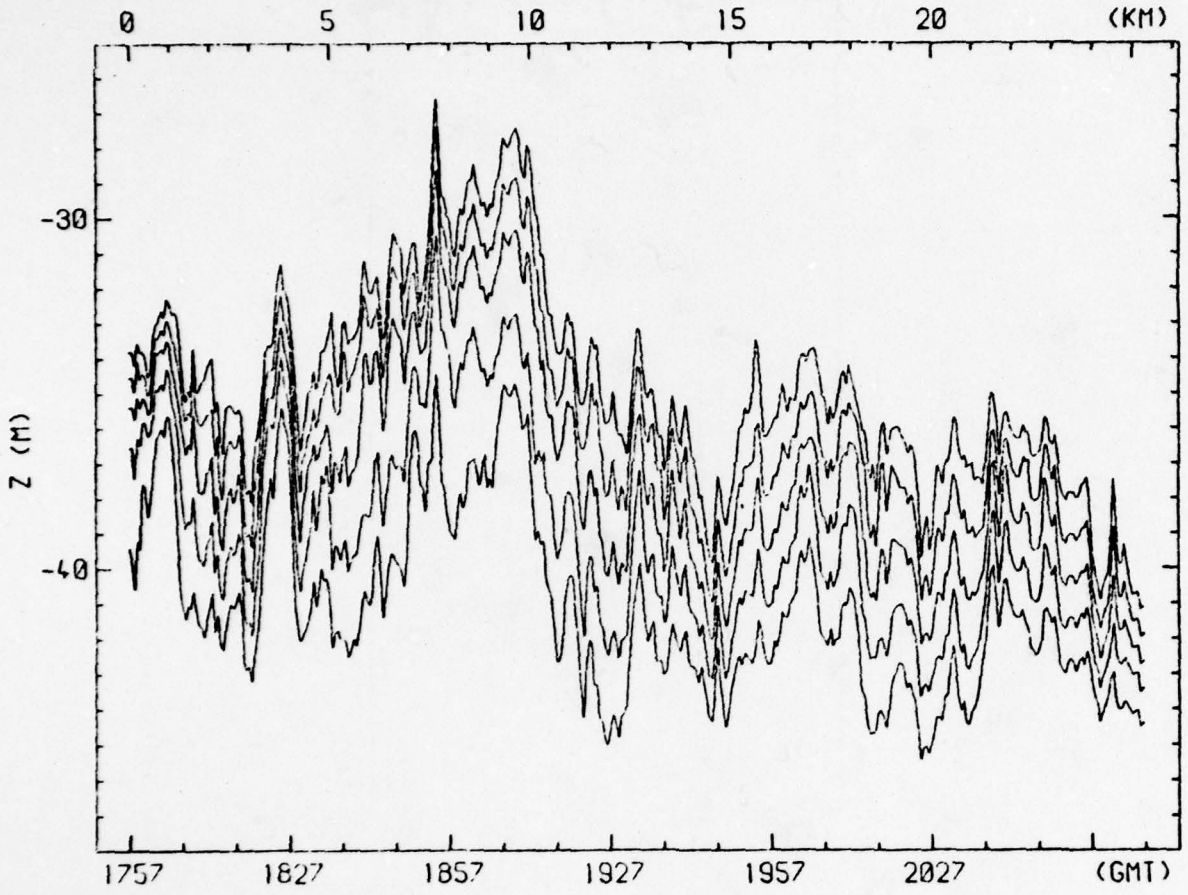

RUN 17 1 SEP 77 EDITED ISOTHERMS VS TIME/DISTANCE

T = 7.0 TO 9.0 DEG C IN 0.5 DEG INCREMENTS

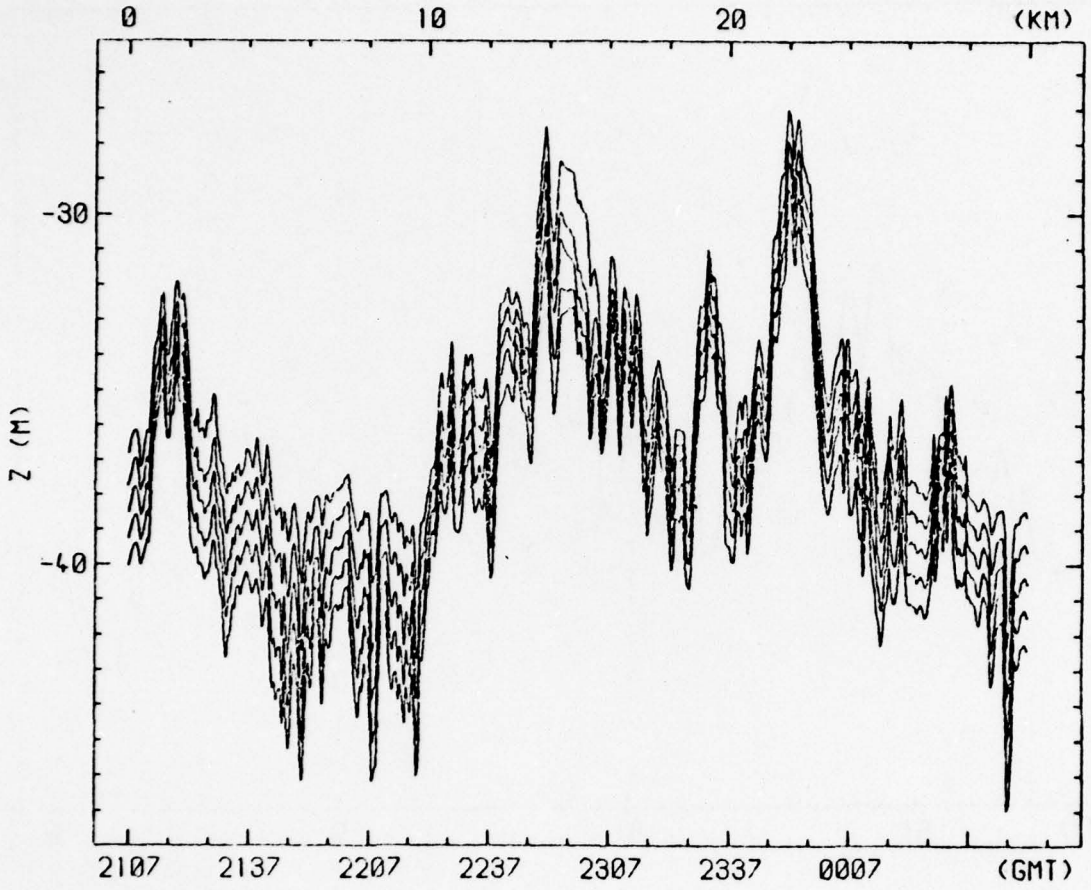

RUNS 17-18 1 SEP 77 EDITED ISOTHERMS VS TIME/DISTANCE

T = 9 5 TO 11.5 DEG C IN 0.5 DEG INCREMENTS

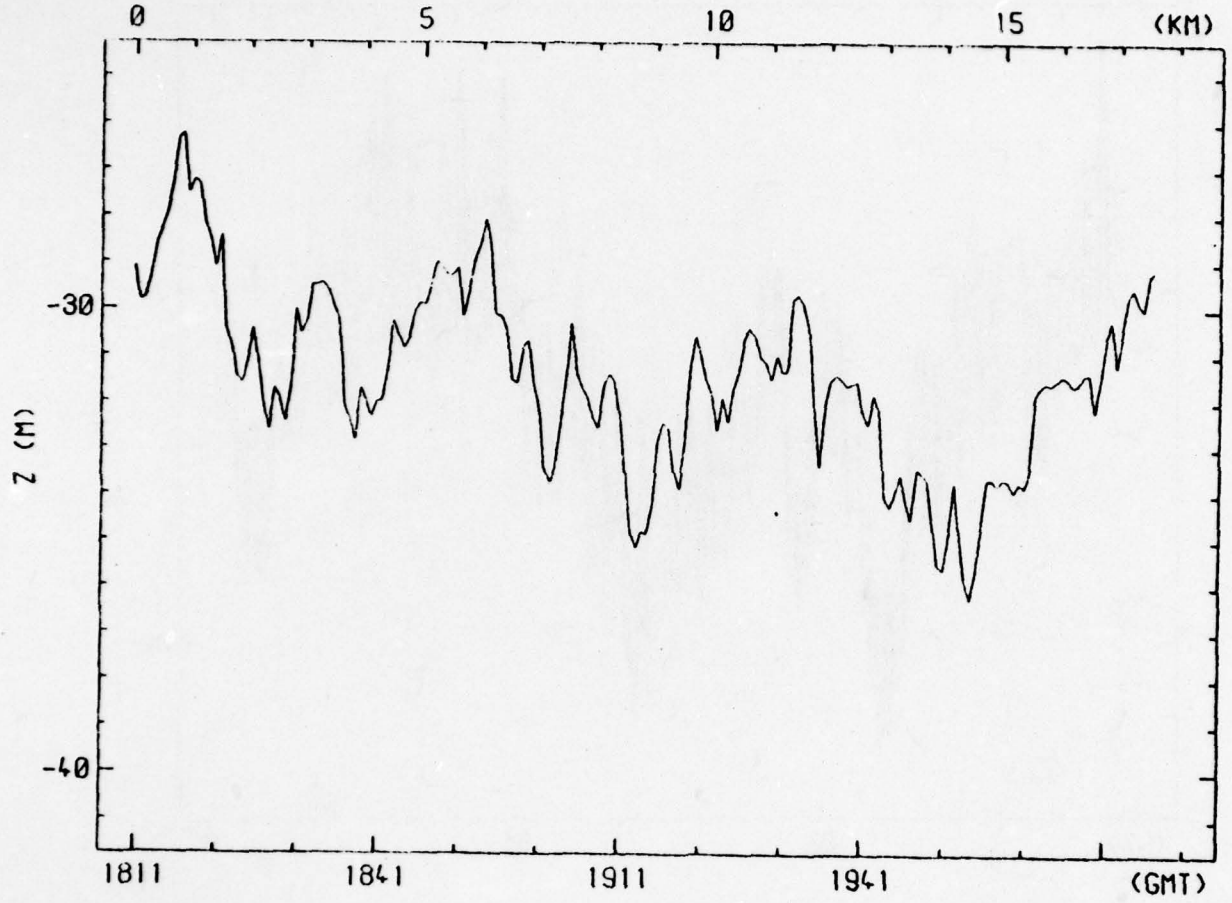

RUN 19 3 SEP 77 EDITED ISOTHERM VS TIME/DISTANCE

T = 12.35 DEG C

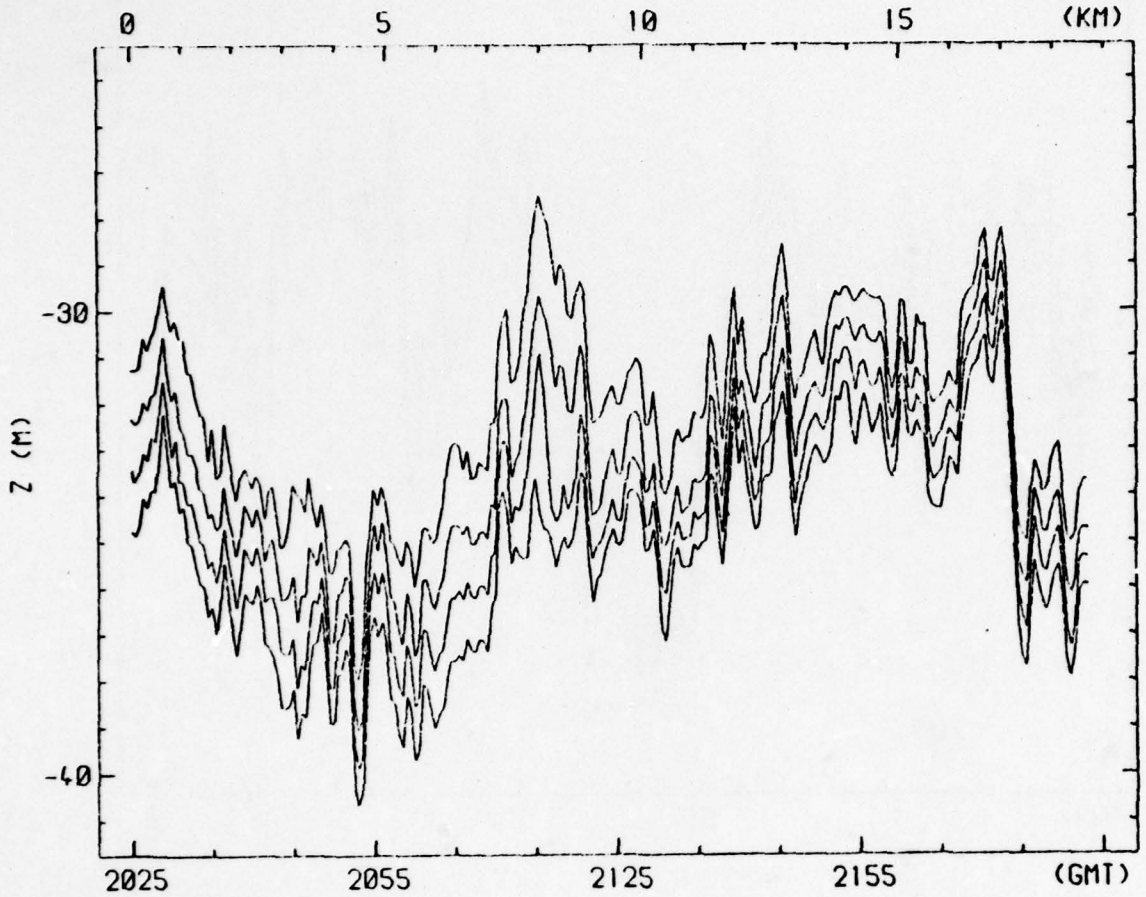

RUN 20 3 SEP 77 EDITED ISOTHERMS VS TIME/DISTANCE

T = 10.5 TO 12.0 DEG C IN 0.5 DEG INCREMENTS

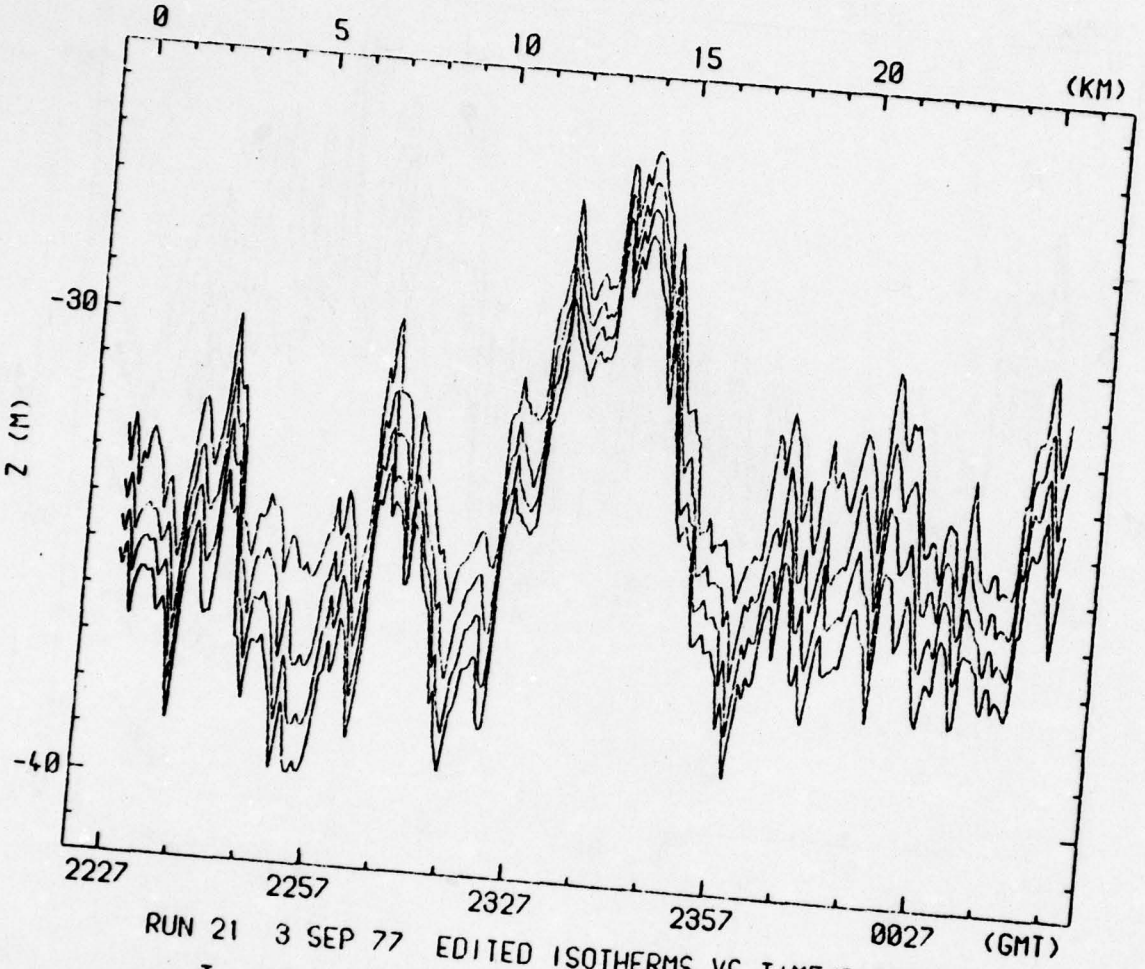

RUN 21 3 SEP 77 EDITED ISOTHERMS VS TIME/DISTANCE
T = 10.5 TO 12.0 DEG C IN 0.5 DEG INCREMENTS

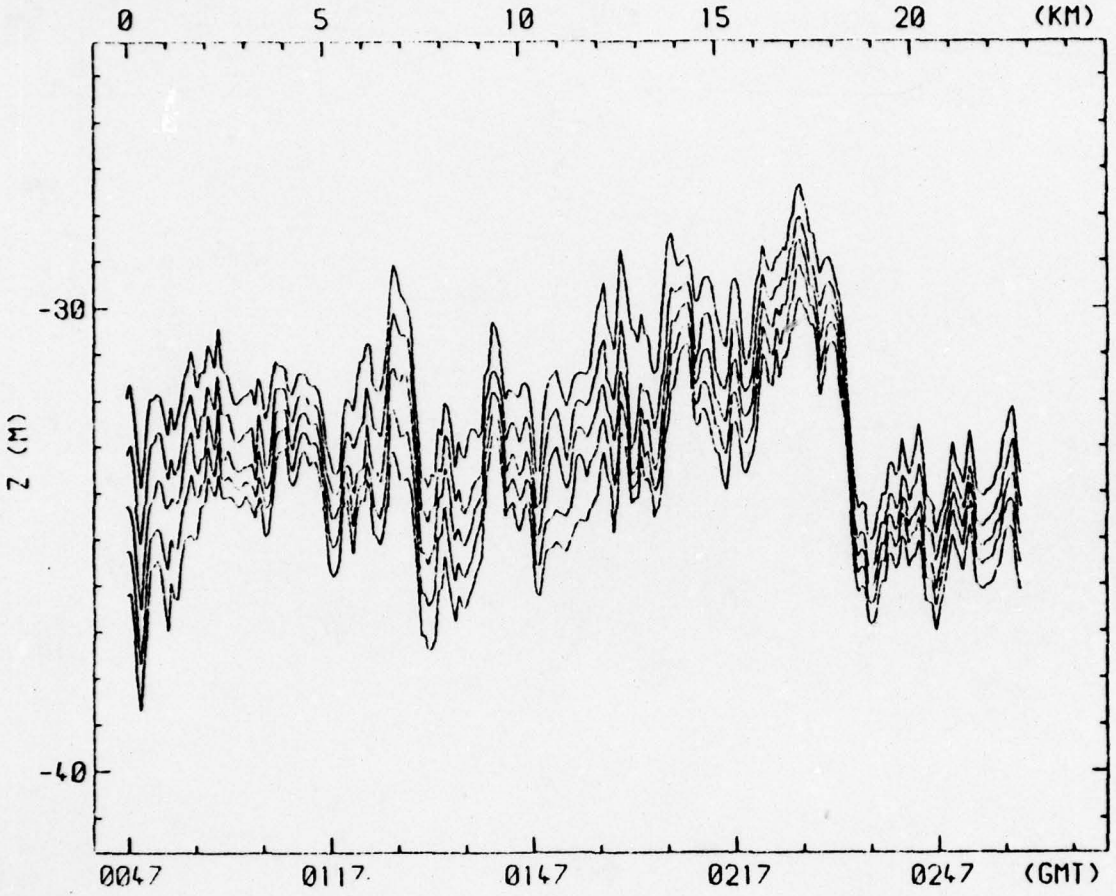

RUN 21 4 SEP 77 EDITED ISOTHERMS VS TIME/DISTANCE

T = 9 5 TO 11 5 DEG C IN 0.5 DEG INCREMENTS

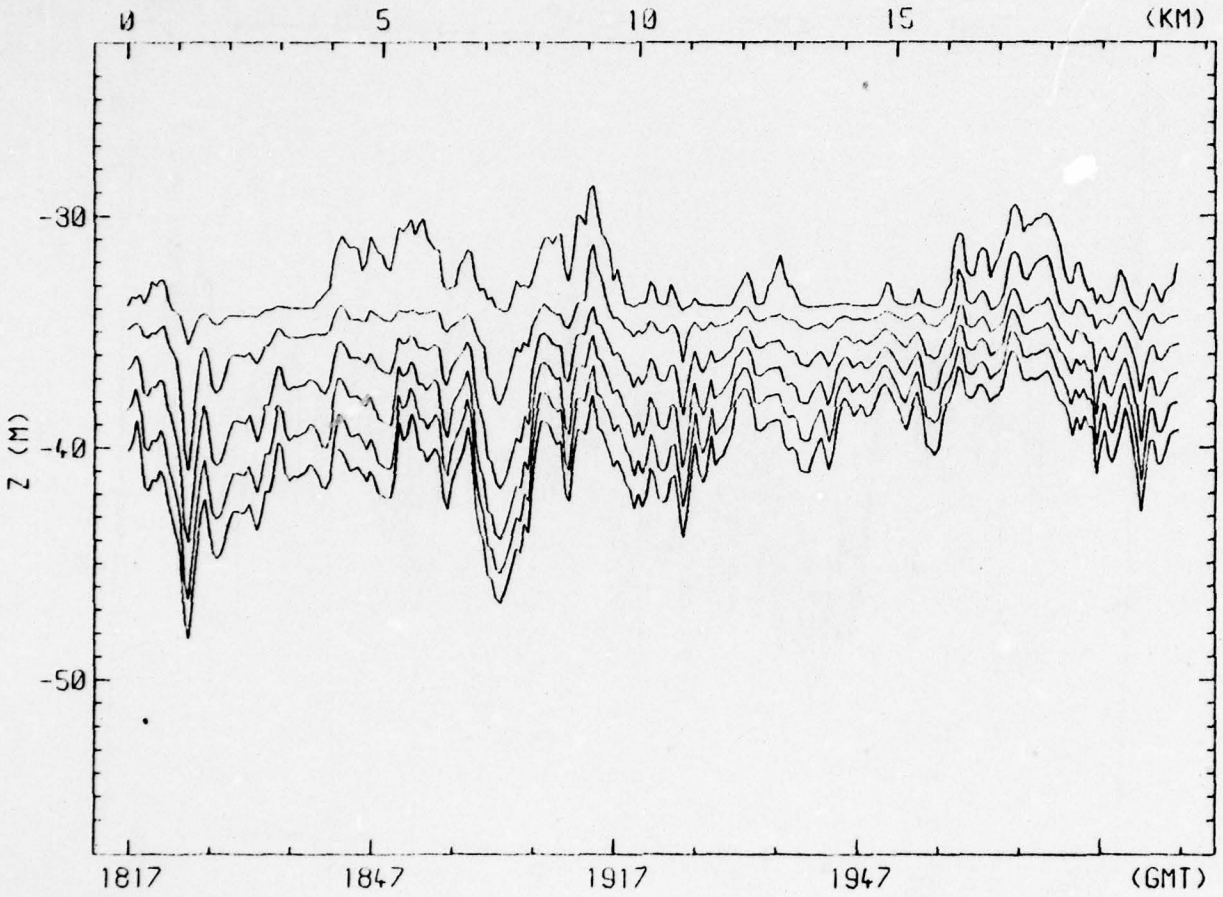

RUN 22 5 SEP 77 EDITED ISOTHERMS VS TIME/DISTANCE

T = 10.0, 10.5, 11.0, 11.5, 12.0, 12.3 DEG C

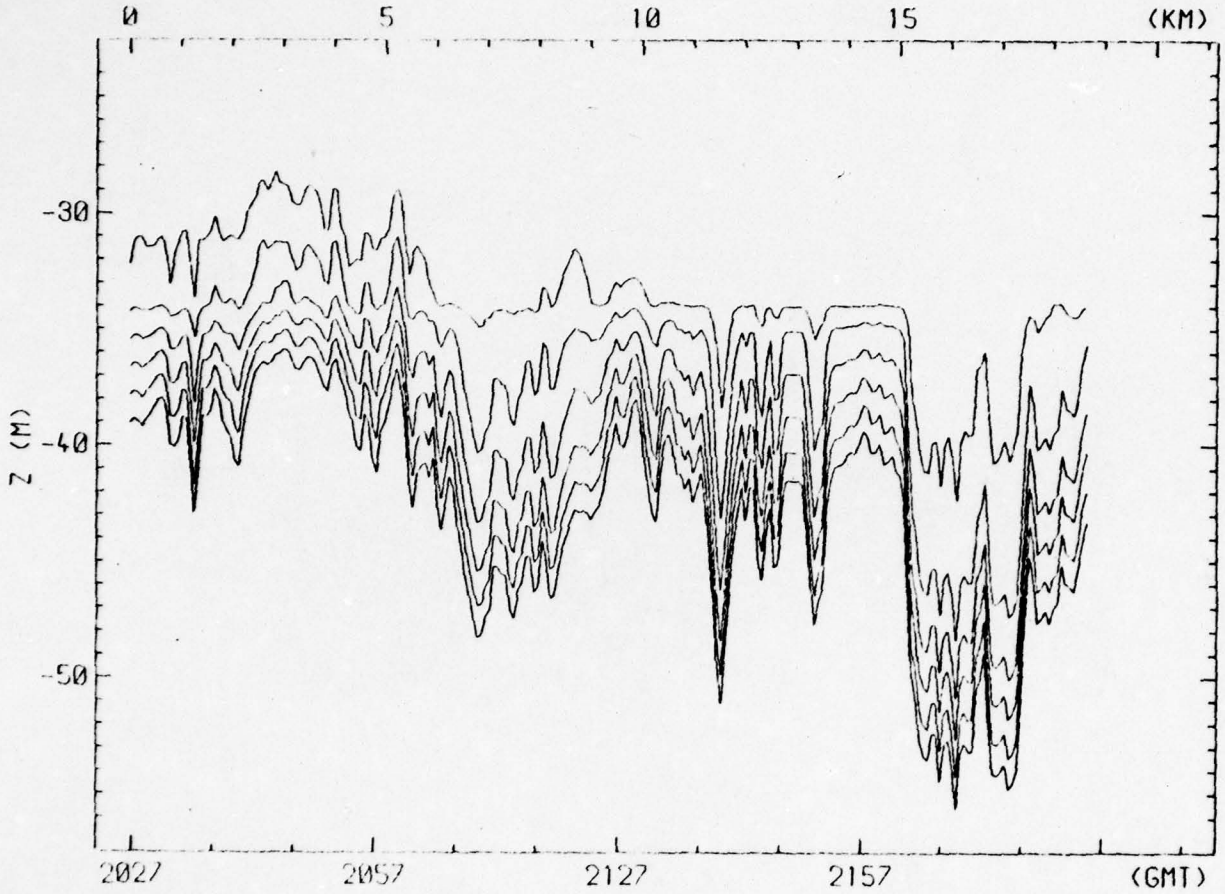

RUN 22 5 SEP 77 EDITED ISOTHERMS VS TIME/DISTANCE

T = 10.0, 10.5, 11.0, 11.5, 12.0, 12.3 DEG C

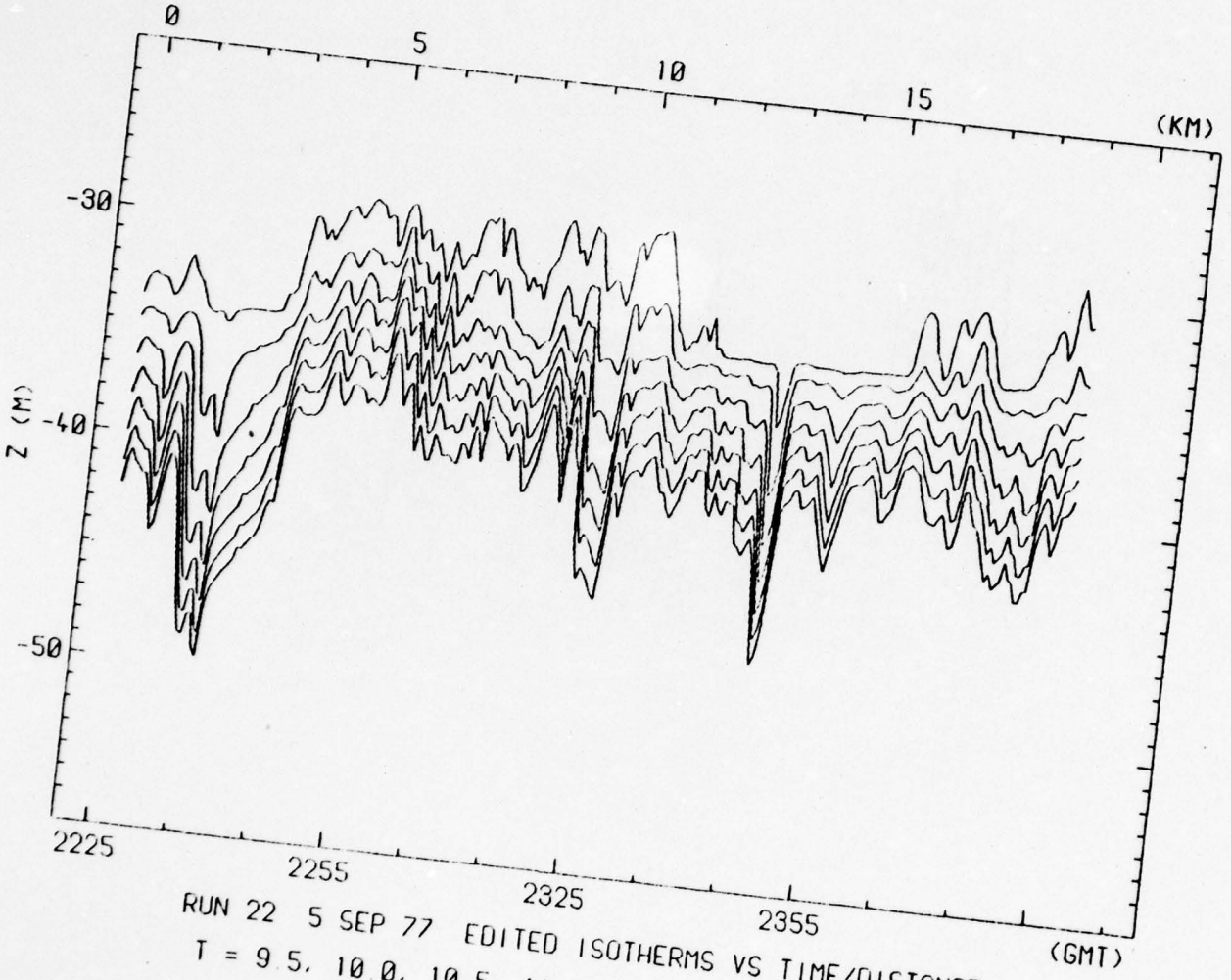

RUN 22 5 SEP 77 EDITED ISOTHERMS VS TIME/DISTANCE

T = 9.5, 10.0, 10.5, 11.0, 11.5, 12.0, 12.3 DEG C

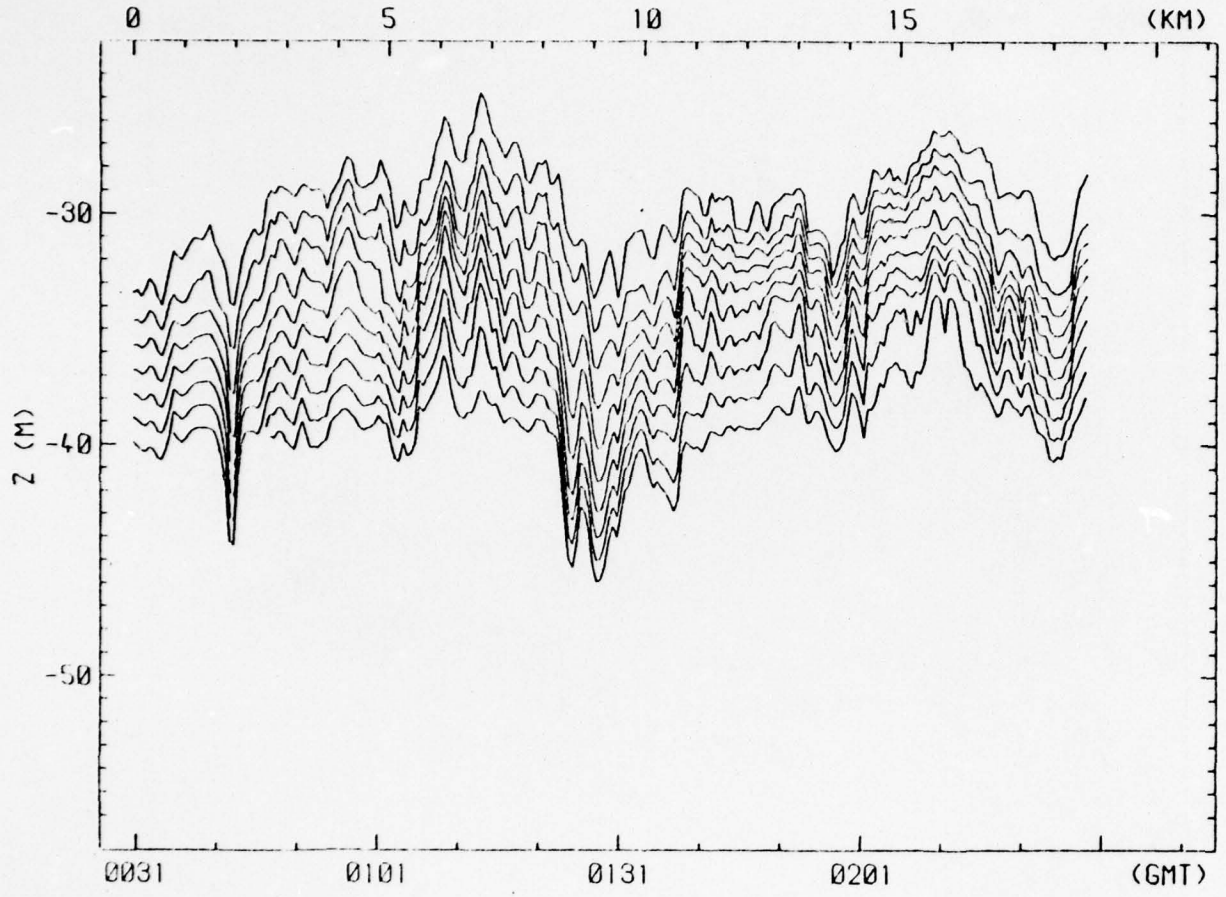

RUN 23 6 SEP 77 EDITED ISOTHERMS VS TIME/DISTANCE

T = 7.5 TO 12.0 DEG C IN 0.5 DEG INCREMENTS

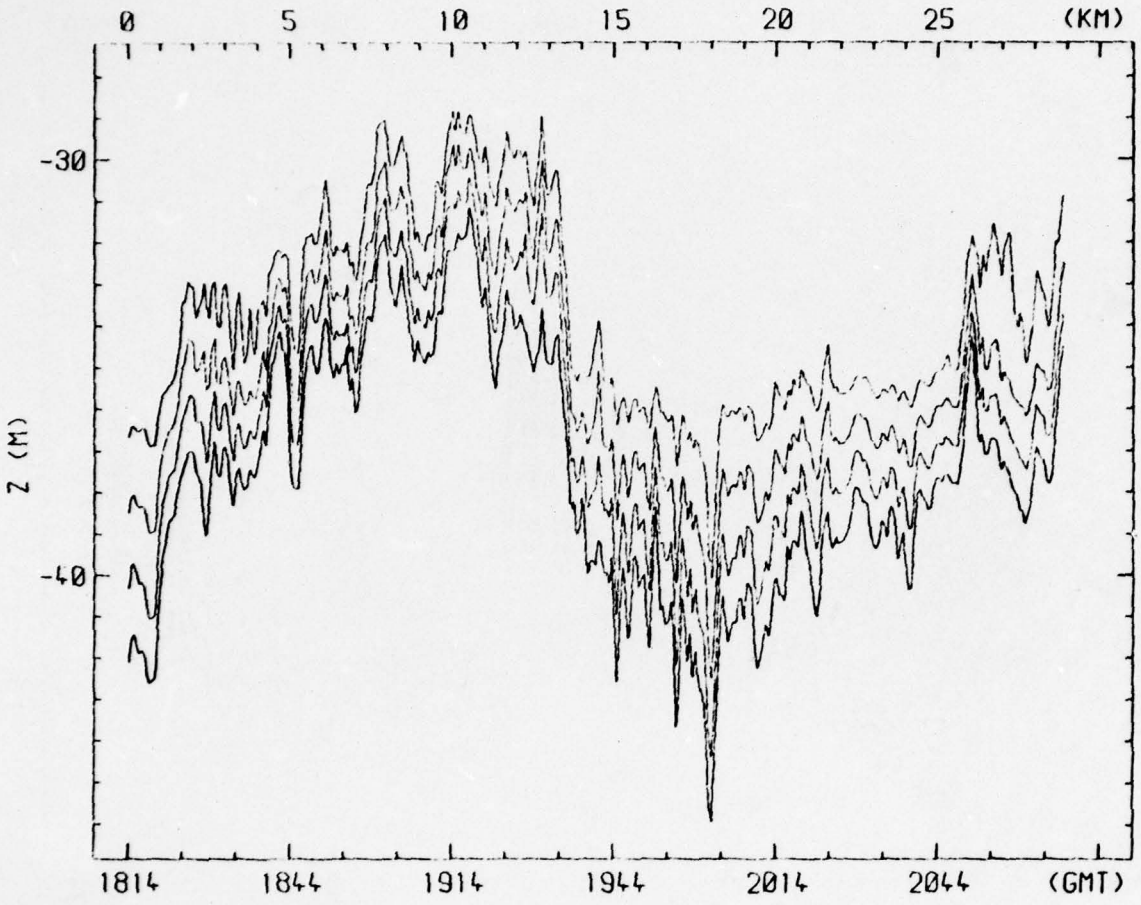

RUN 24 8 SEP 77 EDITED ISOTHERMS VS TIME/DISTANCE

T = 10.5 TO 12.0 DEG C IN 0.5 DEG INCREMENTS

APPENDIX C

Buoyancy Frequency Profiles

Plots of the horizontally averaged buoyancy frequency are presented in this section. The computational method is described in Appendix A. The values at the midpoints between thermistors are plotted. All plots use the same scales, which are shown only on the following page.

AD-A074 273 OREGON STATE UNIV CORVALLIS SCHOOL OF OCEANOGRAPHY F/G 8/3
TOWED OBSERVATIONS OF INTERNAL WAVES IN THE UPPER OCEAN.(U)
JUL 79 T J SPOERING N00014-76-C-0067
UNCLASSIFIED REF-79-10 NL

2 OF 2
AD A074273

END
DATE FILMED
10-79
DDC

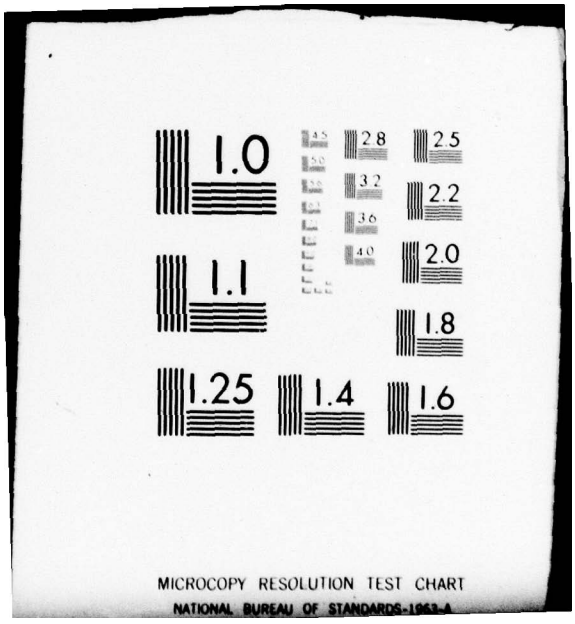
1.0
1.1
1.25
1.4
1.6
1.8
2.0
2.2
2.5
2.8
3.2
3.6
4.0
MICROCOPY RESOLUTION TEST CHART
NATIONAL BUREAU OF STANDARDS-1963-A

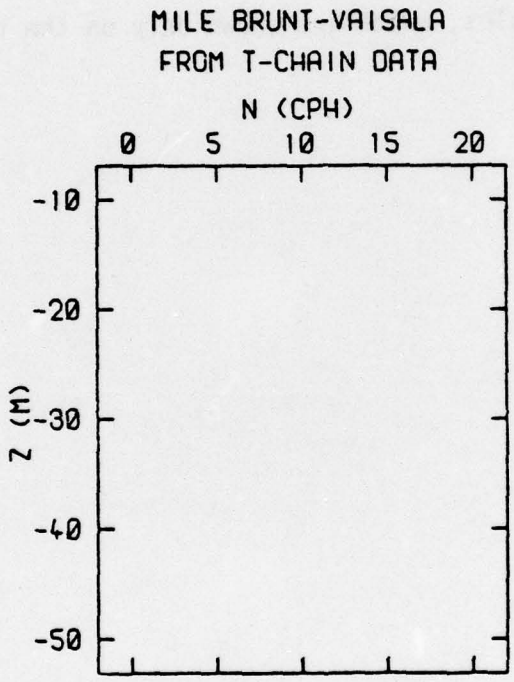
MILE BRUNT-VAISALA
FROM T-CHAIN DATA
N (CPH)
0
5
10
15
20
-10
-20
-30
-40
-50
Z (M)

RUN 01

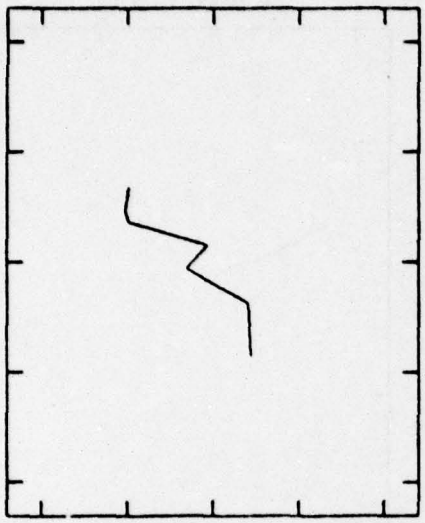

RUN 02

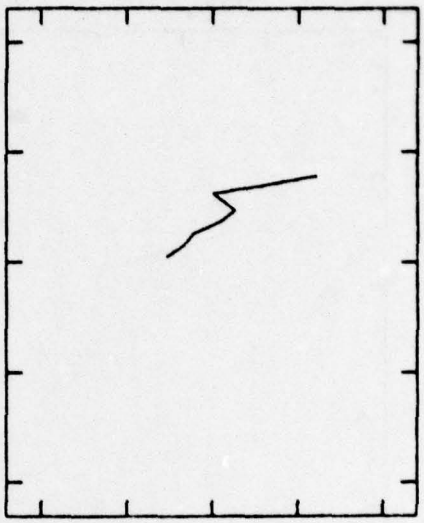

RUNS 4-5

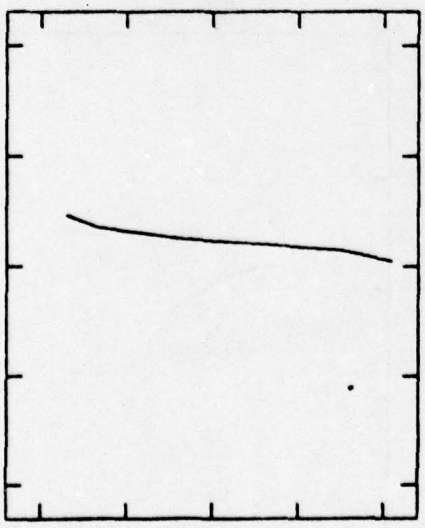

RUN 11A

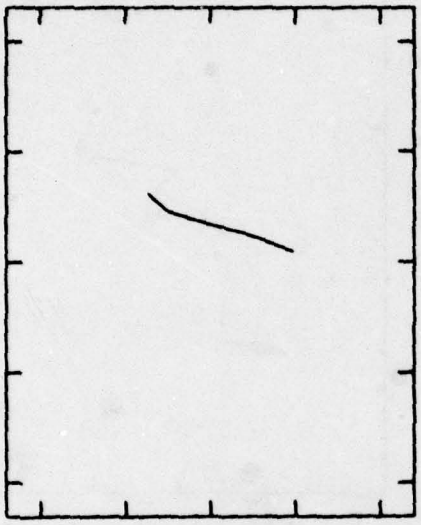

RUN 11B

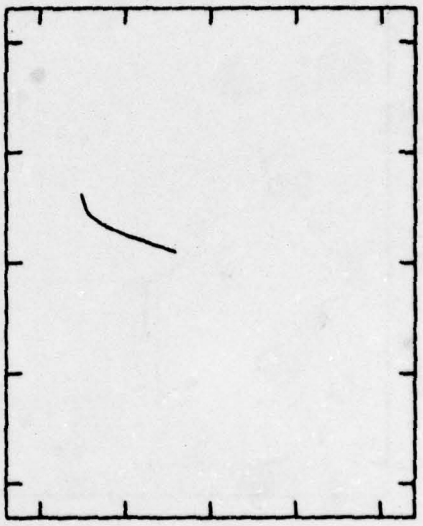

RUN 12A

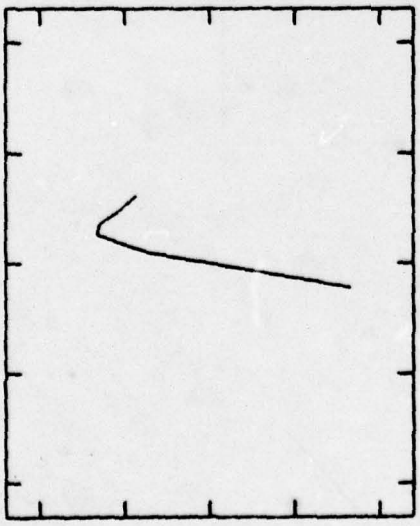

RUN 12B

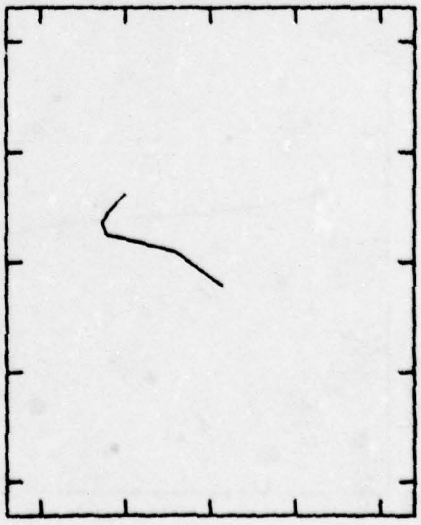

RUN 13A

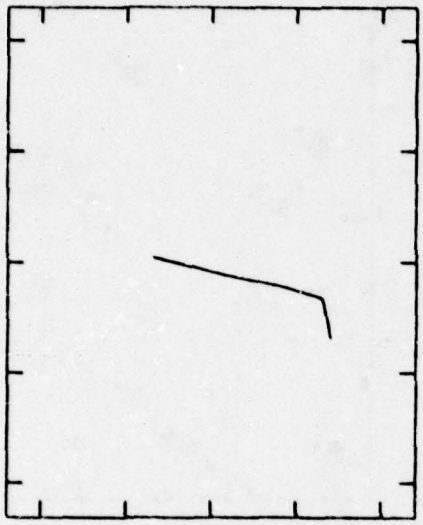

RUNS 13-14

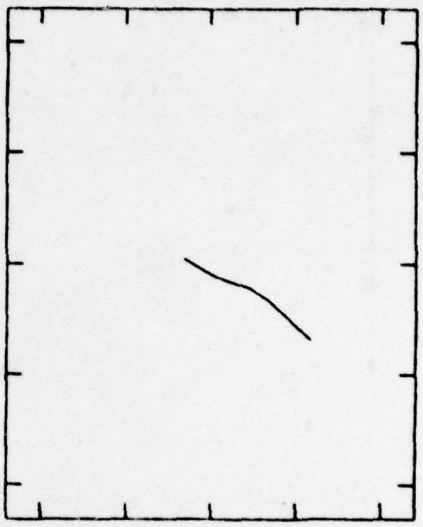

RUN 14B

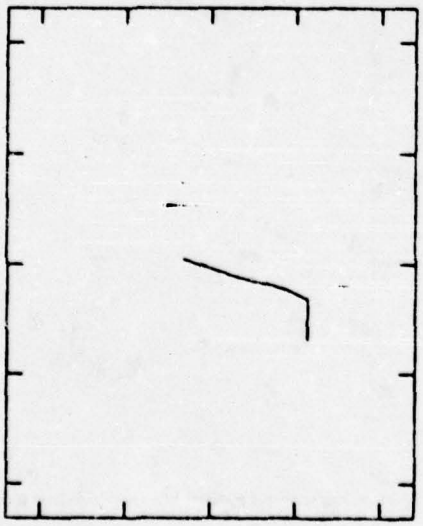

RUN 15A

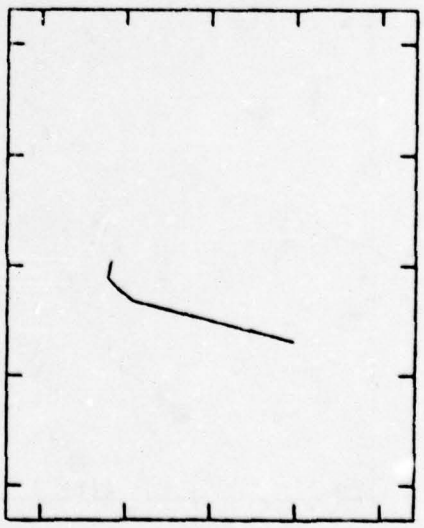

RUN 15B

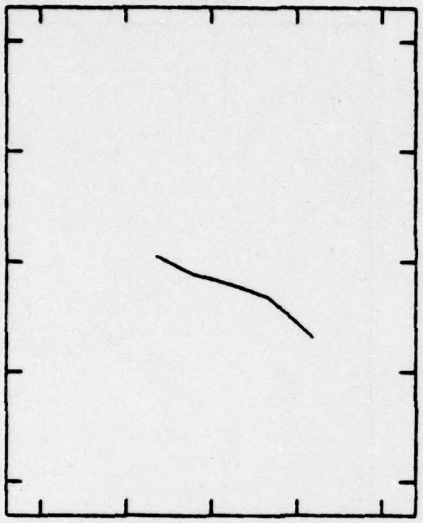

RUN 16

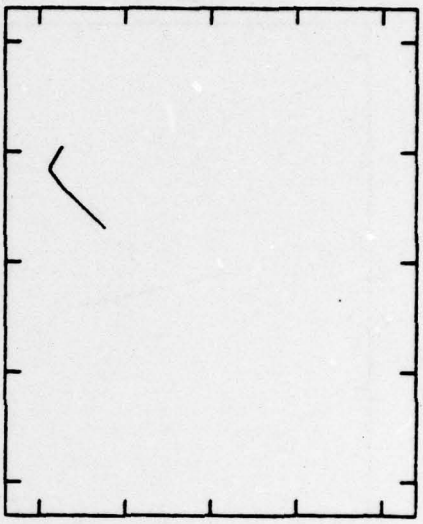

RUN 17A

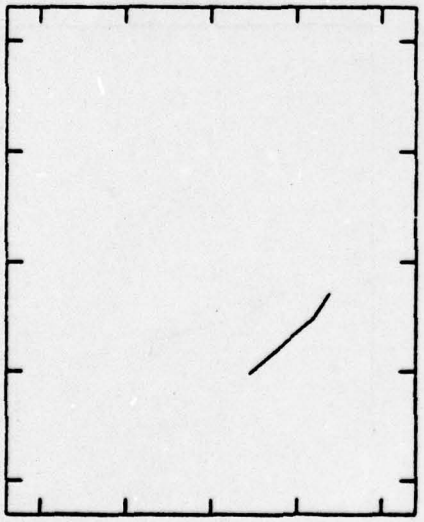

RUNS 17-18

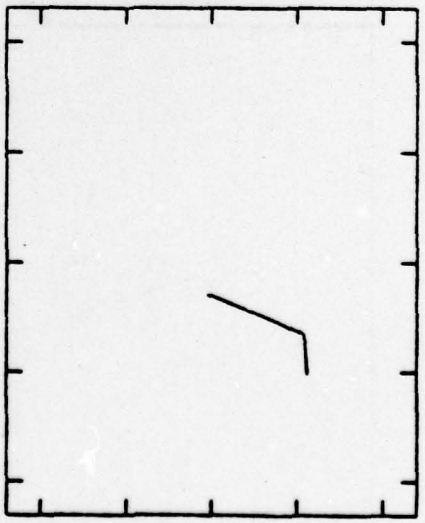

RUN 19

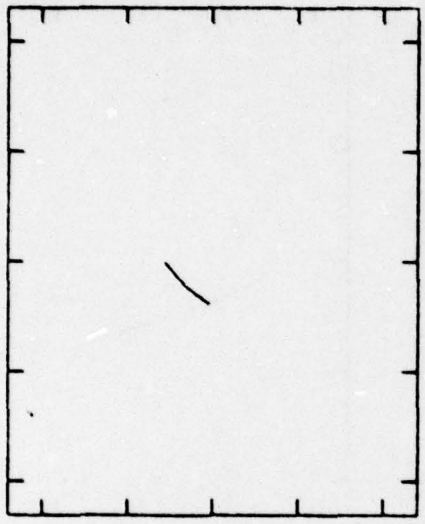

RUN 20

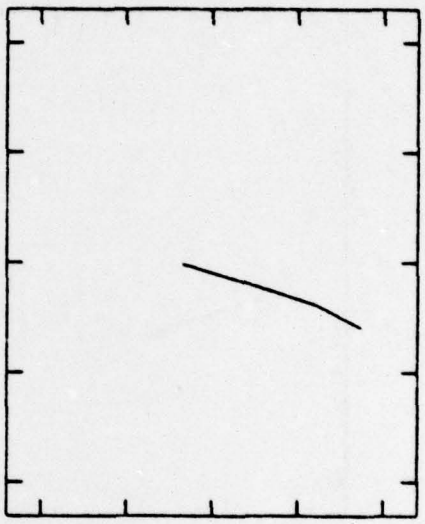

RUN 21A

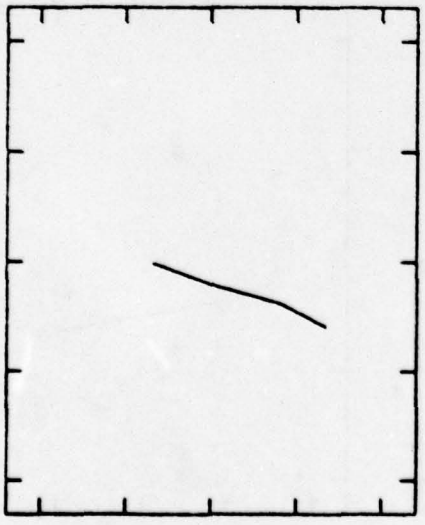

RUN 21B

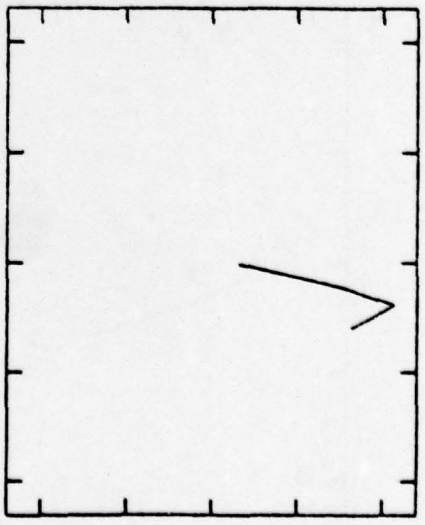

RUN 22A

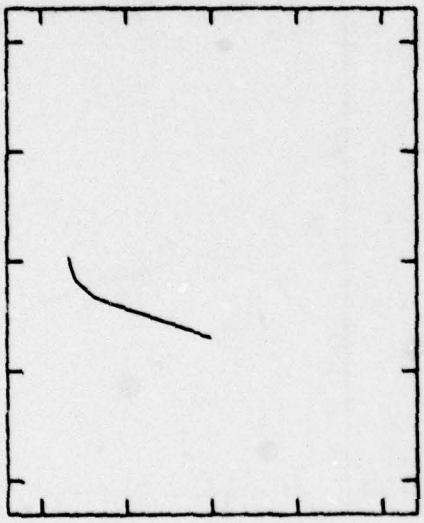

RUN 22B

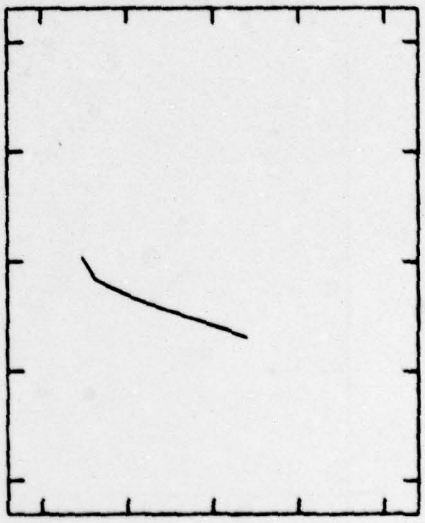

RUN 22C

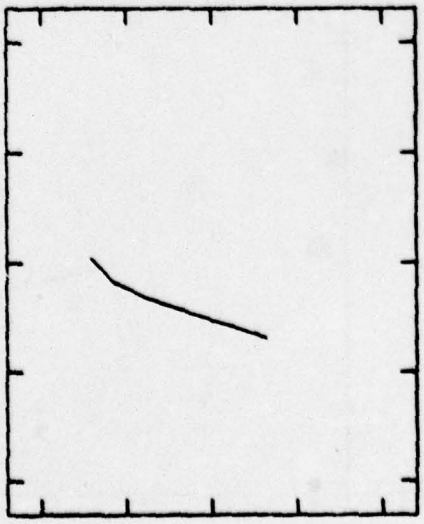

RUN 22D

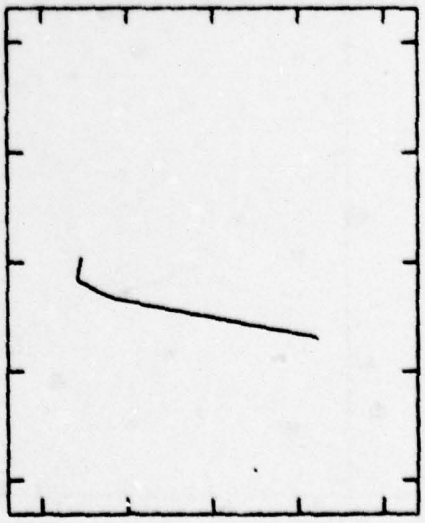

RUN 22E

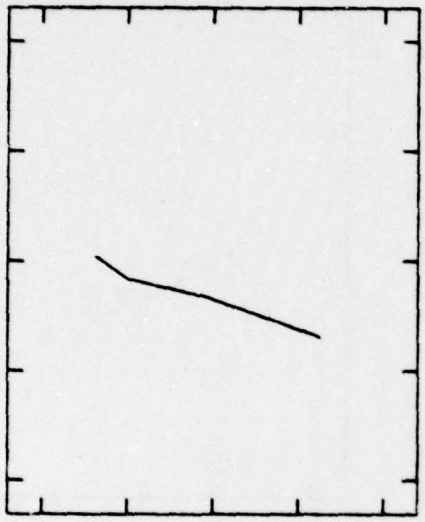

RUN 22F

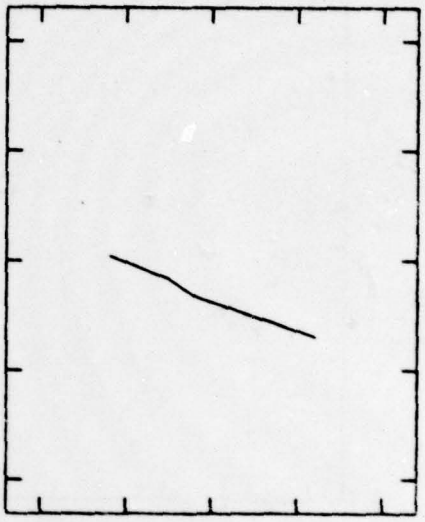

RUN 22G

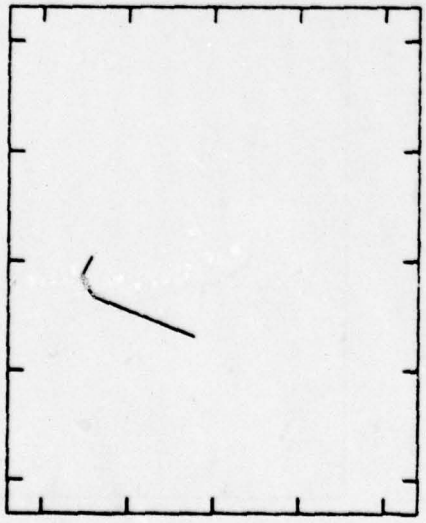

RUN 22H

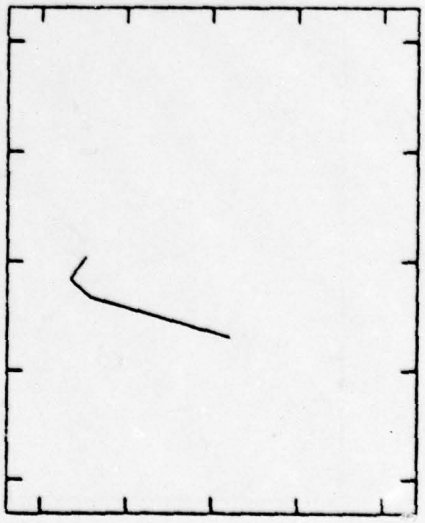

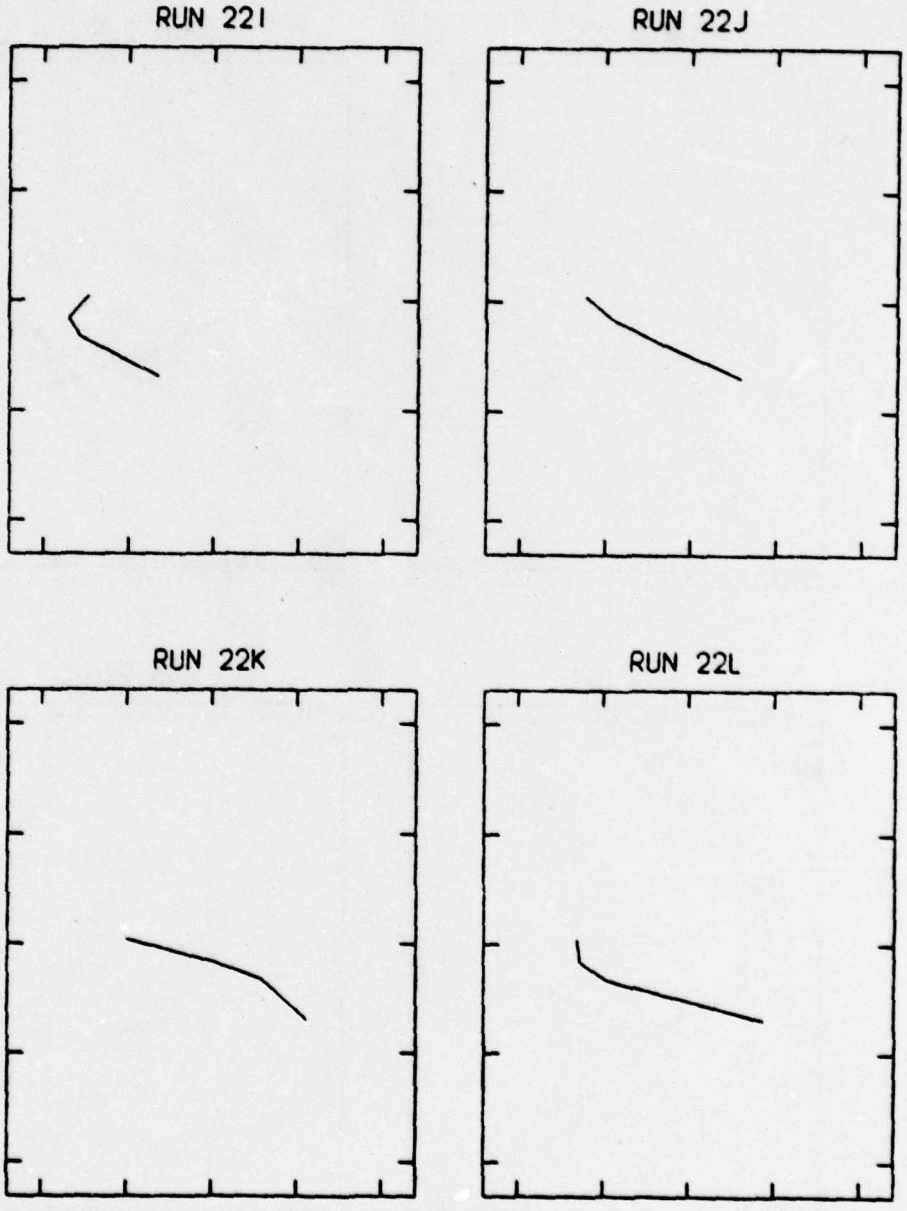
RUN 22I
RUN 22J
RUN 22K
RUN 22L

RUN 22M

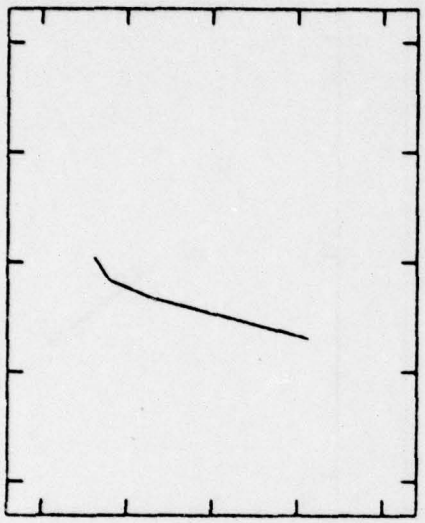

RUN 23A

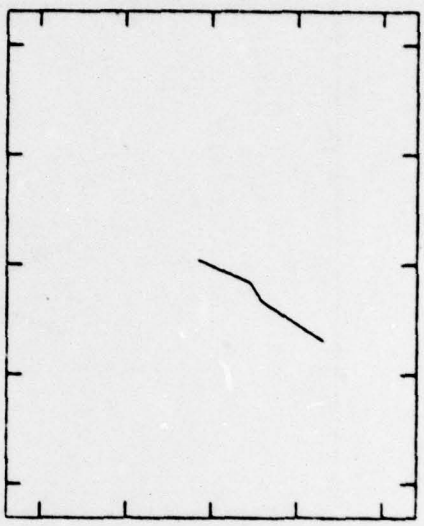

RUN 23B

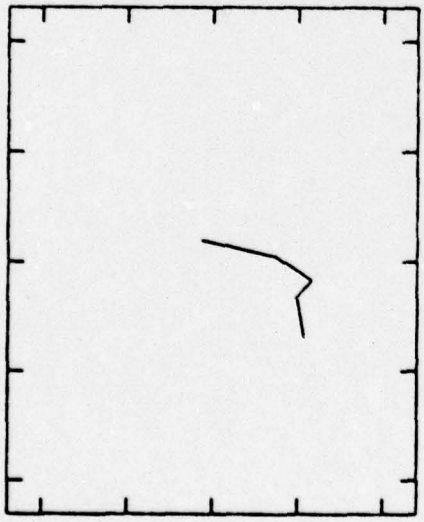

RUN 23C

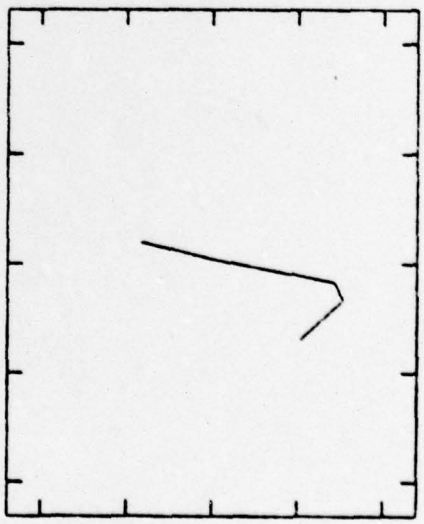

RUN 230

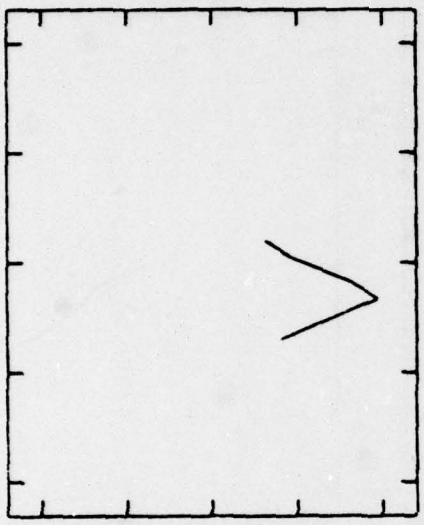

RUN 24

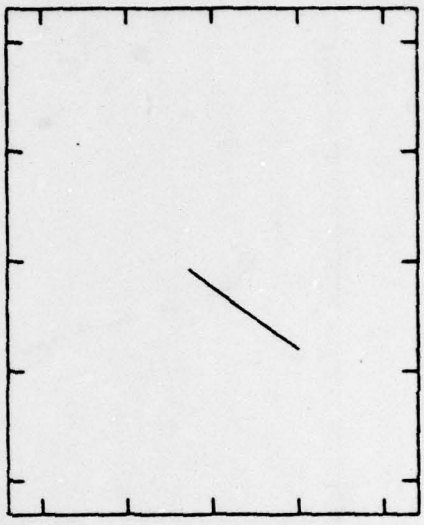

APPENDIX D

Spectral Analysis Methods

Standard spectral analysis techniques were used in processing the data for this study and only pertinent details will be noted here. Excellent references for the subject are the test by Bäth (1974) and the Ph.D. thesis by Andreas[†] (1977).

The complex form of the Fourier coefficients were used in the analysis. That is, a data series x_k, k = 0, 1, ..., N-1 is represented as

$$x_k = \frac{1}{N} \sum_{k=0}^{N-1} X_n \, e^{\frac{2\pi i n k}{N}} \qquad \text{for } k = 0, 1, \ldots, N-1$$

The period of the data series is denoted by T and the sampling interval by Δ, so that $T = N\Delta$. The complex Fourier coefficients are given by

$$X_n = \sum_{n=0}^{N-1} x_k \, e^{\frac{-2\pi i n k}{N}} \qquad \text{for } n = 0, 1, \ldots, N-1$$

Note that in this representation X_n is symmetric about $\frac{N}{2} - 1$, if x_k is a real data series. That is $X_{N-n} = X_n^*$, where X_n^* denotes the complex conjugate of X_n. The power spectrum is then given by

$$P_{xn} = \frac{2}{N^2} X_n X_n^* \qquad \text{for } n = 0, 1, \ldots \frac{N}{2} - 1.$$

The power spectral density is defined as $\phi_{xn} = T \, P_{xn}$. If x_k is a real data series, then P_{xn} are also real. In practice, the terms "spectrum" and "spectral density" are often used interchangeably. The approach taken

[†]Andreas, E. L., 1977: Observations of velocity and temperature and estimates of momentum and heat fluxes in the internal boundary layer over Arctic leads, Ph.D. Thesis, Oregon State University 263 p.

in this study is to use "spectral density" but to refer to it as the "spectrum".

Now suppose a second data series, y_k, k = 0, 1 ..., N-1 exists with Fourier coefficients Y_k. The cross spectrum of the two series is given by

$$P_{xyn} = \frac{2}{N^2} X_n Y_n^* \quad \text{for } n = 0, 1, \ldots \frac{N}{2} - 1$$

and cross spectral density is $\phi_{xyn} = T P_{xyn}$. This series will be complex, with the real part called the cospectrum and the imaginary part the quad-spectrum. The equivalent polar representation is the coherence squared and phase, given by

$$Coh^2_{xyn} = \frac{(Co^2 + Quad^2)^{\frac{1}{2}}}{\phi_{xn}\, \phi_{yn}}$$

$$\phi_{xyn} = \arctan\left(\frac{Quad_{xyn}}{Co_{xyn}}\right)$$

In this study coherence values rather than coherence squared are used.

The spectral estimates are smoothed by bands that are equally spaced on a logarithmic scale. Ensemble averaging of several series is done in a similar manner of the coefficient of the individual series. Confidence limits can be calculated by assuming a chi-squared distribution of the estimates in each band. The variance is used to compute the equivalent degrees of freedom for each band averaged ϕ: $\nu = \frac{2\phi^2}{\text{variance}(\phi)}$. The true value for ϕ, denoted as $\tilde{\phi}$, can then be estimated as being in the interval

$$\frac{\nu\phi}{\chi^2_{\nu:1-\alpha}} < \tilde{\phi} < \frac{\nu\phi}{\chi^2_{\nu:\alpha}}$$

At the 95% confidence level, $\alpha = 0.025$, the χ^2 values can be approximated by

$$\chi^2_{\nu:0.025} \simeq \nu(1 + 9.892\nu^{-3.4})\ (1 - \frac{2}{9\nu} - 1.96(\frac{2}{9\nu})^{\frac{1}{2}})^3$$

$$\chi^2_{\nu:0.975} \simeq \nu(1 - \frac{2}{9\nu} + 1.96(\frac{2}{9\nu})^{\frac{1}{2}})^3$$

For coherence, a 95% significance level is computed for the band averaged values. This level can be determined after Julian (1975):
$\gamma = (1 - p^{1/(n-1)})^{\frac{1}{2}}$, where 1-p is the significance level (here p is 0.05 for 95%) and n is the number of samples averaged.

Various schemes for windowing, detrending, and filtering the series were tried and abandoned. Frankignoul (1974) studied the problems of determining internal wave spectra from short series and found end point jump to be a major source of contamination. One method he suggested to minimize these effects was chosen for the present study. The data series is first pre-whitened by taking the first forward difference:

$$y_k = x_{k+1} - x_k \qquad k = 0, 1 \ldots, N-2$$

$$y_{N-1} = y_{N-2}$$

After the spectrum is computed, it is recolored by division by $2(1 - \cos(\frac{2\pi k}{N}))$, the transform of the differencing scheme.

APPENDIX E

Spectra

Plots of the autospectra for the lowest and highest isotherms of individual tow legs are presented in this appendix. Again, only edited isotherm series that were at least 80% complete before editing were used. All the plots have the same scales, which are given on the following page only. Symbols used on the plots are: X for the spectrum of the lowest isotherm of the leg, and + for the spectrum of the highest. For actual isotherm values and depths, see the listings in Appendix A.

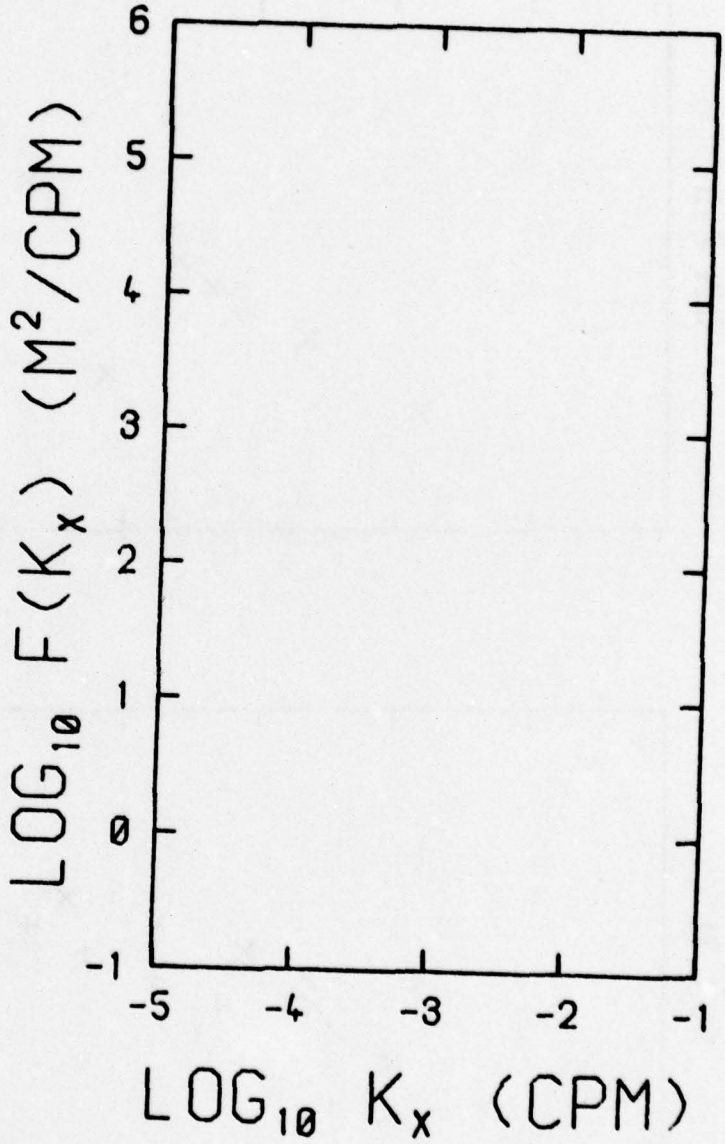
6
5
4
3
2
1
0
-1
-5
-4
-3
-2
-1
LOG10 F(Kx) (M2/CPM)
LOG10 Kx (CPM)

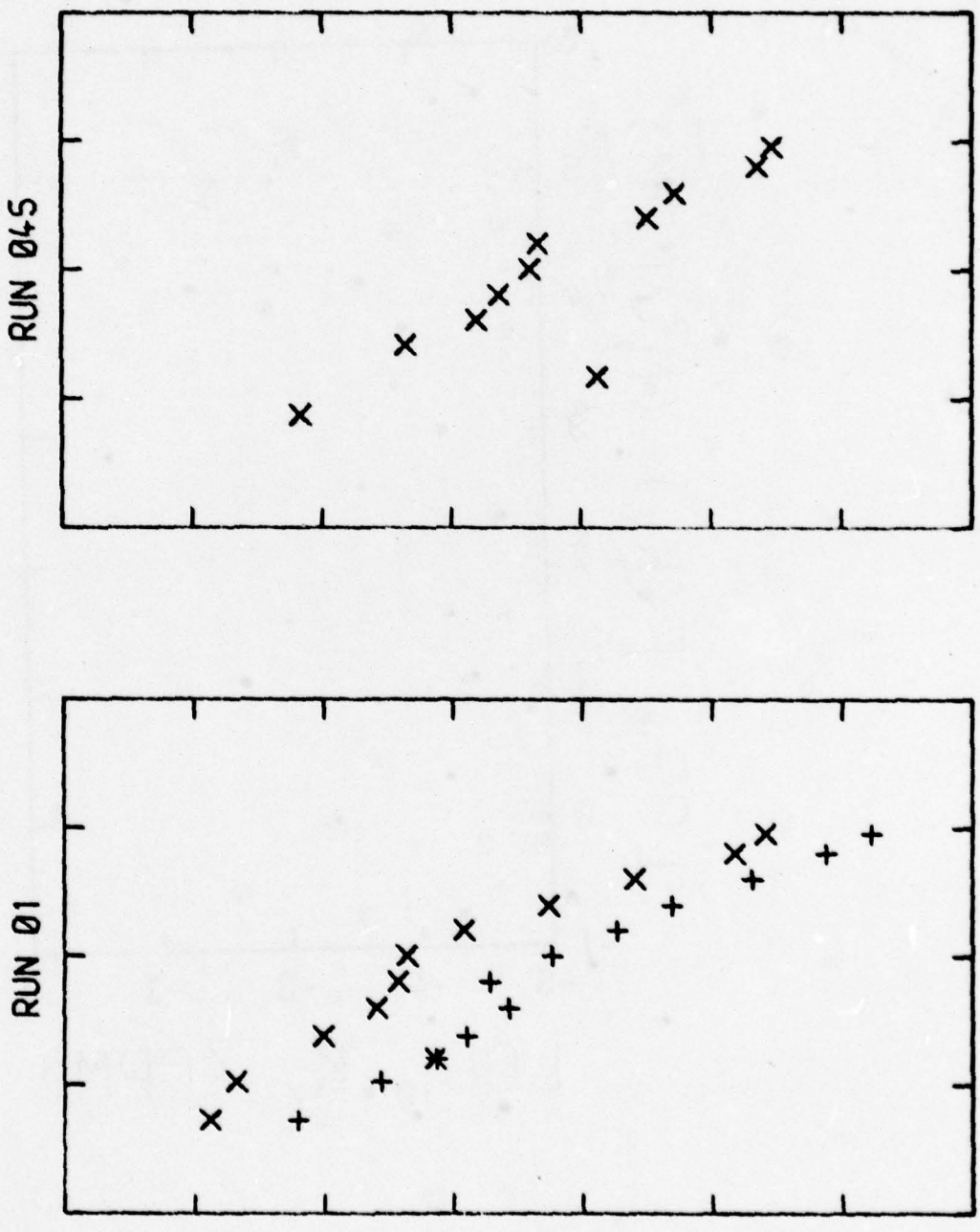
RUN 045
RUN 01

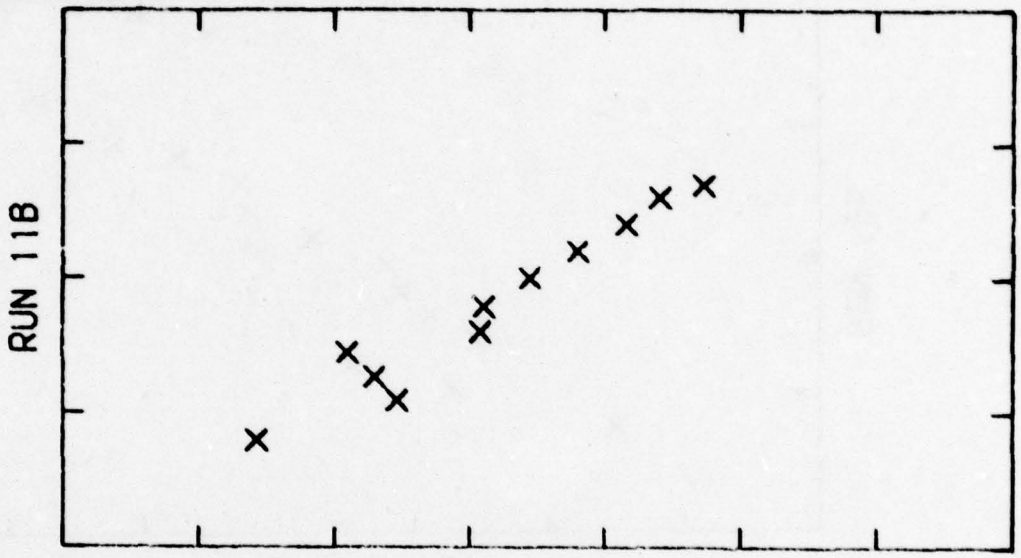
RUN 11B

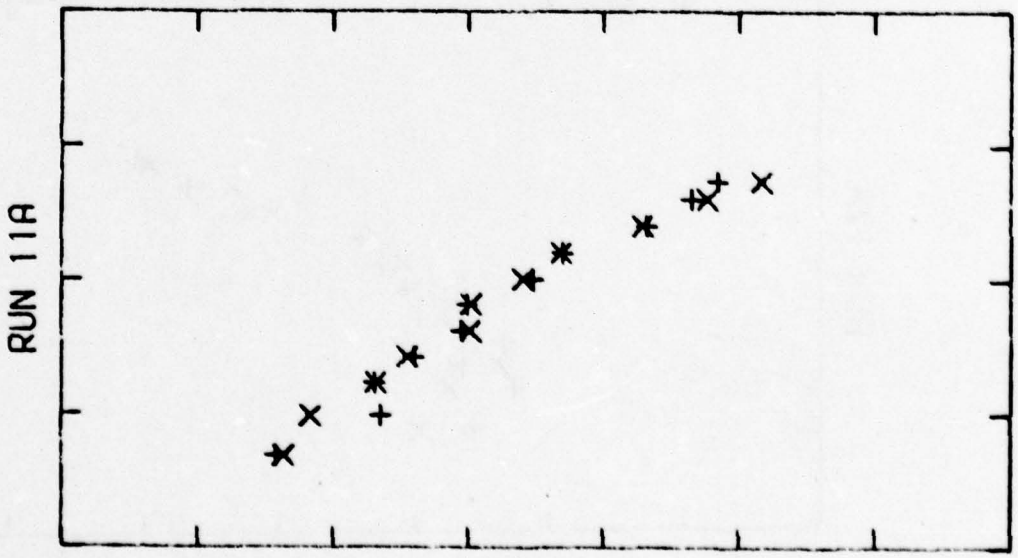
RUN 11A

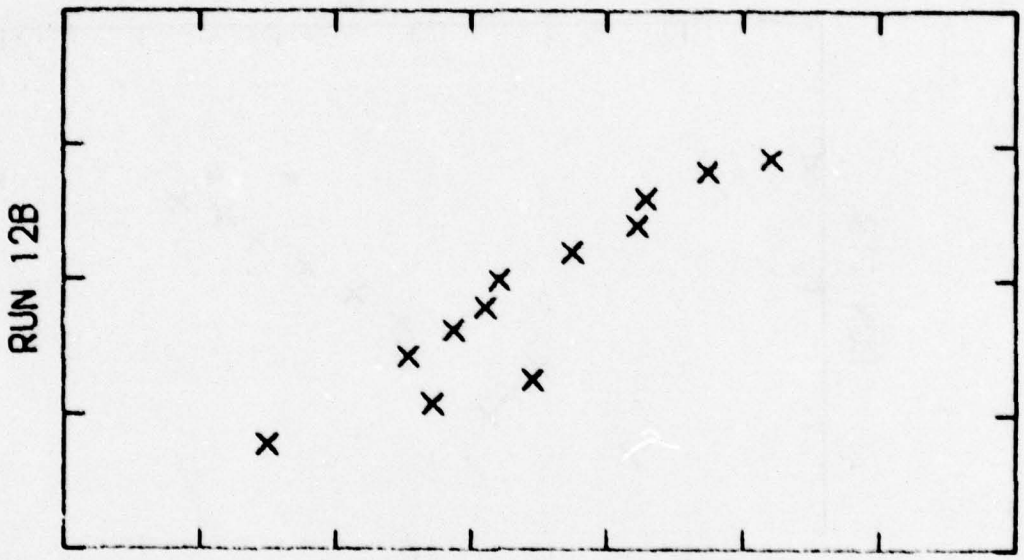
RUN 12B

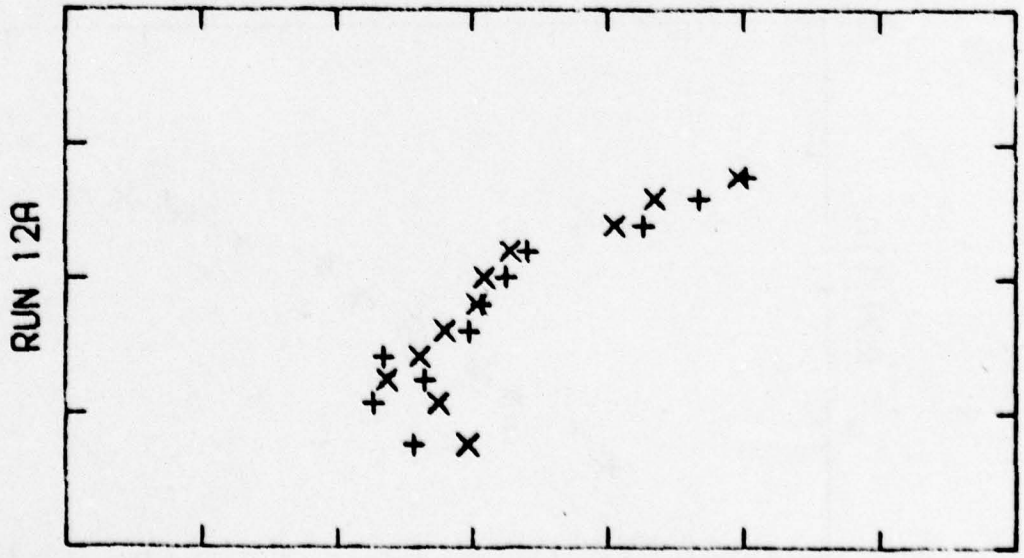
RUN 12A

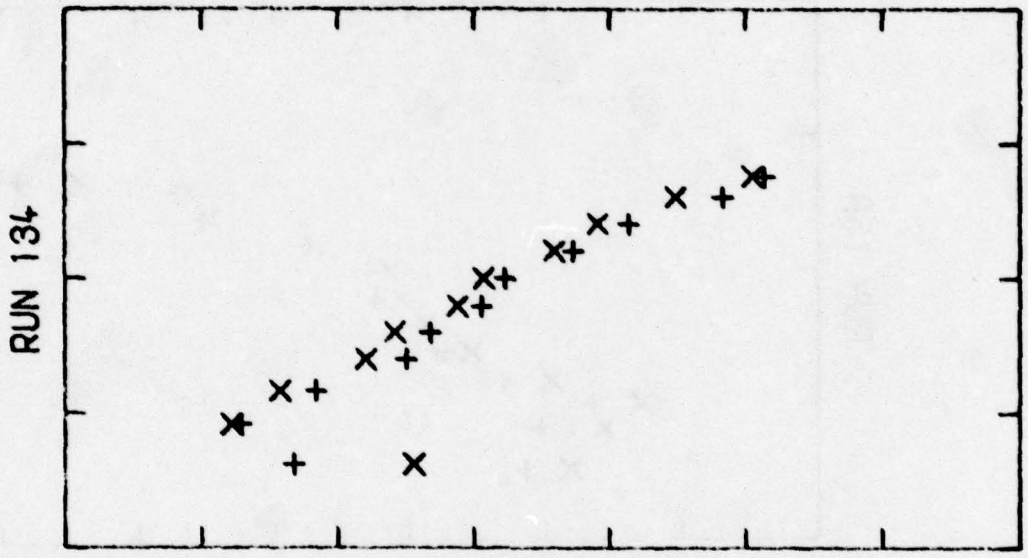
RUN 13A

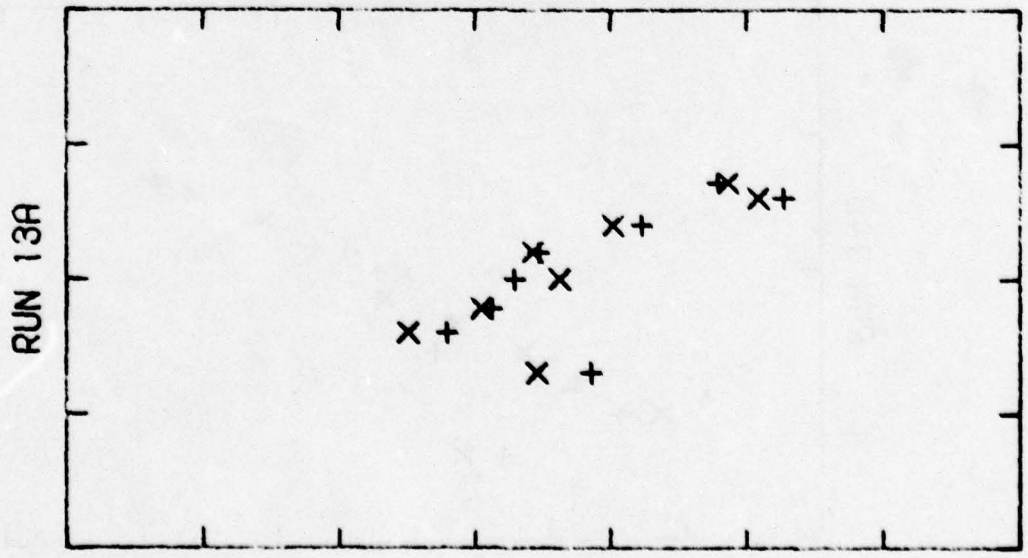
RUN 13A

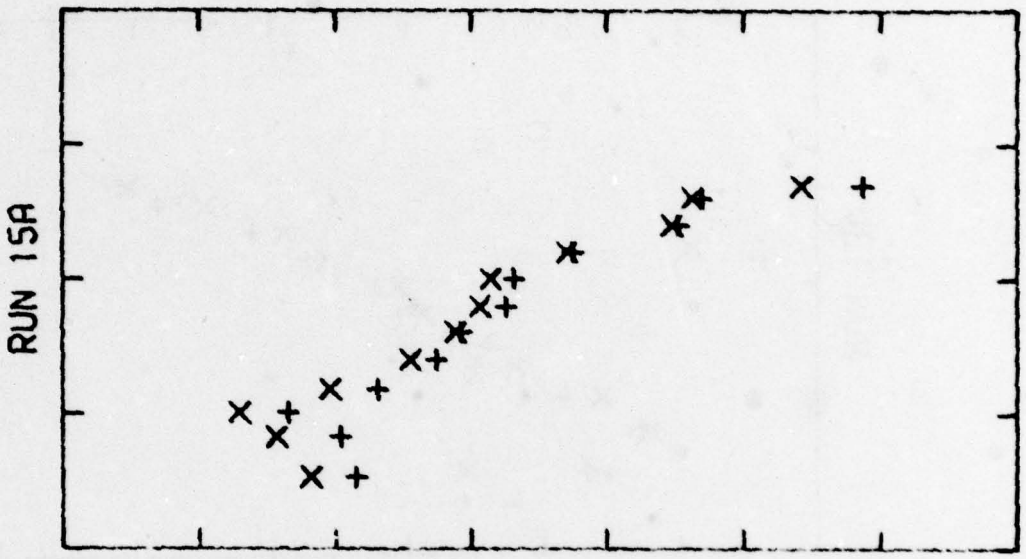
RUN 15A

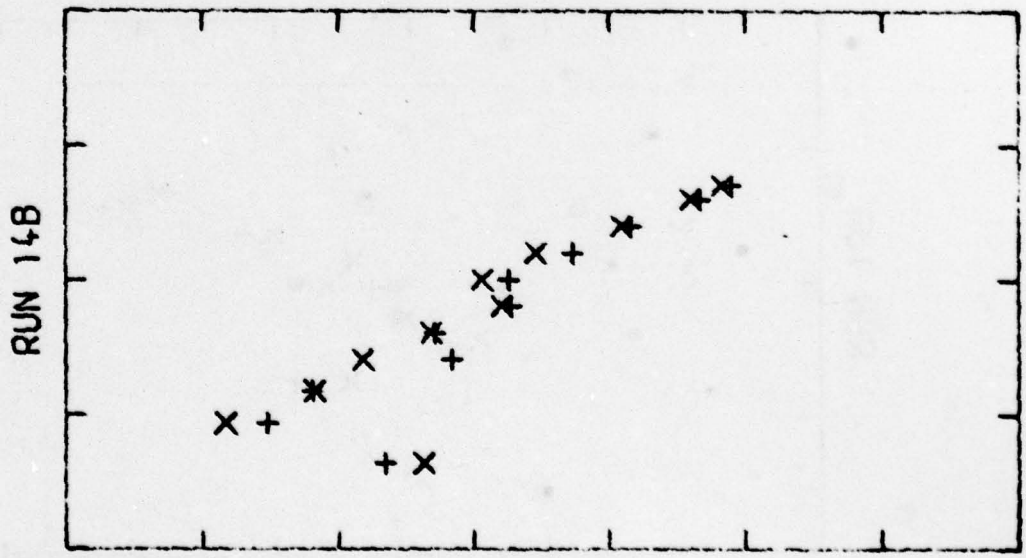
RUN 14B

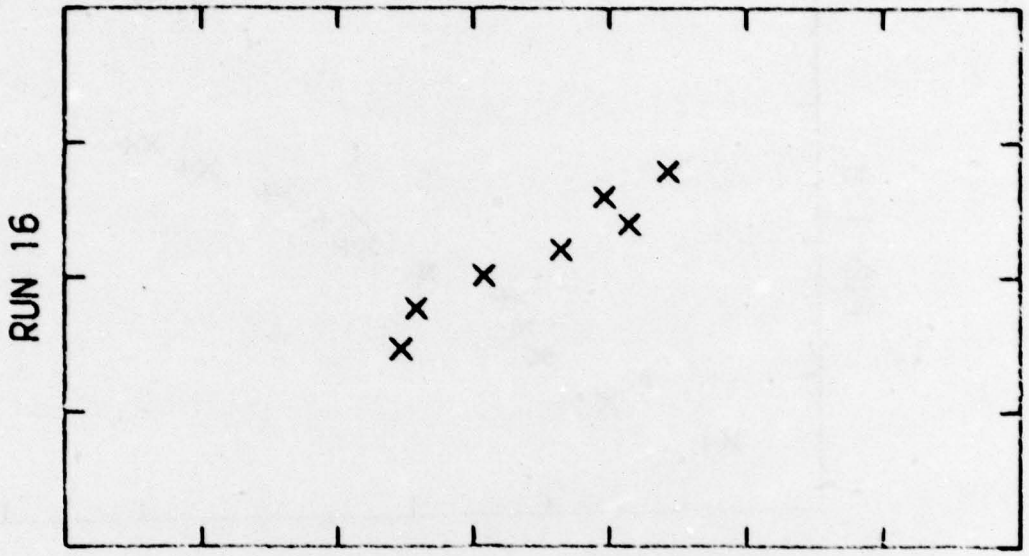
RUN 16

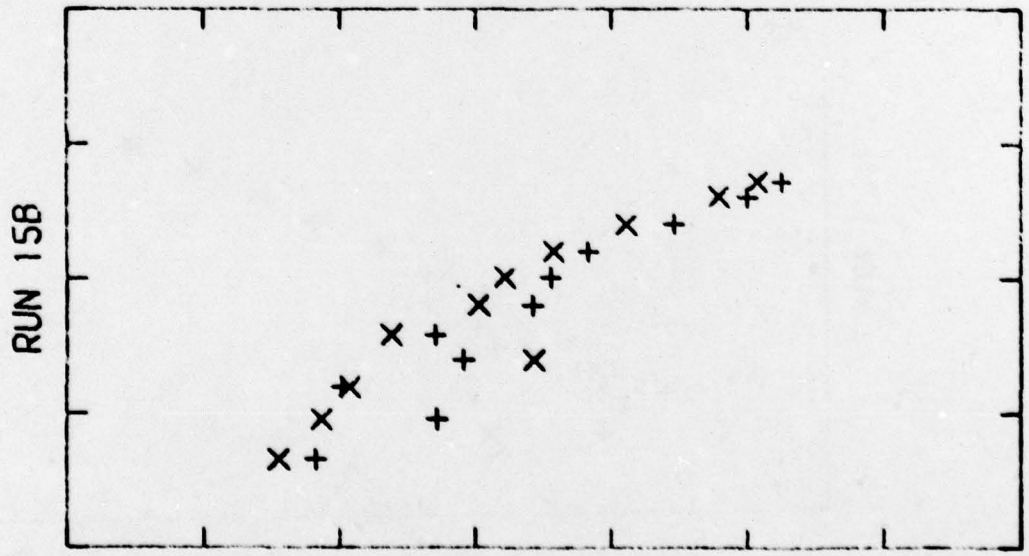
RUN 15B

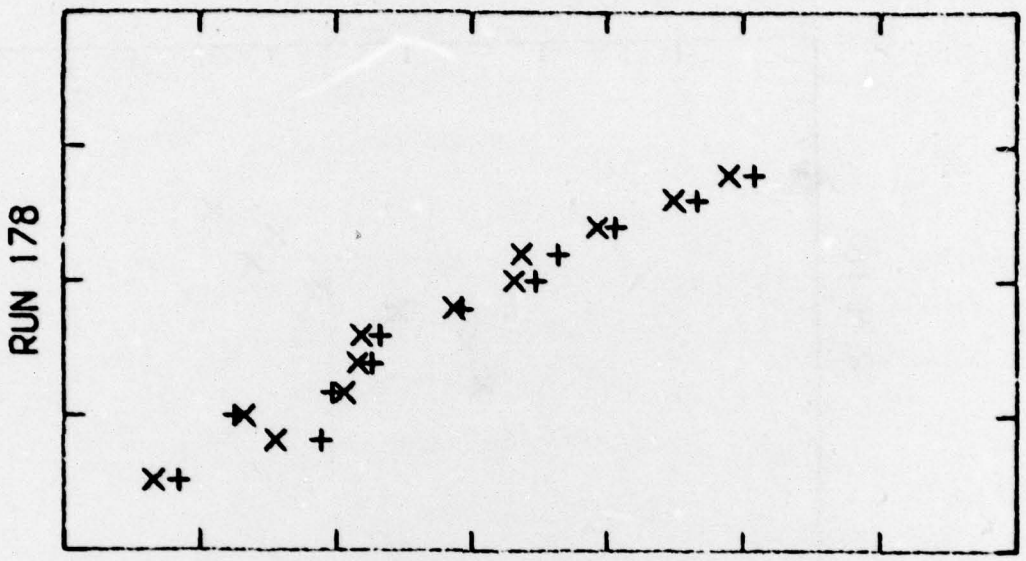
RUN 178


RUN 17A

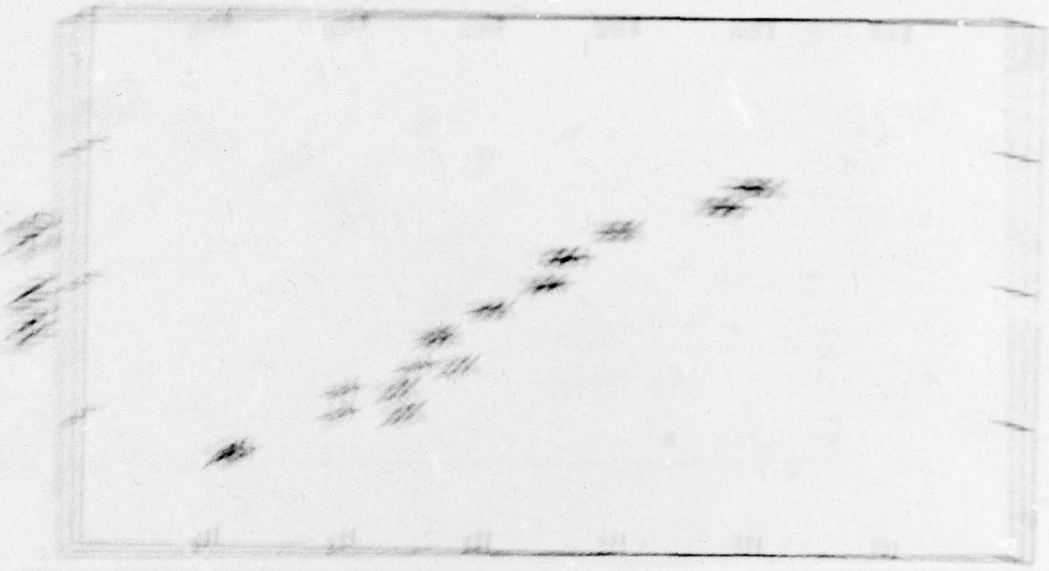

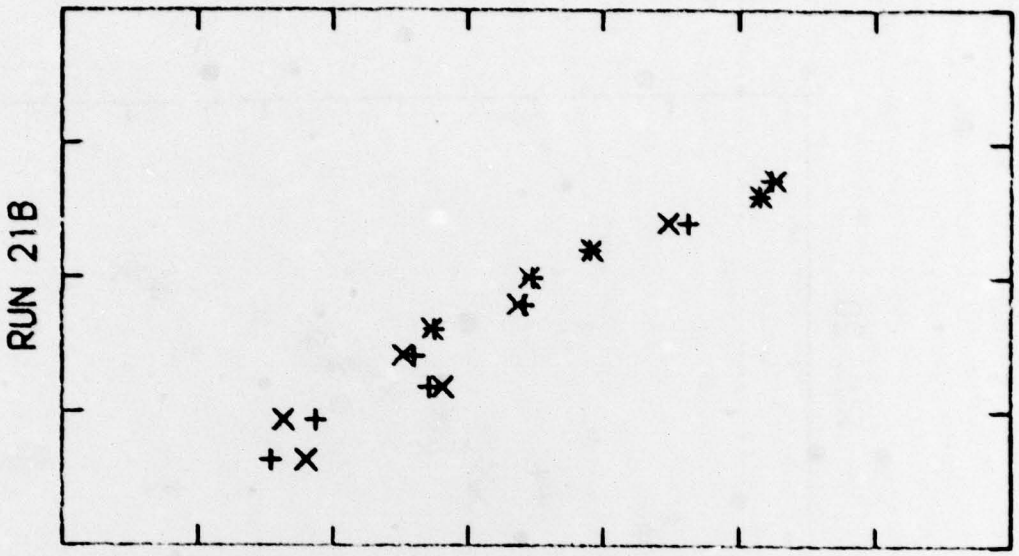
RUN 21B

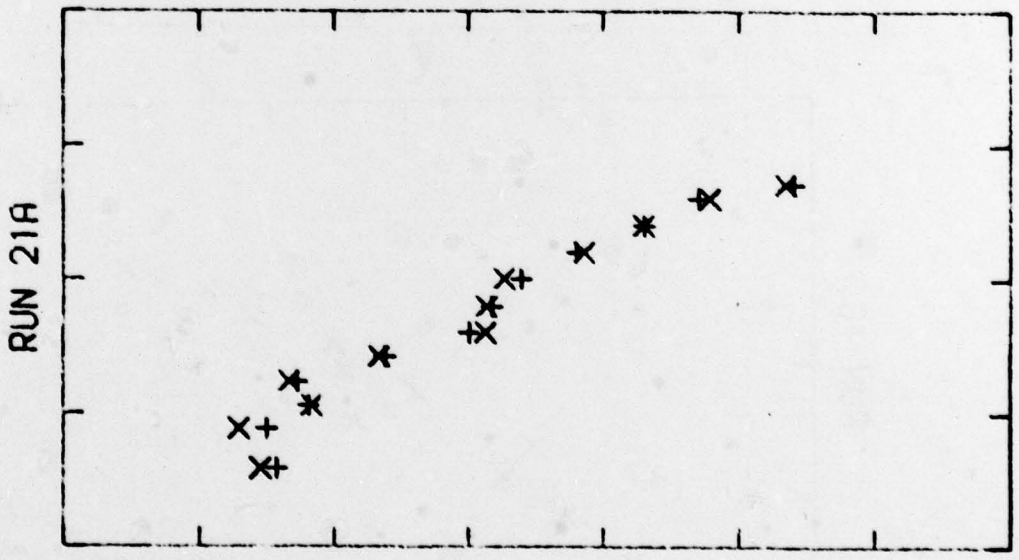
RUN 21A

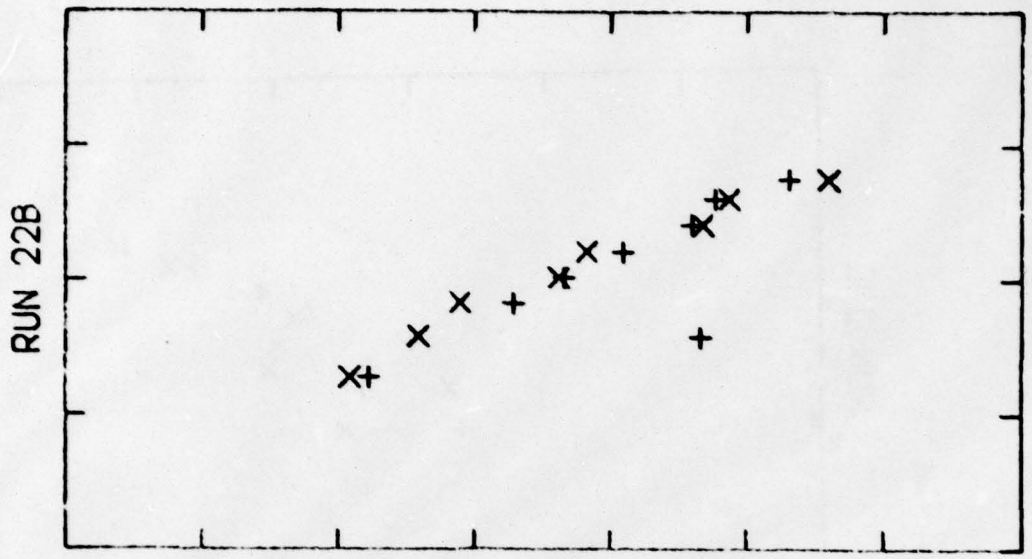
RUN 22B

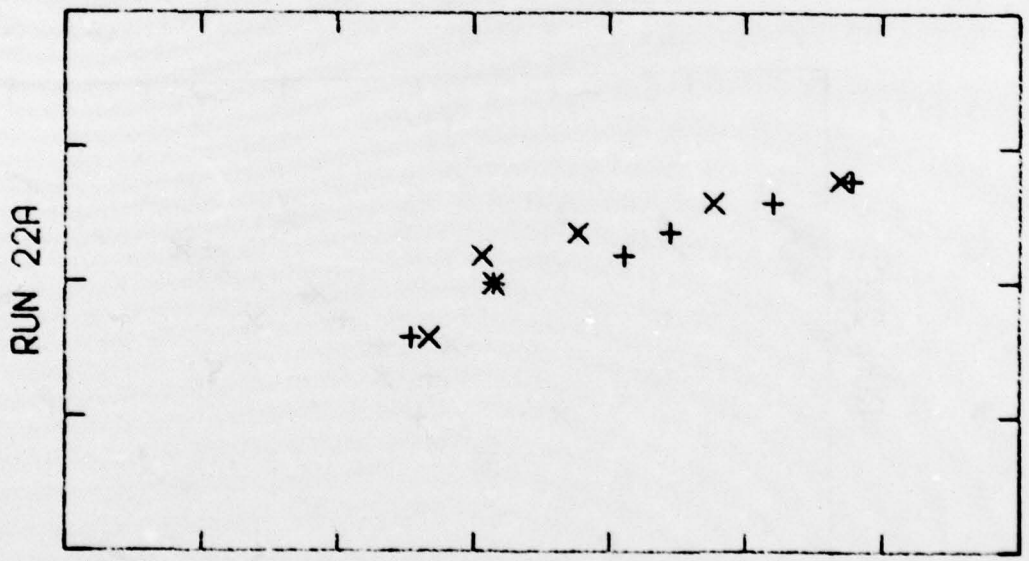
RUN 22A

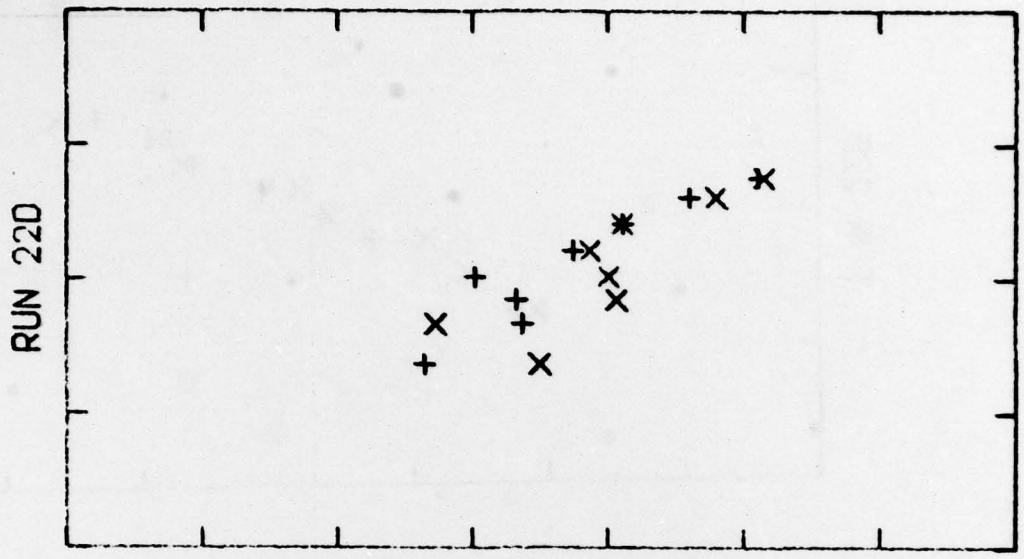
RUN 22D

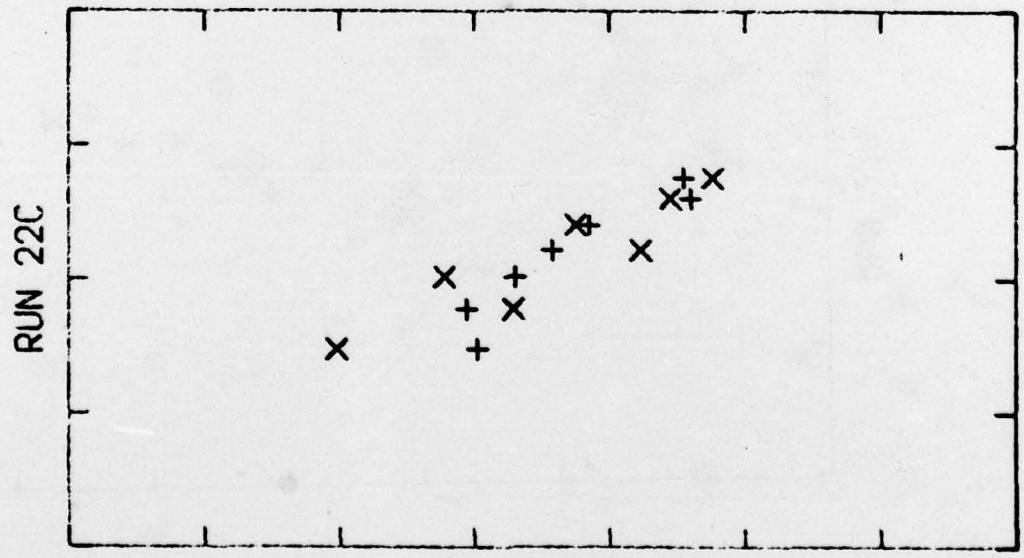
RUN 22C

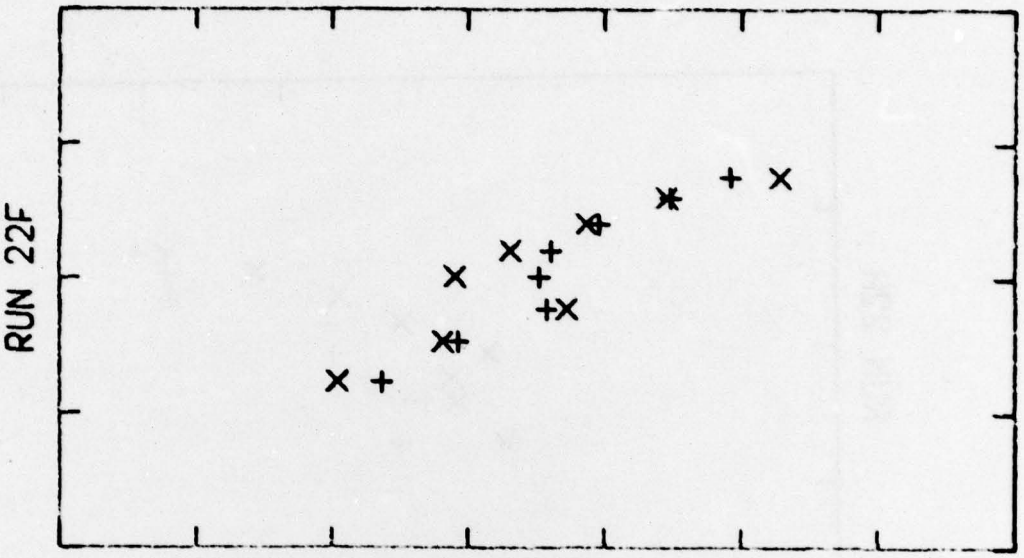
RUN 22F

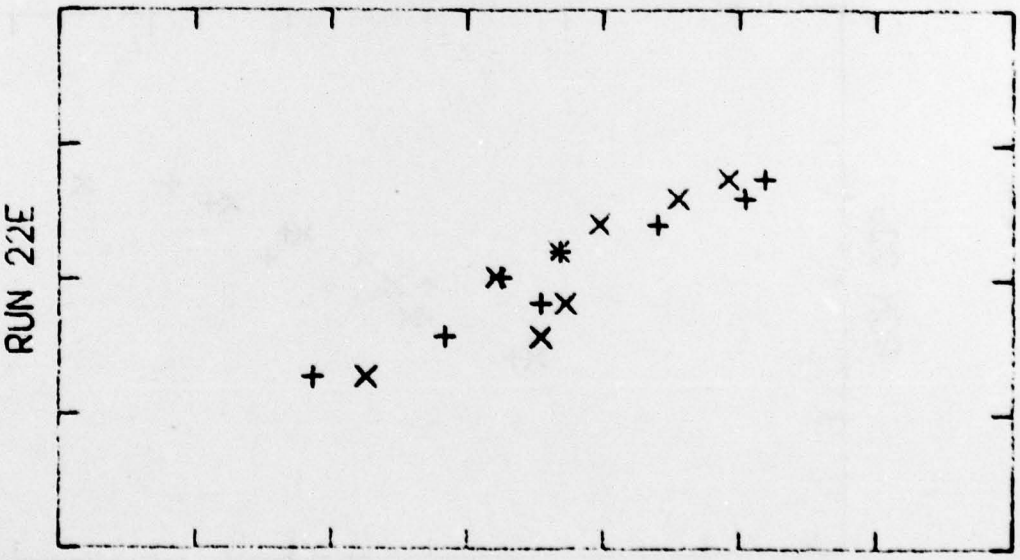
RUN 22E

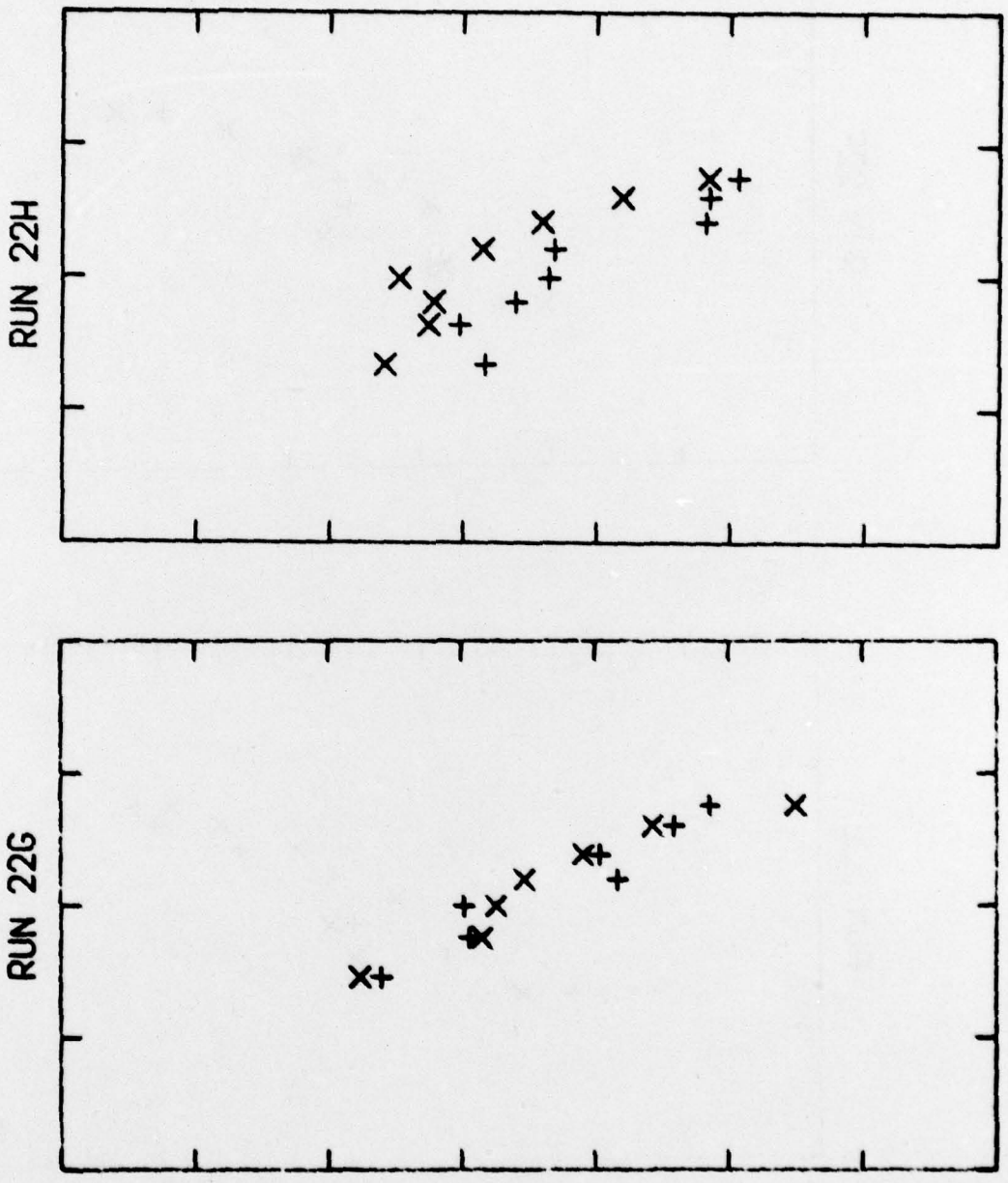
RUN 22H
RUN 22G

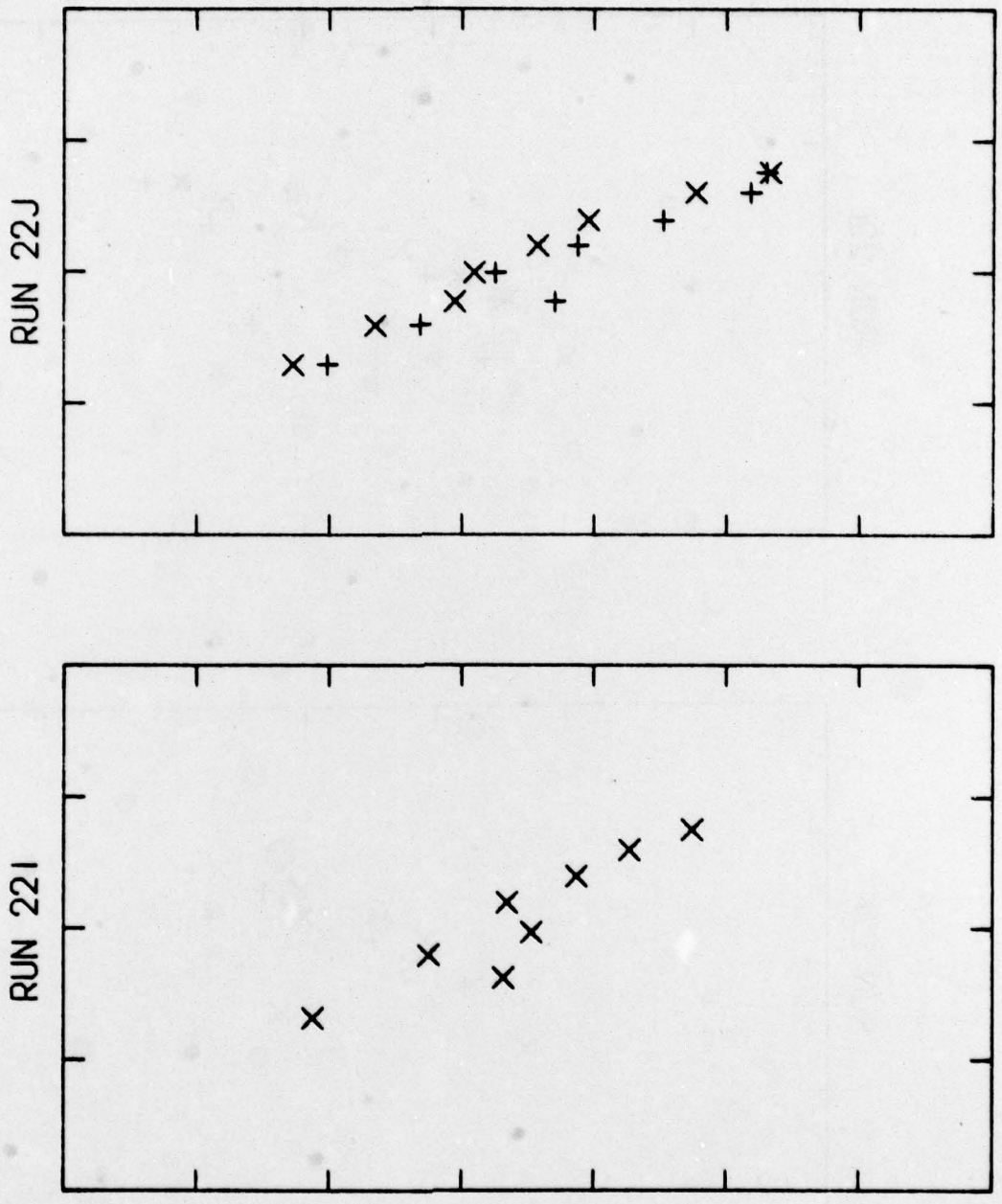
RUN 22J
RUN 22I

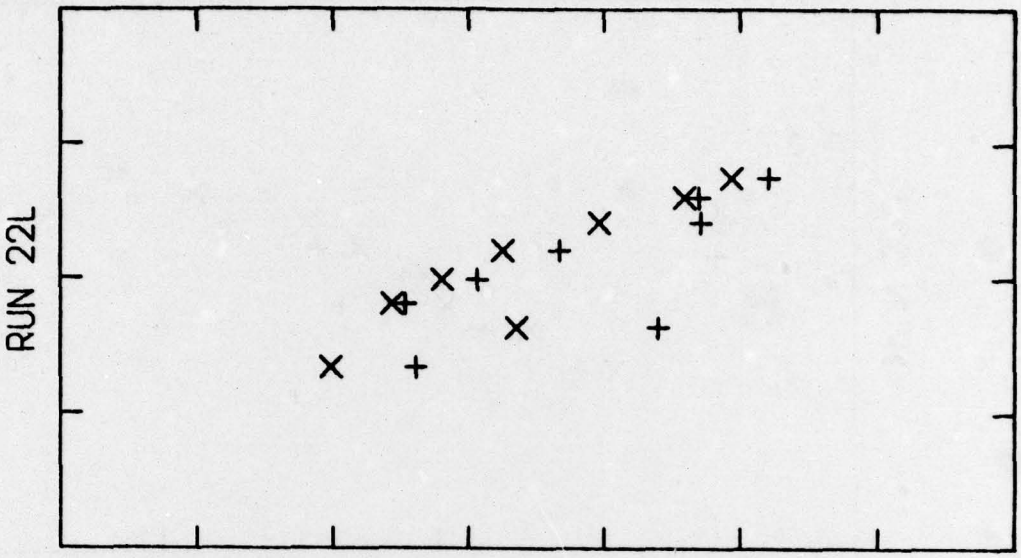
RUN 22L

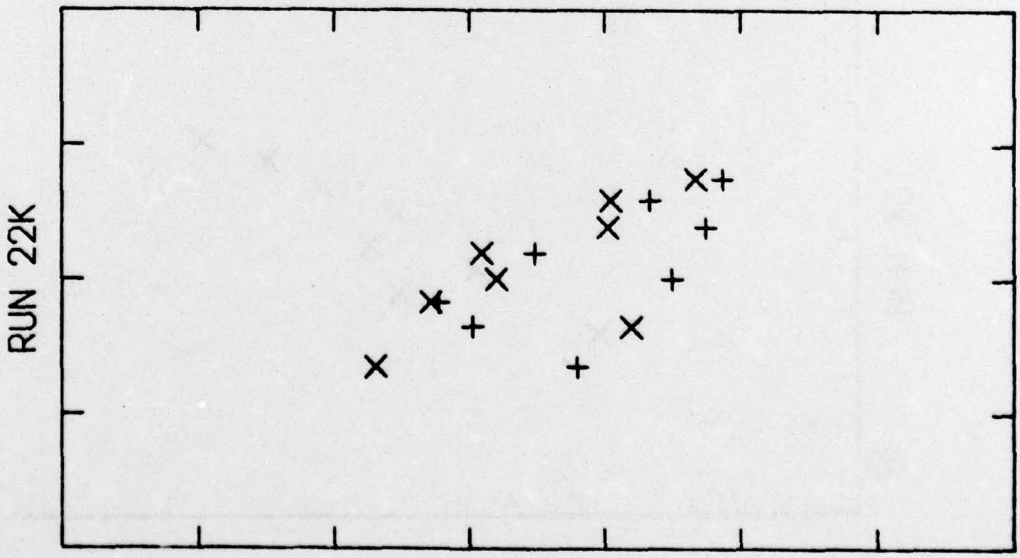
RUN 22K

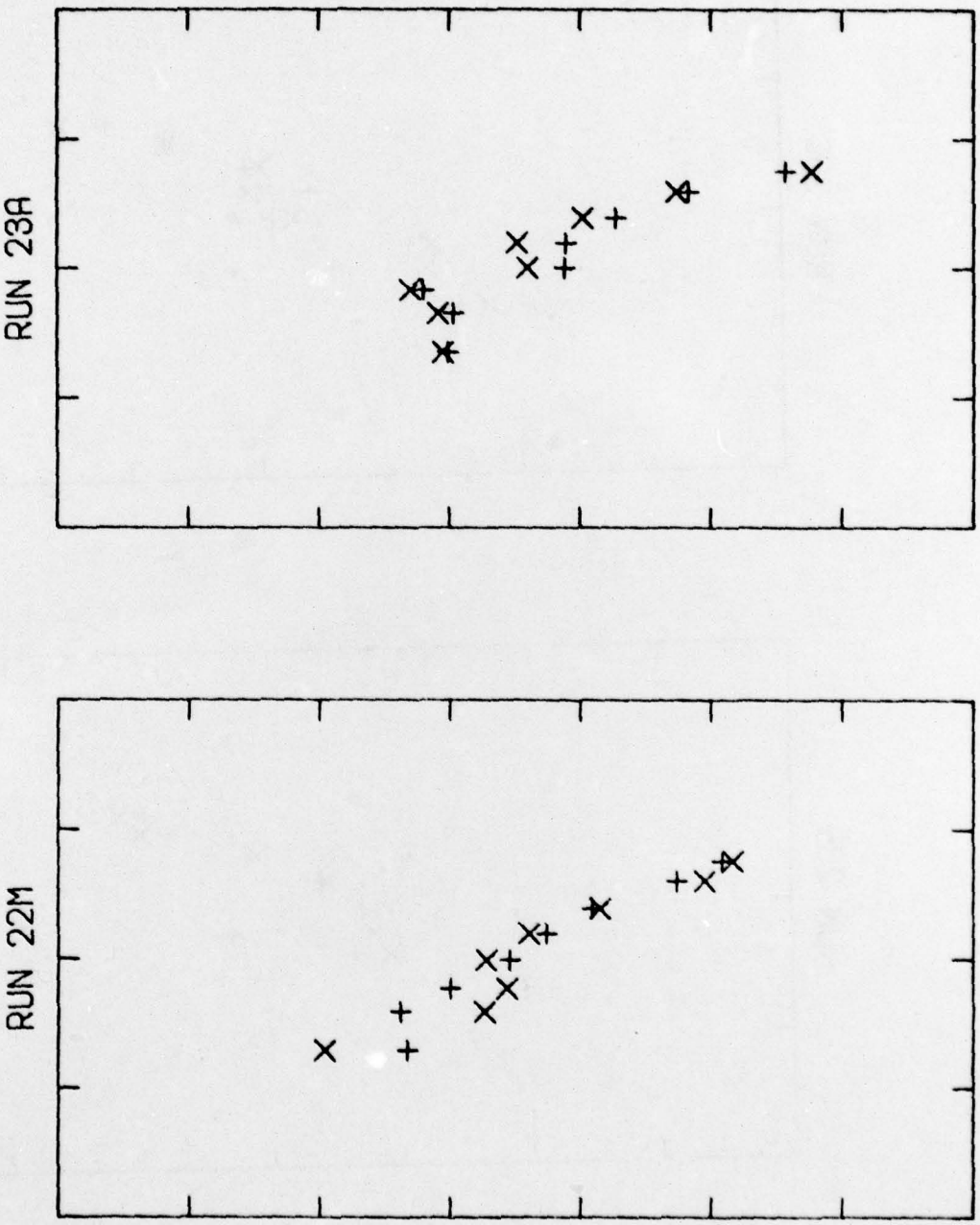
RUN 23A
RUN 22M

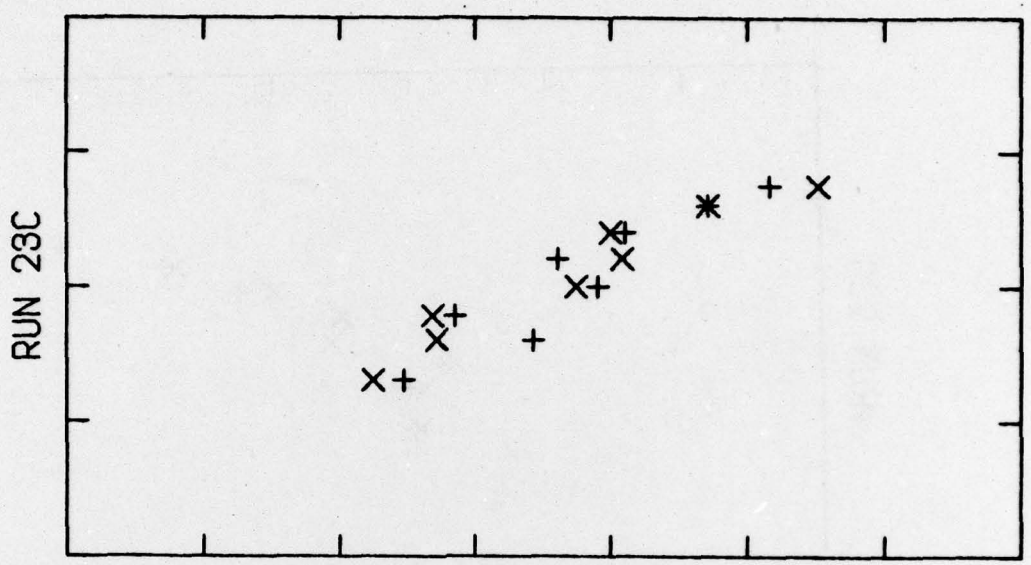
RUN 23C

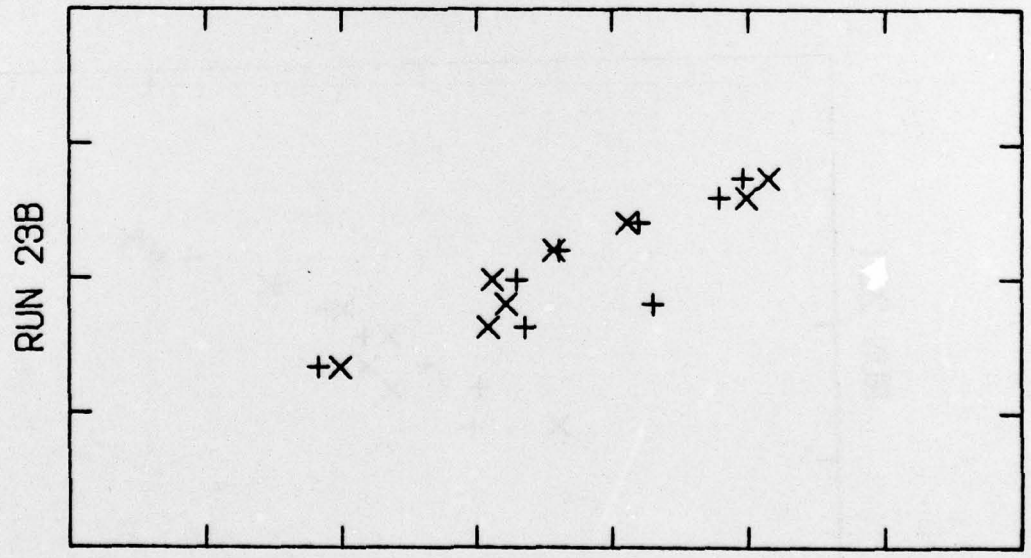
RUN 23B

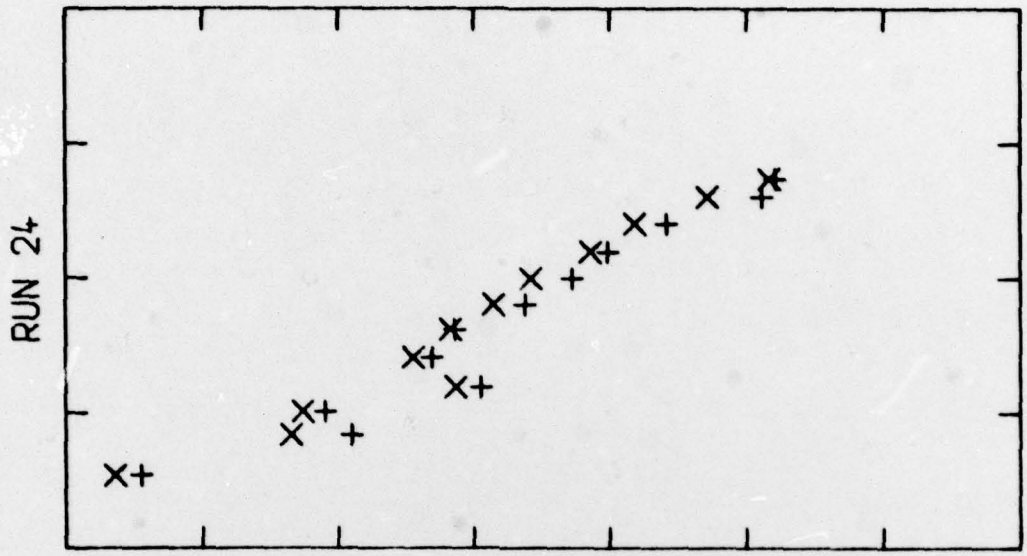
RUN 24

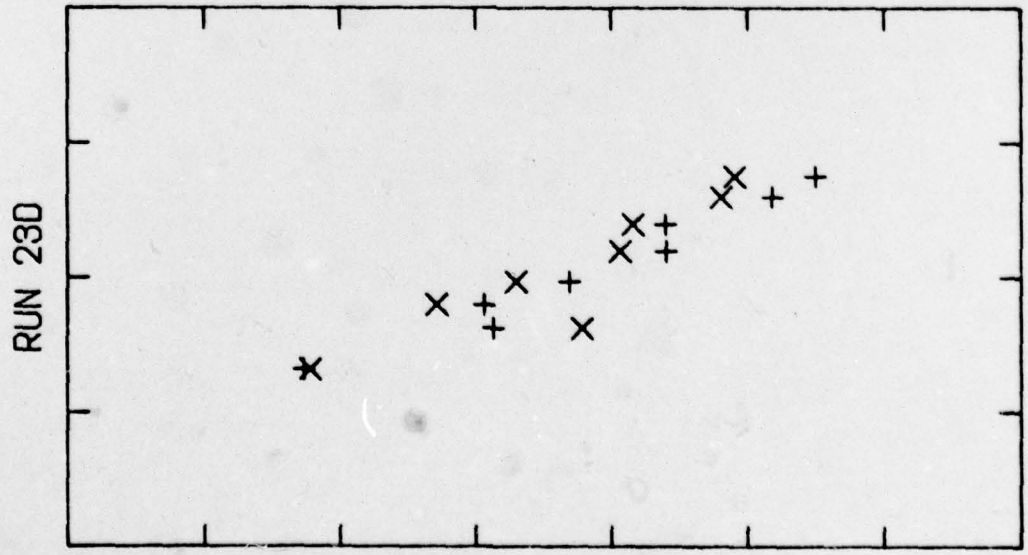
RUN 23D